UNIVERSITA' DEGLI STUDI DI VERONA

DEPARTMENT OF DIAGNOSTICS AND PUBLIC HEALTH

MICROBIOLOGY SECTION

GRADUATE SCHOOL OF LIFE AND HEALTH SCIENCES

DOCTORAL PROGRAM IN APPLIED LIFE AND HEALTH SCIENCES

MICROBIOLOGY AND INFECTIOUS DISEASES

XXIX Cycle Year 2014

PSEUDOMONAS AERUGINOSA INTERACTIONS WITH HOST AND BACTERIAL NEIGHBORS IN CYSTIC FIBROSIS LUNG DISEASE

S.S.D. MED/07

Coordinator: Prof. Giovanni Malerba

Supervisor: Prof. Maria del Mar Lleò

Doctoral Student: Angela Sandri

Pseudomonas aeruginosa interactions with host and bacterial neighbors in cystic fibrosis lung disease

Angela Sandri

Tesi di Dottorato

Verona, 04/07/2017

Contents

1. Aknowledgements - Ringraziamenti

Let's start by saying this will be very long! In the last years, I had the pleasure to meet and work with so many people, and many others walked down this road with me… I hope I won't forget anyone.

Premetto che non sarò breve! In questi anni ho avuto il piacere di incontrare e lavorare con moltissime persone, senza contare chi mi ha accompagnata in questo viaggio… Spero di non dimenticare nessuno.

Mar, questo dottorato è stata un'esperienza unica e formativa sia a livello professionale che umano, e tu sei la prima persona da ringraziare, per avermi dato tutte le migliori possibilità, per avermi sostenuta e guidata attraverso questo percorso non sempre facile, per le discussioni e idee sempre stimolanti, e per il clima amichevole che hai saputo creare. Spero di aver portato i risultati sperati e un po' di soddisfazione.

Gabriella, se dovessi elencare ogni motivo per cui ti ringrazio, stampare questa tesi mi costerebbe un patrimonio. Sei stata un'insegnante e collega eccezionale, oltre ad essere un'amica come poche. Grazie per ogni esperimento, consiglio, rimprovero, fotomontaggio, risata (come solo tu le sai fare), e molto altro ancora. Mai avrei potuto sperare di incontrare di meglio sul mio cammino. E mai avrei creduto di poter adorare così tanto dei bambini, ma al primo "Ancela" mi sono dovuta ricredere.

Alessia, sei stata impagabile come tesista e lo sei tutt'ora come collega, lavorare con te è un piacere e poter contare su di te una grande fortuna. Al di là del lavoro, sei stata una scoperta sorprendente, grazie per essere forse la persona meno noiosa che io conosca, per la curiosità con cui guardi ogni cosa, per gli abbracci che solo tu sai dare, e per essere una brasa cuerta, o ci sarebbe la fila per venire in vacanza con te.

Federico, grazie per avermi mostrato la luce, letteralmente parlando! Oltre che per le innumerevoli ore passate all'Ivis e la tua infinita disponibilità, ti ringrazio di cuore per l'ironia, le risate e le idee geniali sfornate bevendo caffè. La birra luminescente sarà sempre il mio progetto preferito.

Fabio e Francesca, vi devo moltissimo, collaborare con voi è stata un'esperienza costruttiva e interessante che mi ha formata professionalmente. Grazie per gli insegnamenti, il supporto, i meeting tra Parma e Verona, e l'acceso scambio di idee. Con voi ringrazio anche Gaetano Donofrio, per il plasmide che ci ha permesso di fare molto lavoro. Grazie anche a tutto lo staff del CIRSAL dell'Università di Verona, in particolar modo a Daniela, Marta, Giulia, Elisa e il Dr. Morbioli, per la loro competenza e disponibilità.

Marzia e Katia, grazie per essere sempre state partecipi dei miei progetti e risultati, e per avermi dato la possibilità di continuare il lavoro iniziato durante il dottorato. Eleonora, grazie per la tua disponibilità e per i preziosi scambi di idee ed opinioni. È stato un piacere condividere con te il laboratorio, che senza il tuo spirito organizzativo sarebbe stato nella confusione più totale! Con te ringrazio anche Vanessa, Liliana, e Maria, tutte insieme avete contribuito a creare un

bell'ambiente di lavoro e un gruppo affiatato con cui affrontare ogni giornata. 84mila volte grazie. Luisa, Paola, Gloria e Anna, siete il fondamento della sezione, sempre pronte a dare una mano, grazie per la vostra gentilezza e disponibilità. Marco, grazie per il supporto tecnico e le tante pfge. I tesisti, a cui spero di aver anche insegnato qualcosa mentre io stessa cercavo ancora di imparare. Chiara, Debra, Sara, Stefano, un enorme grazie per tutto il lavoro che avete fatto. Assieme a Paula e Giulio, avete creato un ambiente di laboratorio sereno e stimolante. Ilaria ed Enza, la "vecchia guardia", grazie per i preziosi consigli e le belle risate.

Claudio e Paola, con voi ho iniziato quest'avventura, e di questo non vi ringrazierò mai abbastanza. Grazie per questa proficua collaborazione, per il supporto e l'interesse verso il mio lavoro, e per i momenti conviviali passati assieme. Elisa, la mia Svampy, sono così tante le volte in cui mi hai aiutata e sopportata, sei stata semplicemente essenziale, non c'è l'avrei mai fatta senza di te. Grazie per il tanto lavoro, ma anche e soprattutto per la bella amicizia, le sane risate, e la nostra complicità. Federica, grazie per essere una ventata di allegria, iniziare le giornate bevendo un caffè con te le rende già migliori, e non è poco. Valeria, grazie per i kili di plasmide, i litri di surnatanti, e per l'ottimismo che mi infondi. Tutto il Sorio's Lab, da dove sono partita e dove ho sempre trovato rifugio: Marzia, hai sempre la risposta giusta alle mie domande più disparate; Silvia e Luisa, il mio gruppo di sostegno a suon di spritz; Sara, Jan, Zeno, Paola, Anna, sempre gentili e pronti a darmi una mano. Grazie a tutti voi per l'aiuto e per i bei momenti passati assieme in questi anni.

Chiara, grazie per i tanti caffè, i buoni consigli, per il tuo spirito libero e l'incoscienza di gettarci giù dai pendii. Ilaria, grazie per la ventata di freschezza (e tutto il formaggio) che mi hai portato. Elisa, grazie per non aver mollato, non sarebbe stato lo stesso senza di te.

Giovanni Malerba e Maria Grazia Romanelli, grazie per aver coordinato il corso di dottorato con grande competenza e immensa disponibilità. Grazie anche a Stefania Baschirotto e Laura Marcazzan, senza le quali sarei affogata nella burocrazia dei rimborsi.

Grazie ai luoghi vitali per la mia sopravvivenza e vita sociale all'Univr: il bar e le macchinette del caffè.

Søren and Helle, thank you for welcoming me in your group at DTU, it was an amazing experience that I really enjoyed. I've got the chance to learn so much, discuss and expand my ideas and interests, work in a very motivating environment, and win my challenge against Danish winter. Thank you for your great advice, the nice talks about science and much more, for helping and providing me with the perfect strains for my work. Janus, thank you for your magic touch in dosing silicone on flow cells, for teaching me confocal microscopy, giving me a diamond (tip) and an illegal bike ride, for the best Spritz I've ever had, and for your funny attitude that always cheered me up. Alicia, my favorite Spaniard on earth, thank you for bossing me around in such a lovely way, teaching me the secrets of cloning, giving me a home twice, forcing me to do sports, and being just as crazy as you are. Y por los caracoles. Jennie, I always

had the feeling you believe in me way more than I do, and you have no idea how helpful this feeling was to me. Thank you for it, and for improving my English, trying to explain me sequence analysis, cooking so many delicious dinners, and showing me the honey badger path. Ruggero, veniamo dallo stesso paese e siamo dovuti andare in Danimarca per conoscerci… Ed è stata una gran fortuna trovarci proprio lì, a cucinare lasagne e bere vino italiano. Grazie per i consigli e le riflessioni sul lavoro e la vita, le nostre chiacchierate in un ufficio di stranieri, l'ora di psicanalisi quotidiana, e per tutto quel buonissimo ramen. Jakob, thank you for the suggestions about cloning, for your smiling attitude, and for being the first and best fan of my Tiramisù. Biljana, thank you for your help and friendliness, for all the interesting talks and the funny moments we shared. Marilena, quante ore abbiamo passato a giocare con le flow-cells, grazie per tutto l'aiuto e le lunghe chiacchierate al buio. Elio, non fosse per te starei ancora cercando di analizzare le immagini dei biofilm da un vecchio computer danese, grazie per l'aiutino informatico. Lea, tak for your kindness and genuine Danish spirit, you were the best source of interesting facts about Danes habits. Rocio and Fabienne, thank you for the nice time we spent in the cool office, especially on our stolen couch. Tak Kobenhavn, my home in the cold and the dark, but a hygge place where I found lots of light, warmth, cheese and wine.

Eliana, grazie per aver preso un aereo per la Danimarca con me in pieno inverno, un po' per fare un viaggio e un po' per non lasciarmi congelare da sola. Di certezze non ne ho molte, ma una sei tu, che mi raggiungeresti in capo al mondo se mai io ne avessi bisogno. Grazie per i viaggi allo sbaraglio, le lezioni di architettura che sai improvvisare ovunque e con ogni condizione atmosferica, la passione e la determinazione con cui vivi e mi ispiri sempre, e per essere la mia Cosa nel senso più Scrubsiano del termine. Arianna, tu quell'aereo non l'hai preso ma era come se ci fossi. Un'altra certezza su cui non ho dubbi: dovunque io vada, non c'è assenza di campo che possa impedirti di essere lì con me. Grazie perché riesci ad abbattere le distanze, perché mi sai spesso prima e meglio di quanto mi sappia io, perché fai sempre un po' di posto per me, e per aver saputo crescere mantenendo intatto il lato che più amo di te, quello buffo. Ledi e Raffaella, grazie per il calore della vostra ospitalità, per l'amicizia che si è creata tra colazioni e cene, e per farmi ancora sentire coinquilina, seppur part-time. Valentina, Giuseppe, Daniela, Francesco, Miriam, Anna Chiara, Daniele e Nicola, grazie per la vostra amicizia e ospitalità sempre genuina, perché sapete abbattere il tempo e ogni volta ritrovarvi è come non avervi mai lasciati. Grazie a Firenze, la mia casa per caso e per fortuna, dove ho conosciuto la parte che preferisco di me stessa, quella terrona.

Michela e tutta l'Amphora, grazie per avermi insegnato un lavoro e per avermi aiutata quando ne ho avuto bisogno. Oltre al perfetto equilibrio necessario per portare un vassoio, ho imparato da voi che la passione e il sacrificio sono l'ingrediente fondamentale di una buona pizza.

Grazie a tutta la mia famiglia stretta e allargata di zii e cugini che vedo troppo poco, ma che restano sempre aggiornati sui miei spostamenti e traguardi, e fanno sempre il tifo per me.

Mamma e Serena, grazie perché mi sopportate da sempre, e in particolare in questo ultimo periodo di stress e incertezze. Grazie perché avete accettato il mio spirito un po' nomade e la mia valigia sempre pronta, perché ovunque io vada voi siete la mia più grande certezza, le mie radici e le mie ali, perché la distanza non è mai stata un limite per noi, perché mi sostenete sempre e in ogni modo, anche quando non capite le mie scelte. Grazie perché casa non sono quattro mura e un tetto, ma voi.

Grazie alla me stessa diciottenne per quell'errore di troppo in un test d'ammissione. Dei tanti che ha commesso, quello è stato certamente il migliore e più importante, perché l'ha portata esattamente qui, oggi, passando attraverso un decennio di cui non cambierei nulla.

"Devi cambiare la percezione di te e di ciò che ti sta attorno, Calcare. Non può rimanere tutto cristallizzato nel tempo. […] Capisci cosa devi fare, se vuoi andare avanti? Devi svuotare la cache."

"Grazie per avermi aperto gli occhi, amico coccodrillo. Ciò non mi guarirà dalla lacerante nostalgia che mi avvelena la vita, ma mi dona maggior consapevolezza. …Ma mo'? Che faccio?"

"E che devi fà? Continua a raccontare le cose tue. Però come sono adesso."

[Zerocalcare e il coccodrillo di Peter Pan]

2. Abstract

Background: Cystic fibrosis (CF) lung infection is a complex condition where opportunistic pathogens and defective immune system cooperate in developing a constant cycle of infection and inflammation. Despite the polymicrobial nature of this pathology, *Pseudomonas aeruginosa* is considered the major pathogen. Several mechanisms contribute to its successful colonization of CF airways; among these, virulence factors are important players. This thesis includes two studies aimed to evaluate aspects of *P. aeruginosa* interaction with both host and other microorganisms, like the emerging pathogen *Achromobacter xylosoxidans*.

PROJECT 1 - Role of Pseudomonas aeruginosa virulence factors on lung inflammatory response: an in vivo imaging approach

Methods: Pyocyanin, pyoverdine and proteases were measured in bacterial culture supernatant. Lung inflammatory response to bacterial exoproducts was monitored by in vivo imaging in wild-type and CFTR-knockout mice expressing luciferase gene under control of a bovine IL-8 promoter, and by evaluation of immune cells and cytokines in bronchoalveolar lavage.

Results: *P. aeruginosa* grown in presence of sub-inhibitory doses of macrolides azithromycin and clarithromycin showed diminished levels of the secreted virulence factors. Intratracheal challenge with culture supernatant induced a strong inflammatory response in mouse lungs, while lack of virulence factors corresponded to reduction of inflammation. Particularly, inactivation of bacterial proteases by human matrix metalloprotease inhibitors Ilomastat and Marimastat also resulted in decreased lung inflammation, similarly to what previously observed with macrolides.

Conclusions: Our data suggest that virulence factors are involved in *P. aeruginosa* pro-inflammatory activity. Particularly, proteases seem to play a critical role; thus, their inhibition potentially represents an additional therapeutic approach for *P. aeruginosa*-infected CF patients.

PROJECT 2 - Adaptive microbial interactions between Pseudomonas aeruginosa and Achromobacter xylosoxidans

Methods: *P. aeruginosa* and *A. xylosoxidans* clinical isolates were longitudinally collected from a chronically co-infected patient. Genotypic analysis was performed by pulsed-field gel electrophoresis. Phenotype was evaluated in terms of colony morphology, growth rate, adhesion ability, biofilm formation, and protease secretion.

Results: The patient was colonized with the same clonetypes for 3 years. During this time, *P. aeruginosa* underwent phenotypic evolution while *A. xylosoxidans* showed no phenotypic changes. *A. xylosoxidans* could initially affect *P. aeruginosa* growth, adhesion and biofilm formation; later, this inhibitory effect disappeared and the two pathogens could form mixed biofilms. *A. xylosoxidans*

proteases down-regulation was observed over time, along with *P. aeruginosa* increased resistance to these exoproducts.

Conclusions: During long term cohabitation in CF lungs, initial competitive interactions between *A. xylosoxidans* and *P. aeruginosa* seem to evolve towards reciprocal adaptation, which might represent a survival advantage.

General conclusions: Understanding which mechanisms are primarily involved in *P. aeruginosa* successful colonization of CF lungs is essential to prevent the establishment of chronic infection and to find new therapeutic approaches. The studies here presented contribute to this knowledge, pointing at bacterial virulence and inter-species interactions as critical players.

3. Abbreviations

AprA: alkaline protease

ASL: airway surface liquid

BALF: bronchoalveolar lavage fluid

bIL-8-Luc: bovine IL-8 promoter/luciferase reporter

CF: cystic fibrosis

CFTR: cystic fibrosis transmembrane conductance regulator

DPB: diffuse panbronchiolitis

EMEM: Eagle's minimum essential medium

EPS: exopolysaccharide

FEV1: Forced expiratory volume in the 1st second

FVC: forced vital capacity

GFP: green fluorescent protein

KO: CFTR-knockout

IL: interleukin

LB: Luria Bertani medium

LPS: lipopolysaccharide

LasB: elastase B

MIC: minimum inhibitory concentration

MMP: matrix metalloprotease

PFGE: pulsed-field gel electrophoresis

QS: quorum sensing

TSB: tryptic soy broth

WBC: white blood cells

WT: wild-type

4. Background

4.1. Cystic fibrosis

Epidemiology

Cystic fibrosis (CF) is the most common life-threatening recessively inherited disease in the Caucasian population, counting approximately 80.000 diagnosed people in the world. Incidence shows wide geographic variations, ranging from 1 in 1400 to 6000 live births in Europe (excluded Finland, where it is rare). Other areas of high diffusion are North America, Australia and New Zealand, Israel and Lebanon, while it is extremely rare in Asia, especially in China and Japan (Fig. 1). However, it is likely that CF is under-diagnosed in South America, Africa and Asia [1].

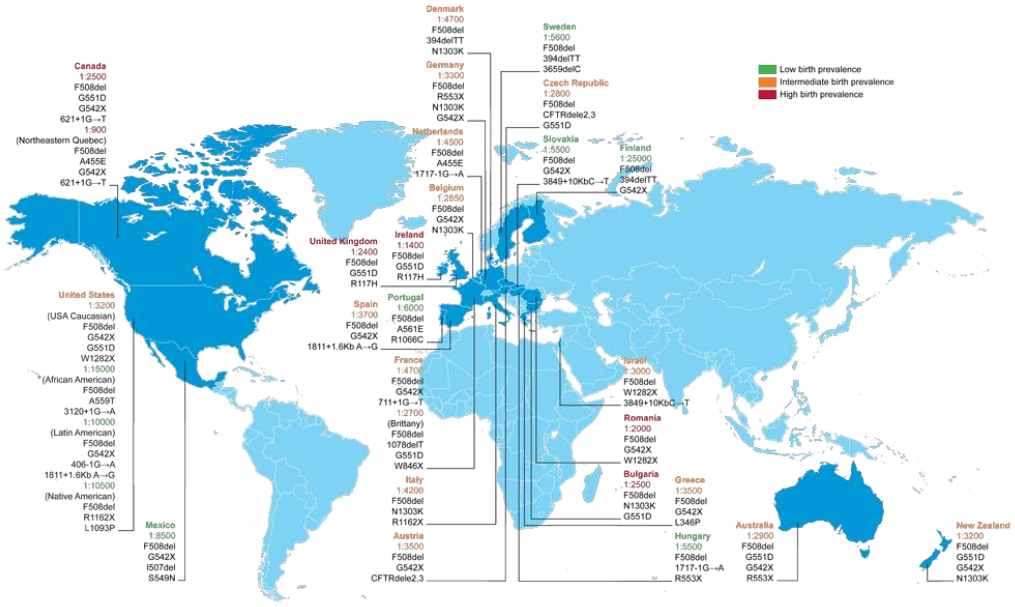

Figure 1. CF prevalence and most common *CFTR* mutations by country. Birth prevalence is reported as number of live births per case of CF. Common/important mutations in each region are listed below the prevalence. The birth prevalence can vary greatly between ethnic groups in a country. (O'Sullivan BP, Freedman SD. *Lancet* 2009)

Genetic defect

The disease is caused by mutations in the *CFTR* (CF transmembrane conductance regulator) gene, situated in the long arm of chromosome 7 (7q31.2) [2, 3] and encoding the CFTR protein, which mainly functions as a chloride channel in exocrine epithelia. Up to date, over 2000 different *CFTR* mutations have been identified (www.genet.sickkids.on.ca), causing CFTR dysfunction through a variety of different mechanisms, categorized in 6 major classes (Fig. 2). Mutations belonging to classes 1 to 3 cause diminished or non-functional CFTR protein at the membrane and are associated with severe CF phenotypes, while class 4 and 5 mutations are associated with residual CFTR-mediated chloride transport and milder phenotypes. Relatively novel class 6 mutations are characterized by high

CFTR turnover at the cell surface, promoting a functional but unstable mature CFTR protein [4, 5].

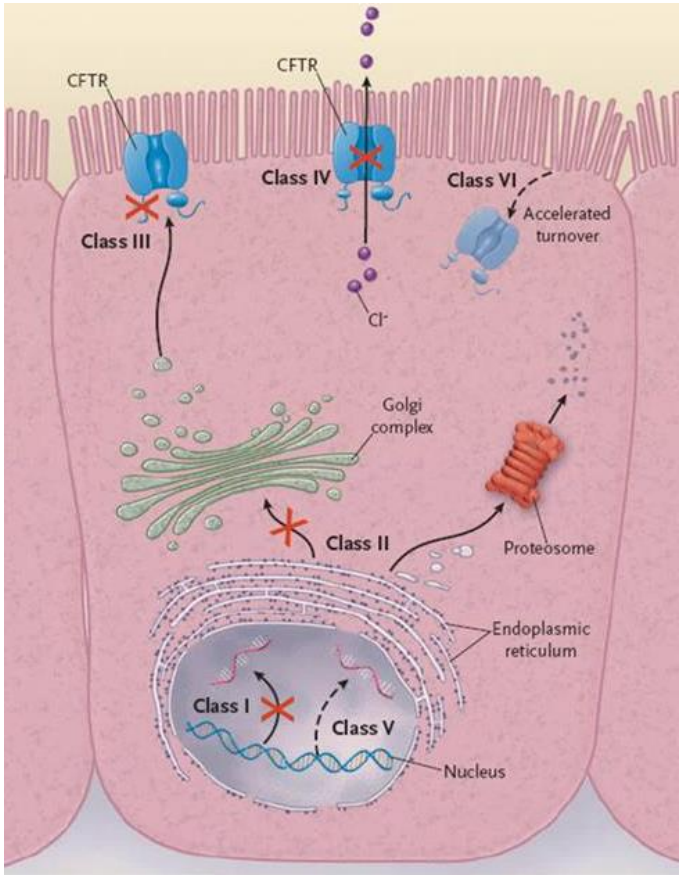

Figure 2. Classification of *CFTR* mutations. Class I: lack of CFTR synthesis; class II: defective protein processing; class III: defective channel regulation or gating; class IV: defective chloride conductance; class V: reduced amount of CFTR protein; class VI: increased turnover of CFTR channel at the cell surface. (Rowe SM, Miller S, Sorscher EJ. *N Engl J Med* 2005).

CFTR functions

The CFTR channel belongs to the superfamily of ABC (ATP binding cassette) transmembrane transporters. It is mainly located in the apical membrane of epithelial cells lining secretory organs, although it is also found in non-epithelial tissues like cardiac myocytes, smooth muscle, erythrocytes and immune cells [6-11]. Structurally, CFTR is a 1480 amino acid membrane-bound glycoprotein comprised of two six-span transmembrane domains, MSD1 and MSD2, each connected to a cytoplasmatic nucleotide-binding domain (NBD) that hydrolyses ATP. These two units are connected through a regulatory domain, which is a unique feature of CFTR within the ABC superfamily [12, 13]. CFTR gating is thought to occur by protein kinase A phosphorylation of the R domain and recruitment of ATP on the NBDs, that induce conformational changes in the protein resulting in channel opening and closing upon ATP hydrolysis (Fig. 3) [14-16].

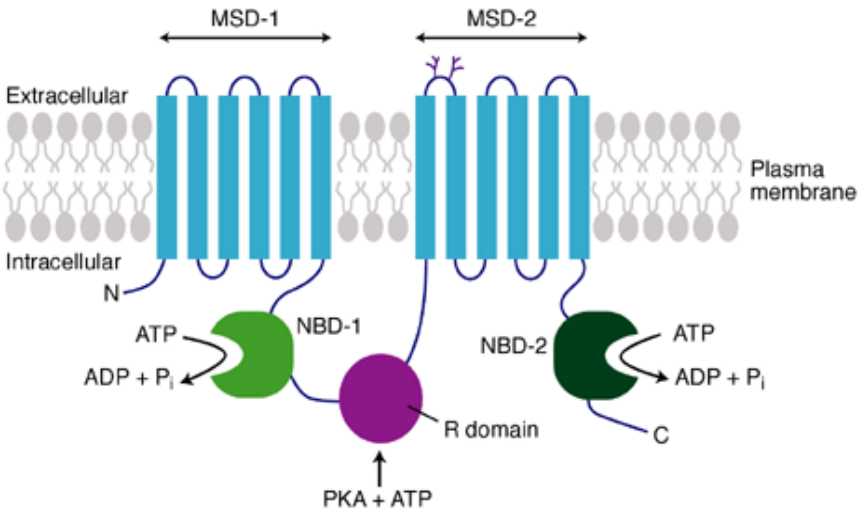

Figure 3. Structure of CFTR channel. CFTR is composed of five domains: two six-span transmembrane domains (MSDs), two nucleotide-binding domains (NBDs), and a regulatory (R) domain. MSD-1 and MSD-2 are each bound to a NBD, forming two units connected through the R domain. The MSDs form the channel pore, phosphorylation of the R domain determines channel activity, and ATP hydrolysis by the NBDs controls channel gating. (Davidson DJ and Dorin JR. *Expert Reviews in Molecular Medicine* 2001)

CFTR has an additional role in the regulation of cell ionic transport, by repressing the epithelial sodium channel ENaC and controlling the renal outer medullary potassium channel ROMK2, the outwardly rectifying chloride channel ORCC, the calcium-activated chloride channel CaCC, the sodium/proton exchanger NHE3, and an aquaporin channel [17-21]. Moreover, CFTR is also involved in bicarbonate-chloride exchange, ATP transfer, intracellular vesicle transport, acidification of intracellular organelles, glutathione extracellular transport, and inflammation processes [22-27].

Clinical manifestations

CFTR absence or low-functioning leads to insufficient chloride secretion in the secretory epithelia, causing excessive reabsorption of ions and water and final dehydration and thickening of secretions. An exception are sweat glands, where CFTR channel function is reverse and its dysfunction produces sweat containing elevated chloride (>60mmol/L) and sodium concentrations [28]. The name "cystic fibrosis" refers to the characteristic fibrosis and cyst formation within the pancreas, due to the stasis of viscous pancreatic juices into pancreatic ducts. The resulting pancreatic insufficiency, observed in around 85% of patients, leads to steatorrhea, malabsorption syndrome, malnutrition, hypoproteinemia, and pancreatitis. Pancreatic abnormalities can also cause CF-related diabetes, which has a prevalence around 25% in patients aged >25 years. Thickened secretions also cause liver problems because of bile ducts obstruction, leading to cirrhosis and yellow jaundice. In addition, ionic imbalance in the biliary tract may lead to increased risk of gall stone and hepatobiliary disease [29]. Early gastrointestinal

manifestations include meconium ileus, occurring in 10-17% of patients within the first days of life [30]. Around 97-98% of male patients are infertile because of atrophic or absent vasa deferentia, while fertility problems due to thickened cervical mucus affect 25% of CF females [31, 32]. While CF is a multiorgan disease, pulmonary involvement is the major cause of morbidity and ultimate mortality. Thickened mucus obstructs distal airways, promoting bronchiectasis and bacterial infections, followed by intense neutrophil recruitment. Chronic infections and progressive inflammation favor tissue degradation, leading to final lung failure [33].

4.2. Lung pathophysiology

Pathogenesis

CFTR is expressed in the submucosal glands and the apical surface of ciliated epithelial cells [34, 35]. In normal airways, mucus is constantly cleared by the mucociliary system thanks to airway surface liquid (ASL) volume autoregulation. Although pathogenesis of CF lung disease is not completely clear yet, studies have suggested that defective chloride and bicarbonate transport, coupled with altered regulation of sodium transport, lead to excessive reabsorption of sodium and water from the airway surface liquid, causing dehydration of the mucus layer and depletion of the periciliary layer, with consequent inability of the cilia to remove the thickened mucus [36]. Mucus stasis promotes airways blockage and bronchiectasis, and impairs clearance of inhaled microorganisms. Relatively minor early infections may induce an exaggerated and prolonged inflammatory response. Infection persistence leads to chronic inflammation and finally to progressive loss of lung function (Fig. 4) [37, 38].

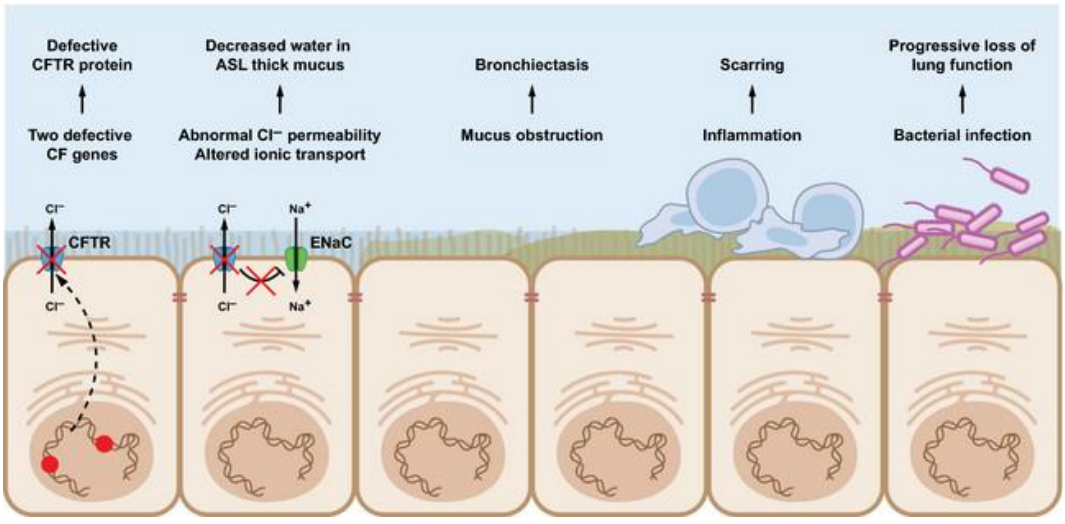

Figura 4. The CF pathogenesis cascade in the lung. The mechanism of CF dysfunction starts with the primary CFTR gene defect, which alters the airway surface volume (ASL) and leads to bronchiectasis, lung damage by a cycle of inflammation and infection, and ultimate severe lung deficiency. (Amaral MD. *Journal of Internal Medicine* 2015).

Inflammation

Normal airways are protected from infection by host defense system, and airway macrophages complement epithelial defenses. In the CF airways, inflammation begins early in life and may occur independently of infection. Chronic inflammation, mainly characterized by neutrophils recruitment, is the result of increased activation of the inflammatory response combined with inability to terminate and resolve inflammation. Inhibition of CFTR production or function in epithelial cell lines was associated with increased activation of the pro-inflammatory transcription factor NFkB, and reduced production of IFN-γ that leads to stimulation of neutrophil chemokines [39-44]. The CF airway contains large concentrations of several pro-inflammatory mediators including TNF-α, IL-1β, IL-6, IL-8, IL-17, IL-33, GM-CSF, G-CSF, and HMGB-1, mainly involved in neutrophil stimulation, clearance regulation, oxidative and secretory responses [44-47]. Particularly, IL-8 and IL-17 are strong promoters of neutrophils recruitment [48, 49]. CF airways are also deficient in several counter-regulatory molecules including IL-10, nitric oxide, and lipoxin-A4, mainly involved in inflammatory response downregulation and termination [45, 50-55]. Thus, an imbalance in anti-inflammatory molecules may be as important as the numerous pro-inflammatory pathways for the persistence of host inflammatory response, helping to explain observations of inflammation in the absence of infection.

Neutrophils normally secrete antimicrobial peptides, eliminate microorganisms through opsonophagocytosis, trap bacteria in extracellular traps consisting of extruded DNA, and digest bacteria intracellularly by autophagy. Recent studies demonstrated that neutrophil phagolysosomes express CFTR, whose absence or defect cause abnormal chlorination of engulfed pathogens and impaired microbial killing [11, 56, 57]. In CF, these potentially malfunctioning neutrophils accumulate in the airways by a combination of excessive influx and decreased clearance. Massive amounts of neutrophil chemoattractants are present in CF airways [58]. Particularly, IL-8 concentration in bronchoalveolar lavage fluid (BALF) has been shown to often correlate with the concentration of neutrophils and their products [48]. Neutrophils are usually removed by cough clearance or alveolar macrophages phagocytosis, but in CF cough clearance is reduced and the ability of macrophages to scavenge apoptotic neutrophils (efferocytosis) also appears abnormal [59]. Rather than clearance by normal apoptotic mechanisms, CF neutrophils often undergo necrosis [60]. Decomposing neutrophils release large amounts of intracellular contents: chemoattractants fuel further neutrophils influx, DNA increases the viscosity of endobronchial secretions, oxidants induce oxidative stress and promote IL-8 production, and proteases mainly damage airways structure [61, 62]. Particularly, neutrophil elastase can disrupt lung tissue, contribute to mucociliary impairment, support neutrophils influx, hinder phagocytosis and efferocytosis, and degrade CFTR [63-69]. Detection of neutrophil elastase in BALF has been shown to predict early bronchiectasis in CF children, and its concentration in sputum correlates with FEV1 decline [70-72]. Recently also macrophages demonstrated to play a critical role in CF inflammation process. Macrophages normally phagocyte microbes, microbial products and cellular debris, and produce pro-inflammatory cytokines in response to pathogen exposure. In CF, macrophages are present in high concentrations in

the BALF of young patients, but appear to be dysregulated: differentiation in cell subtypes is altered, exposure to bacterial lipopolysaccharide induces an excessive production of pro-inflammatory mediators, bacterial killing and efferocytosis abilities are impaired [10, 59, 73-76].

Infection

Ineffective mucociliary clearance and defective innate immune defenses allow bacterial infections to establish in CF airways. Early acquisition of pathogenic bacteria and development of chronic infections are associated with increased morbidity and mortality. Colonization with *Pseudomonas aeruginosa*, the most common pathogen isolated from CF airways, is particularly difficult to eradicate and is associated with acceleration of decline in lung function and with poorer prognosis [77]. Other respiratory pathogens play a role at different stages of the lung disease: *Staphylococcus aureus* and *Haemophilus influenzae* are the main pediatric pathogens, while *Burkholderia cepacia* complex (Bcc), *Achromobacter xylosoxidans*, *Stenotrophomonas maltophilia* and nontuberculous mycobacteria are mainly found in adults (Fig. 5) [78]. Particularly, *A. xylosoxidans* recently gained attention as an important emerging pathogen that can cause severe chronic infection associated with lung inflammation and decline of respiratory function [79-81], further complicated by its innate and acquired multidrug resistance hindering eradication therapies [82, 83]. Bcc is a group of phenotypically similar species of the genus *Burkholderia* that have been associated with worse outcomes and survival in CF patients, and heightened mortality following lung transplantation [84]. Also, anaerobe bacteria seem to have a role in exacerbations [85, 86]. In addition to bacterial infections, many patients present infections with *Aspergillus sp.* and some exhibit the syndrome of allergic bronchopulmonary aspergillosis [87].

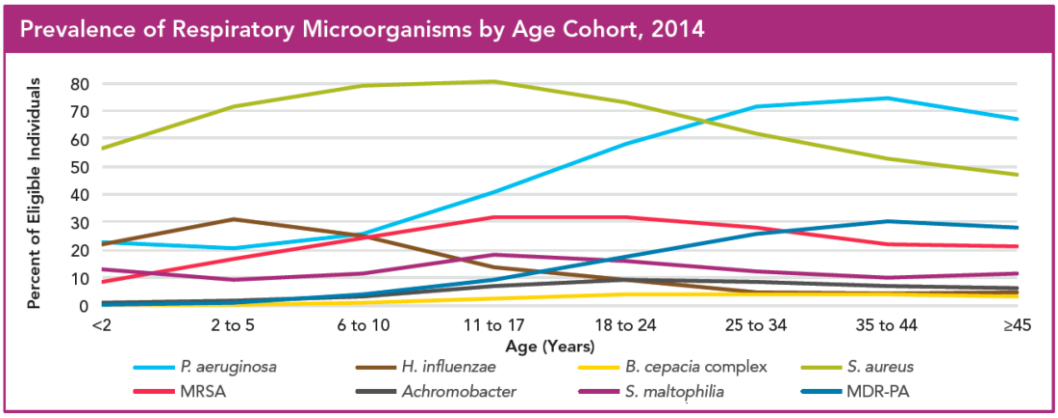

Figure 5. Prevalence of respiratory CF pathogens by age of patients. *S. aureus* and *H. influenzae* are the main pediatric pathogens, while *P. aeruginosa, B. cepacia complex, Achromobacter spp.*, and *S. maltophilia* are mainly found in adults. Multidrug resistant *S. aureus* and *P. aeruginosa* are reported as MRSA and MDR-PA, respectively. (US CFF Patient Registry, Annual Data Report 2014).

Apart from classical pathogens, a large number of microorganisms described as the "CF microbiome" has been identified [88], and CF lung infection has been

highlighted as a polymicrobial condition, highly heterogeneous between patients and fluctuating over time [89]. It is likely that pathogens and commensals could engage intra- and inter-species interactions, acting competitively or synergistically with each other to gain an adaptive advantage through the production of antimicrobial chemicals to compete and signal molecules to cooperate, thereby influencing community composition, resistance to antibiotics, and course of airway disease [90, 91]. Interactions are favored by microbial proximity, promoted by intra- and inter-species co-aggregation in biofilm communities [92, 93]. Biofilm mode of growth, typical of chronic infections, allows bacteria to form highly organized, structured aggregates attached on the epithelial surface, using self-produced extracellular polymeric substance (EPS) containing nucleic acids, polysaccharides, and other macromolecular components like proteins, lipids, biosurfactants, flagella and pili. The EPS matrix imparts both a physical and chemical robustness to the community by resisting mechanical forces and decreasing the penetration of toxic chemicals like antibiotics and host defense molecules [94, 95]. Thus, biofilms decrease bacterial susceptibility to antimicrobial agents, promoting bacterial tolerance and/or resistance, and favoring the failure of eradication therapies [96].

4.3. Pseudomonas aeruginosa

CF airways infection

P. aeruginosa is a Gram-negative rod that can act as an opportunistic pathogen causing chronic respiratory infections in more than 50% of CF patients, with higher prevalence in adults [97-99]. A period of intermittent, recurrent lung colonization with *P. aeruginosa* is described, when antibiotic treatment can temporarily eradicate the infection and recolonization with another genotype occurs [100]. However, a recolonization with the same genotype occurs in approximately 25% of the patients, probably by bacterial aspiration from the sinuses in which the bacteria might adapt before infecting the lung [101, 102]. This intermittent colonization phase, which can last for years, sooner or later transitions into a chronic infection (Fig. 6). In the lower respiratory tract, the biofilm mode of growth of *P. aeruginosa* induces a state of chronic inflammation, which is unable to clear the infection and causes instead pulmonary damage [103]. The gradual decrease in lung function is most likely the result of accumulation of focal infections over time [104]. Increased number of neutrophils, alveolar macrophages and T lymphocytes were found in alveoli of explanted lungs from infected CF patients [105]. Despite the inflammatory response and intensive antibiotic therapy, most infections caused by *P. aeruginosa* persist for long time, eventually leading to respiratory failure and lung transplantation or death [106].

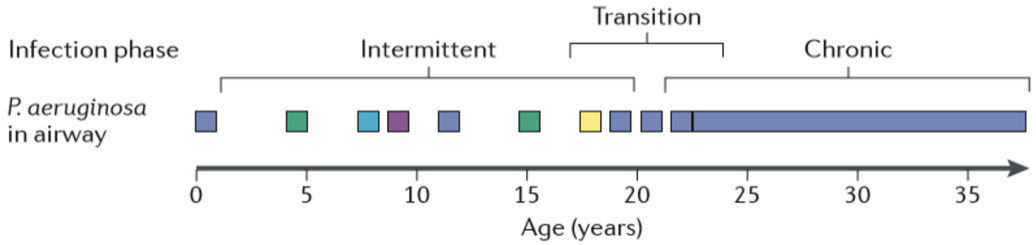

Figure 6. Schematic representation of the typical progression of *P. aeruginosa* infection. Different colors represent phylogenetically independent *P. aeruginosa* clones. Intermittent colonization can be eradicated, and the patients can be negative for *P. aeruginosa* for up to several years. The process is repeated until a chronic infection is established. (Folkesson A et al, *Nature Reviews* 2012)

Genotypic and phenotypic diversification of *P. aeruginosa* occurs both in the lungs and in the paranasal sinuses, with emergence of alginate hyperproducing, mucoid isolates (Fig. 7) [101, 107, 108]. The most common mutations responsible for the mucoid conversion are found in *mucA*, which encodes an inner-membrane-associated anti-σ-factor [109, 110]. *MucA* normally limits the expression of the *algD* operon, which encodes the enzymes required for alginate synthesis, by sequestering the alternative RNA polymerase σ-factor σ^{22}, encoded by *algU* (also known as *algT*) [111-115]. Additionally, σ^{22} regulates a large number of stress response and virulence-associated genes and is involved in the regulation of virulence and motility (Fig. 8) [115-118]. The mucoid phenotype has been associated with biofilm mode of growth, increased endobronchial inflammation, increased antibody response and poorer lung function [119, 120].

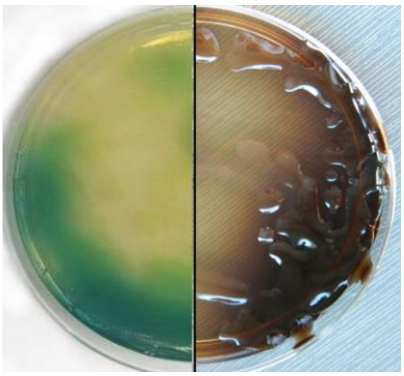

Figure 7. Typical morphology of non-mucoid (left) and mucoid (right) *P. aeruginosa* clinical isolates. Mucoid phenotype is due to alginate overproduction. (Verzè S., unpublished).

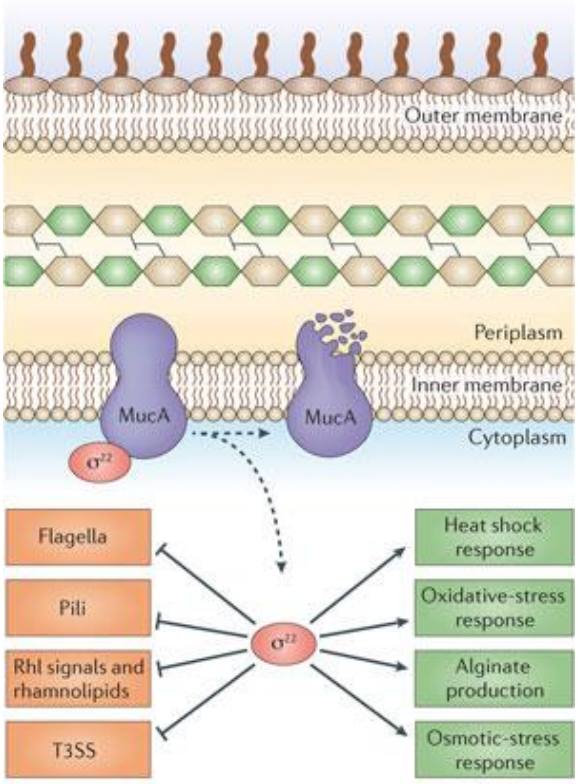

Figure 8. Regulation network of MucA–σ^{22}. The function of the RNA polymerase σ-factor σ^{22} is antagonized through protein–protein binding by the anti-σ-factor MucA. Mucoid *P. aeruginosa* isolates often carry knockout mutations in *mucA*, leaving σ^{22} free to activate transcription of many genes, such as those involved in alginate production and the responses to heat shock, osmotic stress and oxidative stress. σ^{22} also negatively regulates several virulence factors, including flagella, pili, the type III secretion system (T3SS), Rhl quorum sensing signals, as well as Rhl-controlled rhamnolipids. (Folkesson A et al, *Nature Reviews* 2012).

Infections by *P. aeruginosa* are difficult to treat because of its intrinsic ability to resist many classes of antibiotics as well as its ability to acquire resistance. Intrinsic resistance is due to the low permeability of its outer membrane, the constitutive expression of membrane efflux (Mex) pumps, and the natural occurrence of an inducible chromosomal β-lactamase, AmpC. Acquired resistance can result from genetic transfer of resistance genes, or mutations in antibiotic targets or genes regulating intrinsic resistance mechanisms. Adaptive resistance occurs when environmental stressing conditions cause a change in gene expression, resulting in upregulation of genes that can confer resistance [121, 122]. Development of resistance to antipseudomonal drugs is often seen in the non-mucoid isolates and has been associated with occurrence of hypermutability [123]. Acquisition of multidrug-resistant (MDR) *P. aeruginosa* was not found to be associated with decline of lung function in CF patients [124]; thus, MDR *P. aeruginosa* is rather a marker of advanced disease than the cause of it.

Interactions with other bacteria

Given the polymicrobial nature of CF lung infection, *P. aeruginosa* is often co-isolated with other microbial species sharing the same environment, both pathogens and commensals. In the case of chronic co-infections, this cohabitation can last for long time; thus, it is likely that *P. aeruginosa* and its neighbors residing in the same niche can engage interactions, potentially influencing the course of infection and therapies [90, 91].

P. aeruginosa interactions with classical main pathogens *Burkholderia spp.* and *S. aureus* have extensively been studied. Cooperation between *P. aeruginosa* and *B. cenocepacia* was reported: alginate production by *P. aeruginosa* mucoid phenotype contributes to *B. cenocepacia* persistence, co-infection of *P. aeruginosa* and *B. cenocepacia* in mice results in greater levels of biofilm formation and enhanced inflammatory response, polymyxin B-susceptible *P. aeruginosa* appears to benefit from the more resistant *B. cenocepacia* within the same population [125-127]. However, the two species also show competitive interactions: *P. aeruginosa* can inhibit *Burkholderia spp.* by S-type pyocin, a toxin with antibacterial activity [128]. Interestingly, the bactericidal activity of pyocin is greater in anaerobic conditions, and it is also active against cells in the biofilm mode of growth [129, 130]. Interactions between *P. aeruginosa* and *S. aureus* provide a potential explanation for the limited isolation of *S. aureus* in late-stage CF lung disease: *P. aeruginosa mucA* mutants compromise *S. aureus* growth, and *P. aeruginosa* elastase A and tetramic acids exhibit anti-staphylococcal activity [131, 132]. Furthermore, *P. aeruginosa* quinolone signals select for the highly antibiotic resistant *S. aureus* small colony variants, which are able to persist viable inside host cells [133]. This latter finding is supported by clinical data indicating that CF patients with methicillin-resistant *S. aureus* have poorer outcomes when associated with *P. aeruginosa* infection [134].

As regards interactions with emerging pathogens like *S. maltophilia* and *A. xylosoxidans*, the available information has lesser extent, mainly due to the recent identification of these microorganisms as important CF pathogens. Recently, *S. maltophilia* has been reported to have modulatory activity on *P. aeruginosa* virulence in mixed biofilm; further investigations will reveal the outcome of this interaction, which might confer selective fitness advantage to *P. aeruginosa* or, alternatively, increase its virulence leading to pulmonary exacerbation [135]. Up to date, studies about *P. aeruginosa* possible interactions with *A. xylosoxidans* lack, despite the frequent co-isolation of the two microorganisms from sputum samples and the increasing number of patients becoming chronically infected with *A. xylosoxidans* [81, 136, 137].

Virulence factors

Especially during early infection, *P. aeruginosa* expresses a wealth of virulence factors exhibiting strong pro-inflammatory properties (Fig. 9) [138].

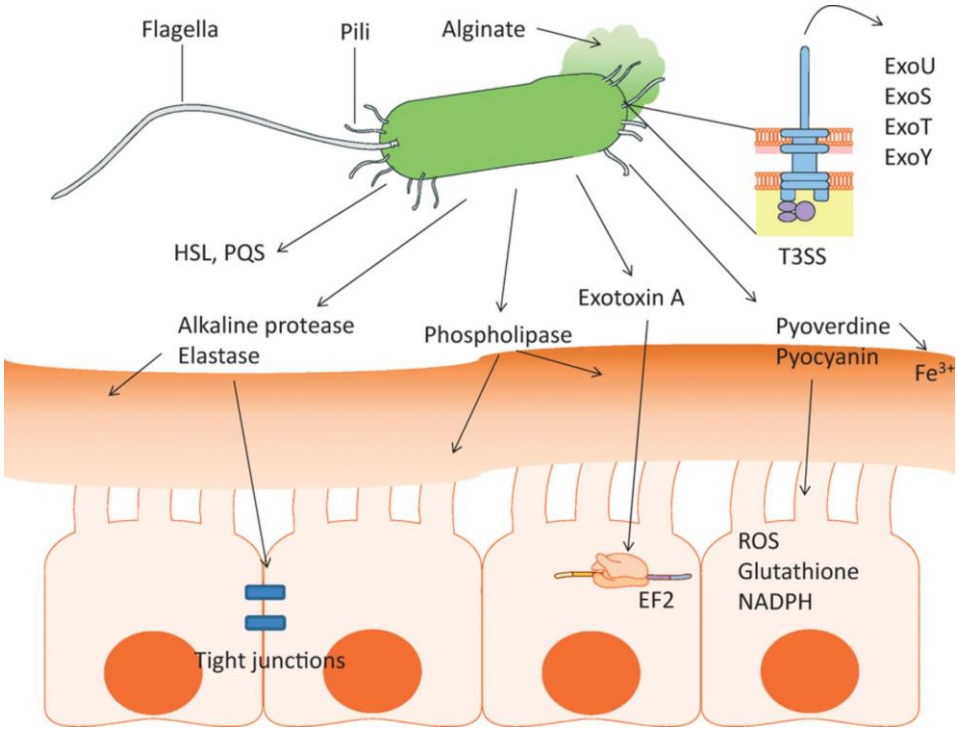

Figure 9. A multitude of virulence factors are produced by *P. aeruginosa*. Flagella and type 4 pili are the main adhesins, T3SS can inject cytotoxins directly into the host cell, and a wealth of secreted factors have various effects on host. (Gellantly SL and Hancock REW. *Pathogens and Disease* 2013).

Flagella and type 4 pili are the main means of motility and adhesion to host epithelial cells. Each *P. aeruginosa* cell possesses a single polar flagellum and several type 4 pili, also localized at a cell pole. The flagellum, responsible of swimming motility, can bind to host epithelial ganglioside asialoGM1 and can elicit a strong NFkB-mediated inflammatory response [139]. Many isolates from chronic infections demonstrate downregulation of flagella and flagella-mediated motility [140]. Type 4 pili are responsible of twitching motility and, together with flagella, facilitate swarming motility, a coordinated form of motility on semi-solid surfaces [141, 142]. Moreover, they contribute to formation of biofilms, promoting bacteria aggregation on target tissues [143, 144]. Pili are also involved in bacterial phagocytosis by macrophages, and pili-deficient mutants demonstrated reduced virulence [145].

Lipopolysaccharide (LPS) is a component of the outer membrane and has roles in antigenicity, inflammatory response, exclusion of external molecules, and in mediating interactions with antibiotics [146]. *P. aeruginosa* produces a three-domain LPS consisting of a membrane-bound lipid A, a core region, and a highly variable O-antigen. While penta-acylated lipid A form is predominant in laboratory strains, isolates from chronically infected CF lungs show hexa- and sometimes hepta-acylated species with increased inflammatory properties, and the extent of these modifications appears to increase with the severity of lung disease [147]. “O-specific” polysaccharide is an O-antigen variable which elicits a strong

antibody response [146]. Interestingly, many chronic *P. aeruginosa* isolates lose the expression of this variable over time [148].

Type 3 secretion system (T3SS) can inject toxins directly into host cells. As such, its expression is frequently associated with acute invasive infections and has been linked to increased mortality in infected patients [149, 150], while T3SS mutants displayed attenuated virulence [151]. Nearly all strains express one of the two major exotoxins exoU or exoS (rarely both) and minor exotoxins exoY and exoT [150, 152]. Recently, it was reported that nucleoside diphosphate kinase is also translocated into host cells by T3SS [153]. The exact contribution of each effector to pathogenesis is unclear, but it is thought that the T3SS may allow *P. aeruginosa* to exploit breaches in the epithelial barrier by antagonizing wound healing during colonization, and to promote cell injury [150].

Quorum sensing (QS) small membrane-diffusible molecules, called autoinducers, are the mediators of bacterial coordinated adaptation to the lung environment. These molecules are constitutively produced by each bacterium and act as cofactors of specific transcriptional regulators when they reach high enough threshold concentrations. When the bacterial population increases to a critical mass (i.e. “quorum”), the concentration of autoinducers becomes sufficient to cause activation of specific downstream genes, resulting in a coordinated response across the entire bacterial population. It is estimated that 10% of genes and more than 20% of the expressed bacterial proteome are regulated by QS [154]. *P. aeruginosa* produces three autoinducers: two acyl homoserine lactones (AHLs) and the *Pseudomonas* quinolone signal (PQS), regulated by Las and Rhl systems [154, 155]. Cell survival, biofilm formation, and virulence are controlled by these systems; thus, strains deficient in any of these systems show reduced pathogenicity [149, 156, 157].

P. aeruginosa secretes several proteases, which can degrade host complement factors, mucins, surfactant and disrupt tight junctions between epithelial leading to dissemination of the bacteria [156, 158, 159]. Alkaline protease (AprA) is a type 1-secreted zinc metalloprotease known for its degradation of host complement proteins and fibronectin [160]. It can also modulate inflammatory and immune responses by reduction of the bioavailability of several cytokines and inhibition of RANTES [161-164]. In a murine model of sepsis, AprA in combination with exotoxin A administered as an inactivated toxoid vaccine demonstrated significant protection against subsequent infection by *P. aeruginosa* [165]. Moreover, AprA has been shown to degrade free flagellin monomers, thereby helping *P. aeruginosa* to avoid immune detection [166]. Furthermore, AprA has been reported to proteolytically activate ENaC channel, contributing to alter fluid secretion and pathogens clearance in CF airways [167]. *P. aeruginosa* also produces two elastases, LasA and LasB, which are regulated by QS and secreted via type 2 secretion system [168, 169]. LasB is a metalloprotease that can degrade lung surfactant proteins A and D [170] and cause ruptures in the respiratory epithelium through tight-junction destruction, increasing epithelial permeability and facilitating neutrophil recruitment [171]. It can also decrease host immune response through alteration of key membrane receptors such as proteinase-activated receptor 2 and urokinase-type plasminogen activator receptor, and

inactivation of inflammatory cytokines such as TNF-α and IFN-γ [164, 172, 173]. Interestingly, *lasB* mutants are less virulent and more susceptible to phagocytosis [174]. LasA is a serine protease, thought to enhance the proteolytic activity of LasB [169, 175]. Another serine protease is protease IV, which can degrade complement proteins, immunoglobulins, and fibrinogen. Protease IV degradation of host surfactant proteins A and D inhibits the association of *P. aeruginosa* with alveolar macrophages, helping *P. aeruginosa* survival during infection [176].

The blue-green pigment pyocyanin causes host cells oxidative stress by disrupting mitochondrial electron transport and cellular protective mechanisms of host enzymes catalase, superoxide dismutase and glutathione peroxidase [177-179]. Purified pyocyanin can induce apoptosis in neutrophils as well as inhibit the phagocytosis of apoptotic bodies by macrophages [180-182]. It is also able to modulate IL-2, IL-8 and RANTES expression by airway epithelial cells and suppress cilia beating [183-187]. Moreover, pyocyanin is thought to play a protective role against the reactive oxygen and nitrogen species produced by phagocytic cells, to induce increased levels of neutrophil elastase, and to contribute to biofilm formation by promoting extracellular DNA release [188-191].

The siderophore pyoverdine is both able to sequester iron from host depots and to act as a signaling molecule. Iron chelation is a vital part of establishing infections, as the host environment has little free iron due to its own sequestration molecules. Iron-bound pyoverdine starts a cell-surface signaling cascade which directs the transcription of several genes involved in the regulation of exotoxin A, endoprotease, and pyoverdine itself [192, 193]. The dual function of pyoverdine in iron uptake and virulence renders this siderophore essential for *P. aeruginosa* infectivity, as demonstrated in different mouse models [194, 195]. Pyoverdine production was found to be influenced by several environmental signals and regulatory pathways, including oxygen and nutrient availability, oxidative stress, cellular aggregation [196, 197].

Exotoxin A inhibits host cell elongation factor 2 (EF2), thereby inhibiting protein synthesis and leading to cell death. It is also involved in repression of the host immune response and can induce apoptosis [198-200]. In the presence of iron ions, exotoxin A expression is upregulated by pyoverdine [193].

Lipase and phospholipase can target lipids in the lung surfactant and phospholipids in host cell membranes [156]. Surfactants degradation by phospholipase causes an increase in surface tension [201].

4.4. Achromobacter xylosoxidans

Infection

Achromobacter species are ubiquitous Gram-negative bacilli, widely distributed in aquatic environments and soil, increasingly found in nosocomial setting. They are opportunistic pathogens in certain populations, such as subjects with CF, where these microorganisms can survive for long time in both lower and upper airways [308]. Among CF patients, the most often isolated species is *A.*

xylosoxidans, whose chronic lung colonization has been associated with decline in respiratory function and lung inflammation [81, 308, 309]. Infection results either from acquisition from the environment or from direct/indirect transmission [310, 311], and is usually complicated by the innate and acquired multidrug resistance carried by these microorganisms. Approximately 50 drug-resistance associated genes have been predicted in *A. xylosoxidans* type strain, and a rich variety of mobile genetic elements carrying resistance genes have been identified in clinical isolates [312, 313]. All together, these features characterize *A. xylosoxidans* as an important emerging CF pathogen.

Virulence factors

Similar to other gram-negative pathogens, *Achromobacter* spp. express cell membrane-bound virulence factors, like the Vi capsular polysaccharide, involved in surface adhesion and protection from phagocytosis and toxins, and the O-antigen, which elicits host immune response [314]. LPS as well induces key inflammatory cytokines [315]. *A. xylosoxidans* is also equipped with various secretion systems that mediate the release of molecules to provide capability for invasion of the host cells [316, 317], but few is known about its exoproducts. Genome analysis showed the presence of genes encoding colicin V, a protein cytotoxic to similar bacteria, and AepA, involved in cellulase and protease regulation [316]. In addition, production of phospholipase C and ability to inactivate *P. aeruginosa* quinolone signal molecule were observed [318, 319]. Moreover, a heat-stable cytotoxic factor, associated with increase of pro-inflammatory cytokines in vitro, was identified [320]. Jakobsen and collegues also investigated the presence of secreted virulence factors known to be important for other CF pathogens like *P. aeruginosa*, but reported the absence of extracellular proteases, chitinase and rhamnolipids [316].

As regards the biofilm mode-of-growth, *Achromobacter* spp. is highly motile (swimming) via long, peritrichous flagella but lacks twiching motility, which is considered necessary for the development of surface-attached biofilm, as it probably contributes to stabilize interactions with the surface [321]. Indeed, poor adhesion ability in vitro was reported [316]. Reduction of surface attachment over time of infection was also shown in sequential CF clinical isolates, in association with acquisition of mutations in genes with a presumptive role in surface adhesion [317, 322]. However, a recent study from Nielsen and collegues highlighted *Achromobacter* spp. ability to form unattached or loosely attached aggregates, held together by polysaccharides forming a peripheral shell around the bacterial cells [322].

4.5. Anti-inflammatory therapy in cystic fibrosis

Macrolides

Macrolide antibiotics are 14-, 15-, and 16-member lactone monocycles, known to have antibacterial properties (Fig. 10). They bind to the 23S rRNA in the 50S subunit of the bacterial ribosome, thereby inhibiting protein synthesis and bacterial growth [202]. In addition, 14- and 15-members have also

immunomodulatory effects. They act through different mechanisms at the level of the immune system, ultimately interfering with immune activation and cytokines production (Fig. 10) [203, 204].

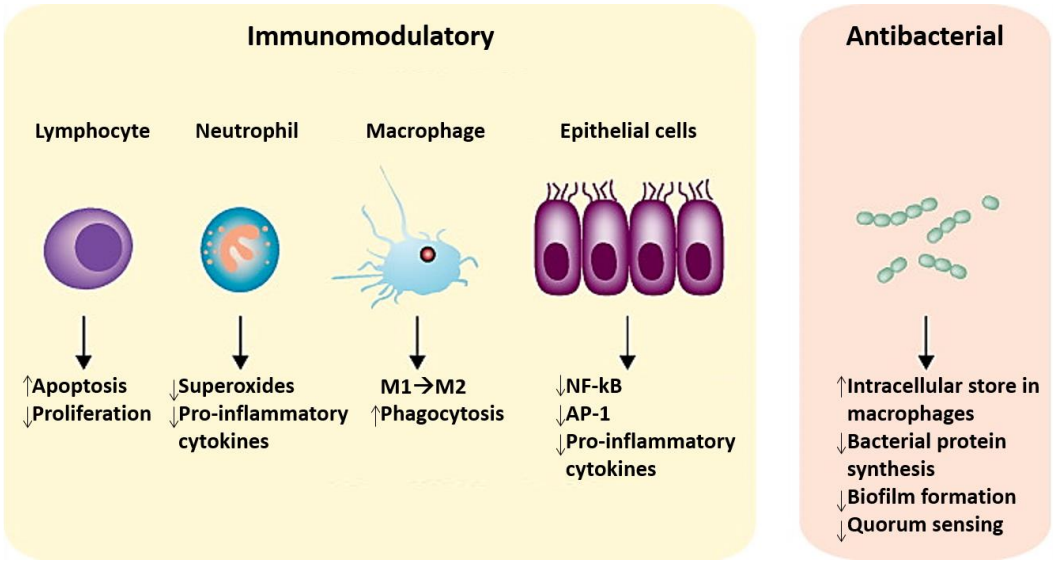

Figure 10. Immunomodulatory and antibacterial activity of macrolides. On the host side, macrolides induce macrophages activation, downregulate lymphocytes, and reduce the release of pro-inflammatory cytokines from neutrophils and epithelial cells. On the bacterial side, they favor phagocytosis and downregulate protein synthesis and biofilm formation mainly by interfering with quorum sensing system. (Wong EH et al. *Lancet Respiratory Medicine* 2014).

Azithromycin is a 15-member macrolide widely used as low-dose continuous treatment in *P. aeruginosa* chronically infected patients. Although it has no bactericidal activity against *P. aeruginosa*, several clinical investigations have revealed that azithromycin treatment improves respiratory function and reduces the occurrence of pulmonary exacerbations and the frequency of courses of antibiotic therapies [205-208]. It has also been demonstrated that the amounts of neutrophils and some plasma inflammatory markers are significantly reduced by azithromycin treatment; these changes are associated with the improvement of respiratory function [209, 210]. Although the mechanisms are still not clear, it is thought that azithromycin beneficial effects are due to a combination of anti-pseudomonal and immunosuppressive activity [211]. Sub-inhibitory azithromycin concentrations can downregulate protein synthesis in *P. aeruginosa* and suppress motility and production of several virulence factors, including proteases, pyocyanin, exotoxin A, phospholipase C, and EPS [212-219]. Azithromycin also interferes with QS system, down-regulating the expression of many QS-dependent genes, as those encoding pili, flagellum, and oxidative stress response proteins [220-222]. Moreover, azithromycin can increase *P. aeruginosa* susceptibility to serum bactericidal activity, probably by altering lipopolysaccharides and outer membrane proteins, and to some antimicrobials, and promote killing of stationary-phase and biofilm-forming cells [223-227]. Azithromycin has also anti-inflammatory effects independent from its anti-virulence activity, since it can

reduce various serum inflammatory markers and increase pulmonary function in non-infected patients, although with less extent than in chronically infected patients [209, 210, 228]. Beneficial effects have so far been documented in CF patients treated with azithromycin for up to 6 months, while reduced efficacy was associated with longer treatment duration, probably due to development of bacterial resistance to its anti-virulence activity [228, 229].

Clarithromycin is a 14-member macrolide known to modulate pro-inflammatory cytokine expression, probably due to downregulation of NF-κB and other pro-inflammatory pathways [48, 230, 231]. Clarithromycin treatment was evaluated in several chronic respiratory diseases characterized by airways inflammation. Low-dose clarithromycin demonstrated clinical effectiveness in treating diffuse panbronchiolitis (DPB), which shares many similarities in clinical and pathological characteristics with CF and is often treated with erythromycin, another 14-membered macrolide [232-234]. In patients with bronchiectasis, clarithromycin treatment decreased inflammatory cytokines and leukocytes number in BALF, exhaled breath condensate and peripheral blood [231, 235]. Moreover, short term clarithromycin administration demonstrated to reduce chronic airways hypersecretion [236]. Different studies evaluating clarithromycin therapy in CF patients were conducted, reporting contrasting results. In a study in which patients were treated with 250 mg clarithromycin on alternate days for a year, the treatment resulted in a marked reduction of cytokine levels in both sputum and plasma as well as a significant improvement in both FEV1 and FVC [237]. In contrast, in two studies examining daily administration of 500 mg clarithromycin, there was no significant difference in the pulmonary function, in neutrophils number and inflammatory cytokines in the sputum after the treatment [238, 239]. In an additional study using 15 mg/kg/day clarithromycin for 3 months, the treatment led to a decrease in acute pulmonary exacerbations and improvement in clinical status, but it did not cause a significant fall in inflammatory cytokines in the BALF of CF patients [240]. Although low-dose clarithromycin might be more effective as supported by its low-dose (200 mg/day) benefits in treatment of DPB [232], the comparison of the outcomes of these studies is limited by the different treatment regimens, drug doses and formulations, and clinical factors evaluated; thus, further trials are necessary to assess the effects of clarithromycin treatment in CF patients. As regards *P. aeruginosa* infection, clarithromycin has no bactericidal activity against the microorganism, like other macrolides. Nonetheless, it showed to have inhibitory activity against *P. aeruginosa* protease expression, twitching motility and biofilm maturation, promoting biofilm permeability and favoring penetration of other antimicrobial agents like ciprofloxacin and tobramycin [217, 241-248]. Clarithromycin formulation as dry powder inhaler (DPI) for aerosol administration is currently under investigation [249, 250]. At present, the only antibiotic available as DPI is tobramycin; therefore, clarithromycin-tobramycin local co-administration in the airways represents an interesting therapy for the treatment of chronic *P. aeruginosa* pulmonary infection [251].

Protease inhibitors

Excessive and dysregulated secretion of host and bacterial proteases in the CF lung strongly contribute to exacerbation of the inflammatory response and lung damage (Fig. 11). Although the main source of protease activity is thought to be activated neutrophils, it became evident that exogenous *P. aeruginosa* proteases disrupt key host processes by several means such as activation of cascade pathways, disruption of cytokine signaling, inactivation of cell receptors and host protease inhibitors [252]. Therefore, protease-inhibiting molecules could target the damaging effects of bacterial secreted proteases limiting host inflammatory response and lung damage.

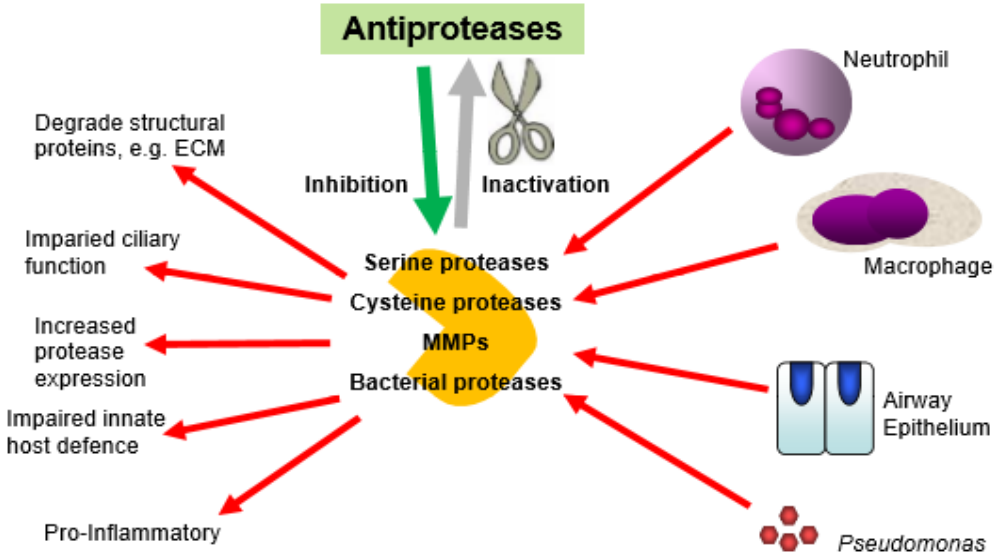

Figure 11. Proteases in CF airways. The overwhelming of the airway innate anti-protease shield by excessive and dysregulated secretion of host and bacterial proteases in the CF lung leads to exacerbation of the inflammatory response and lung damage. (Quinn DJ et al, *The Open Respiratory Medicine Journal* 2010).

The most potent protease inhibitors are hydroxamate-based broad spectrum matrix metalloprotease (MMP) inhibitors, which mimic collagen structure, thus binding to the enzyme active site and inactivating it by chelation of the catalytic zinc ion. Interestingly, their inhibitory effect can apply also to bacterial metalloproteases, as it has been demonstrated by Ilomastat (Galardin, GM6001) ability to inhibit thermolysin and *P. aeruginosa* elastase [79, 253-257]. Ilomastat is under evaluation as treatment for sulfur mustard inhalation injury and chemical burns, ocular implantation, dental caries, and as inhaled treatment for chronic obstructive pulmonary disease [258-262]. Several MMP inhibitors also entered clinical trials as anticancer agents during the 90's, but their clinical performance was disappointing [263, 264]. The first MMP inhibitor to be clinically tested was Batimastat, an injectable drug. Although effective for malignant ascites and malignant pleural effusion, due to its poor solubility and very low oral bioavailability trials were stopped during phase III in favor of the newer, orally available analogue Marimastat [265, 266]. During clinical trials Marimastat showed a favorable pharmacokinetic profile, high systemic bioavailability, linear dose-plasma relationship, balanced excretion (75% hepatic, 25% renal), an

elimination half-life compatible with twice-daily dosing, and modest efficacy in delaying disease progression; however, significance could not be established due to dose-limiting toxicity, identified with appearance of musculoskeletal symptoms reversible upon drug discontinuation [264, 267-269].

Targeting of bacterial proteases involved in chronic infection processes such as dysregulation of the inflammatory response would be a useful addition to CF therapeutic treatments. Furthermore, unlike traditional antibiotics which target fundamental processes thereby creating enormous selection pressures, anti-protease therapy should be less likely to result in the generation of resistant pathogens [252].

4.6. Mouse models for studying CF lung inflammation

CF models

CF animal models are powerful tools that enable the study of the mechanisms and complexities of human disease. Murine models have several intrinsic advantages compared with other animal models, including lower cost, maintenance, and rapid reproduction rate. Up to date, eleven CF transgenic or knockout mouse models have been characterized (Tab. 1) [270]. With an overall aminoacid sequence homology of 78% between murine and human CFTR, these models have facilitated significant strides in our understanding of this complex disease. The first loss-of-function null murine model (CFTRtm1UNC) was generated by insertion of a stop codon in exon 10 of the CFTR coding sequence, termed S489X mutation, in embryonic stem cells [271]. Following this model, many others knockout models were developed on various genetic backgrounds (CFTRtm1CAM, CFTRtm1HSC, CFTRtm3BAY, CFTRtm3UTH, CFTRtm1HGU, CFTRtm1BAY) [272-275, 286]. To overcome the limitations imposed by the severe intestinal disease presented by many knockout strains, "gut-corrected" hybrid strains were created using a transgene expressing CFTR from a promoter specific for the intestinal epithelium [307]. In addition to the CF knockout models, various knock-in mutants were also developed. Specific CF-causing mutations were introduced in the endogenous mouse CFTR gene to bear mice carrying the class II ΔF508 (CFTRtm1EUR, CFTRtm1KTH, CFTRtm2CAM) and G480C (CFTRtm3HGU) mutations, the class III G551D (CFTRtm2HGU) mutation, and the class IV R117H (CFTRtm2UTH) mutation [276-280, 286]. However, intra-mutant variations in the survival, disease severity, and pathology of these animals have been reported. Although not a typical CFTR murine model, the β-ENaC mouse model has also been considered. The channel, in concert with CFTR-mediated chloride secretion, plays an important role in the proper regulation of ASL volume and in the adequate clearance of inhaled microorganisms and environmental particulates by the mucociliary system [281].

Table 1. CF mouse models

Identifier	Mutation	References
CFTR^{tm1UNC}	Exon 10 replacement	[271]
CFTR^{tm1CAM}	Exon 10 replacement	[272]
CFTR^{tm1HSC}	Exon 1 replacement	[275]
CFTR^{tm3BAY}	Exon 2 replacement	[274]
CFTR^{tm3UTH}	Exon 4 replacement	[286]
CFTR^{tm1HGU}	Exon 10 insertion	[286]
CFTR^{tm1BAY}	Exon 3 insertion	[273]
CFTR^{tm2CAM}	ΔF508, exon 10 replacement	[278]
CFTR^{tm1KTH}	ΔF508, exon 10 replacement	[277]
CFTR^{tm1EUR}	ΔF508, exon 10 insertion (hit and run)	[276]
CFTR^{tm2HGU}	G551D, exon 11 replacement	[280]
CFTR^{tm3HGU}	G480C, exon 10 insertion (hit and run)	[279]
CFTR^{tm2UTH}	R117H, exon 4 replacement	[286]
Tg(FABPCFTR)	Transgene expressing *CFTR* in intestinal villus epithelia	[307]
Tg(CCSPScnn1b)	Transgene expressing *Scnn1b* in airway surface epithelia	[281]

Lung disease in CF models

While the upper respiratory tract of the murine models is representative of the upper airways of humans with CF, the lower airways represent an entirely different picture. No CFTR mouse model develops spontaneous lung inflammation without challenge, limiting their usefulness in the study of pulmonary disease progression in CF [271-273, 275-277, 279, 280, 282]. The lack of severe spontaneous lung pathology in these mouse models has been partially attributed to the expression of a non-CFTR calcium-activated chloride channel (CaCC) in certain mouse tissues: its expression might rectify the ion imbalance underlying CF lung disease. Only a congenic strain of the CFTR^{tm1UNC} mouse model, termed B6-CFTR^{tm1UNC}, in which the murine-expressed alternative chloride channel is absent, was reported to develop spontaneous lung disease including impaired mucociliary clearance and tissue fibrosis even when bred in a pathogen-free environment. These congenic mice also displayed impaired control of *P. aeruginosa* infection [283, 284]. The development of chronic pulmonary inflammation and bacterial persistence has been reported in the CFTR^{tm1UNC}

model following intranasal challenge with *B. cepacia*, with increased neutrophil counts and cytokine levels [285]. Significant pulmonary inflammation and associated pathology were also induced in $CFTR^{tm1UNC}$ mice following intratracheal delivery of *P. aeruginosa*-embodied agarose beads [286]. Furthermore, low ATP12A proton-pump expression levels in CF mice may allow for normal ASL pH and unimpaired airway host defenses. Such findings may explain why CF mice exhibit increased protection from pulmonary infection [287].

Lung inflammation: methods and models

In vivo studying lung inflammation is essential for the development of new therapies and for the characterization of the pathological processes. Frequently in mouse models, inflammation is induced by invasive lung challenge with bacterial cells or bacterial products with pro-inflammatory activity such as LPS. Inflammation is then monitored by recovery of BALF from the killed animals and by analyzing the presence of inflammatory markers such as immune cells and cytokines. Thus, the conventional assessments of inflammation in mice often rely on invasive ex vivo measurements which cause the death of the animal and are consequently particularly onerous when expensive transgenic mice are utilized. Moreover, when applied to CF transgenic mice this protocol may not be fully reproducible, probably due to the heterogeneity of airway inflammation in CF. Furthermore, although this approach is extensively used and highly validated, it precludes the possibility to repeat longitudinally the assessment of test animals [288-290]. However, in vitro and in vivo new protocols in animal models have been used to study the mechanism of lung inflammation in chronic diseases and to evaluate the anti-inflammatory role of some candidate molecules [291, 292]. Recently emerging non-invasive imaging technologies such as magnetic resonance imaging (MRI), micro-CT and optical imaging have been applied to longitudinal monitoring of airway remodeling and inflammation in murine models [293-296]. The clinical imaging system used in MRI, CT and PET, have been further adapted to murine models of asthma [293, 297-299], to serve as a preclinical and translational step between basic discovery and clinical practice, whereas optical imaging technologies developed in experimental settings may also slow-down their way into the clinical practice, especially in the context of intra-operative activities [300, 301]. Recently, a mouse model transiently expressing the luciferase reporter gene under the control of a bovine IL-8 promoter has been generated. Although mice do not express IL-8 or a clear homologous, the cell signaling and transcriptional apparatus could specifically activate the exogenous IL-8 promoter [302].

5. Objectives

The main objective of this study was to evaluate some aspects of *P. aeruginosa* interaction with both CF host and other co-infecting microorganisms, like the emerging pathogen *A. xylosoxidans*.

To this purpose, the thesis is divided in two projects:

- Regarding *P. aeruginosa* interaction with host, we studied *in vivo* lung inflammation induced by *P. aeruginosa* exoproducts, and evaluated the anti-inflammatory effects of molecules inhibiting the synthesis/activity of *P. aeruginosa* secreted virulence factors, to better understand their role in CF lung inflammatory disease. For this study, an innovative in vivo imaging approach was developed and applied to CF animals.

- About *P. aeruginosa* interactions with co-infecting microorganisms, we observed inter-species interactions between *P. aeruginosa* and *A. xylosoxidans* longitudinal isolates chronically co-infecting the same patient, in order to investigate the possible competitive/synergistic effects of their long-term cohabitation and the role of bacterial interactions on their survival and persistence in the human host.

6. PROJECT 1 - ROLE OF *P. AERUGINOSA* VIRULENCE FACTORS ON LUNG INFLAMMATORY RESPONSE: AN IN VIVO IMAGING APPROACH

In the present study, using non-invasive imaging techniques we monitored mouse lung inflammation induced by virulence factors released by *P. aeruginosa* and evaluated the anti-inflammatory action of molecules inhibiting the synthesis/activity of bacterial factors involved in pathogenicity. The mouse model here used allowed to detect in vivo the activation of an exogenous bovine IL-8 promoter via a luciferase reporter, responsible of bioluminescence emission. Although mice do not bear a clear IL-8 homologous, activation of the exogenous promoter could be detected in different mouse strains.

6.1. Materials & Methods

Bacterial strains

Two *P. aeruginosa* clinical isolates were selected, VR1 and VR2. The strains were isolated from sputum samples from two intermittently infected patients followed at the Cystic Fibrosis Center of Verona. Strains were stored in Microbank™ (Pro-Lab Diagnostics, Neston, UK) at -80°C.

Minimum inhibitory concentration assay

P. aeruginosa strains were streaked on Blood Columbia agar plates (Oxoid, Milan, Italy) and incubated at 37°C for 24-48 hours. 1-2 colonies were inoculated in 10 ml LB (Luria-Bertani) broth shaking at 37°C for 16 hours. OD_{600} was measured, cultures were diluted to 0.1 OD/ml and inoculated in 96-wells microtiter plates with increasing concentrations of azithromycin and clarithromycin. Plates were incubated at 37°C for 16 hours and OD_{600} was measured. The minimum inhibitory concentration value corresponds to the lower dose of antibiotic causing a complete inhibition of the culture turbidity.

Bacterial growth and culture supernatant collection

P. aeruginosa strains were streaked on LB or TSA (tryptic soy agar) plates and incubated at 37°C for 24-48 hours. 1-2 colonies were inoculated in 30 ml LB, KB (King's broth) or TSB (tryptic soy broth) shaking at 37°C for 16 hours. OD_{600} was measured and cultures were diluted to 0.1 OD/ml in 30 ml of the same medium, with/without sub-MIC azithromycin (8 µg/ml) or clarithromycin (45 µg/ml). After shaking at 37°C for 16 hours, cultures were diluted to 0.2 OD/ml and centrifuged at 7000 g for 30 min at 4°C. Supernatants were collected and sterile-filtered.

Virulence factors measurement:

- *Pyocyanin*

Pyocyanin was chloroform-extracted from LB supernatants. Briefly, 3 ml chloroform were added to 5 ml supernatant, and the lower phase was mixed with 1 ml 0.2 M hydrogen chloride. OD_{530} was measured in the upper phase and pyocyanin concentration was calculated by multiplying for its ε^{-1} (17,072 µg/ml cm) and normalizing for the optical distance.

- *Pyoverdine*

OD_{405} of KB culture supernatants was measured and pyoverdine concentration was calculated using its ε (19 mM^{-1} cm^{-1}) and normalizing for the optical distance.

- *Proteases*

Protease activity in TSB culture supernatants was determined by azocasein assay. Briefly, 350 µl reaction mixture containing 0.1 M Tris-HCl, pH 8.0, and 1% azocasein (Sigma-Aldrich, previously resuspended in 0.5% $NaHCO_3$) was added to 150 µl supernatant, with/without protease inhibitors (Ilomastat, Marimastat, Batimastat), and incubated at 37°C for 20 minutes shaking. After addition of 1 ml 7% ice-cold perchloric acid, the solution was centrifuged. 150 µl 10 N sodium hydroxide were added to the clear supernatant and OD_{430} was measured. One protease unit was calculated as the amount of enzyme producing an increase of 0.1 OD per hour.

- *Metalloproteases*

Metalloprotease activity in TSB culture supernatants was assayed by gelatin zymography. 20 µl of supernatant in non-reducing sample buffer (0.125 Mm Tris base pH 6.8, 1.25% SDS, 5% glycerol, trace bromophenol blue) were loaded in a polyacrylamide gel containing 0.1% gelatin. The gel was run at 200 V, 14 mA for 1-1.5 hours, washed twice in 2.5% Tryton X-100 for 20 minutes shaking and incubated in renaturing buffer (10 Mm Tris-HCl pH 7.5, 1.25% Triton X-100, 5 mM calcium chloride, 1 µM zinc chloride) at 37°C for 16 hours shaking. After Coomassie Blue staining and water destaining, areas of degradation appeared as clear bands against a dark background.

- *Alkaline protease*

Alkaline protease in TSB culture supernatants was quantified by western blot using a specific anti-AprA antibody (kind gift of Prof. Gerd Döring, University of Tubingen, Germany). 20 µl of TCA-precipitated supernatant in reducing sample buffer (0.05 mM Tris base pH 6.8, 1 % SDS, 5% glycerol, 5% β-mercaptoethanol, trace bromophenol blue) were run in a polyacrylamide gel at 200 V, 14 mA for 1.5 hours. Proteins were then transferred on a PVDF membrane at 100 V, 120 mA for 1 hour. The membrane was blocked for 1 hour shaking in 5% BSA, then incubated overnight with the anti-AprA primary antibody at 4°C shaking. After 1 hour incubation with anti-rabbit secondary antibody, chemiluminescent images were acquired using ECL Western Blotting Substrate (Promega, Milan, Italy). Total proteins were quantified by electrophoresis in a polyacrylamide gel in reducing conditions and Coomassie Blue staining.

Supernatant concentration

TSB supernatants were concentrated using 30 kDa cut-off Amicon Ultra-15 centrifugal filter units (Merck Millipore, Tullagreen, Cork, Ireland) pre-coated with 10 mg/ml bovine serum albumin. Concentrate was centrifuged at 27.000 rpm to remove cell debris, supernatant was sterile-filtered and stored at -20°C.

Reporter construct

Eukaryotic cells and experimental animals were transfected with the bIL-8-Luc construct, containing the luciferase gene under the control of bovine IL-8 promoter (kind gift of Prof. Gaetano Donofrio, University of Parma, Italy). Plasmid was transformed in competent *E. coli* DH5α cells by heat shock and purified by Qiagen Plasmid Maxi Kit (Qiagen) followed by phenol:chloroform extraction with precipitation in isopropanol and 70% ethanol. Plasmid identity was verified by KnpI digestion and agarose gel electrophoresis. Concentration and purity were measured using NanoDrop 2000c spectrophotometer.

Eukaryotic cells

Mouse lung adenoma LA-4 cells were cultured in Dulbecco's modified essential medium (DMEM, Lonza) with 2 mM L-glutamine and 10% fetal bovine serum, and detached with 0.25% trypsin-EDTA. Cell culture plates or flasks were incubated at 37°C with 5% CO_2 in humidified atmosphere.

Cell transfection

LA-4 cells were plated in 24-wells plates (30.000 cells/well) and grown overnight. 80% confluent cells were transfected with bIL-8-Luc construct alone or co-transfected with bIL-8-Luc and pEGFP-C3 constructs (9:1 ratio) using Lipofectamine 2000 (Thermo Fisher Scientific). Briefly, 500 ng/well DNA and 1.5 µl/well Lipofectamine were separately diluted in DMEM medium, mixed, incubated at room temperature for 5 minutes and added to the cells (50 µl/well).

Reporter assays

BIL-8-Luc transfected LA-4 cells were treated with 50 µl culture supernatant and luminescence was recorded using Luciferase Assay System (Promega). Briefly, cells were lysed with 100 µl 1X cell culture lysis reagent for 5 minutes, centrifuged at 12.000 g for 2 minutes at 4°C and supernatant was collected. In 96-wells plates, 100 µl/well luciferase assay reagent (LAR) were added to 20 µl/well lysis supernatant and the light produced was measured using Victor2 microplate reader (Perkin Elmer). Prior to LAR addition, EGFP fluorescence in lysate supernatant was recorded (excitation 485 nm, emission 535 nm) as cells vitality control. Alternatively, 150 µg/ml D-Luciferin (Perkin Elmer) was added to the alive cells directly in the 24-wells plates and, after 10 minutes, bioluminescence was recorded using IVIS Lumina (Caliper Life Sciences).

Experimental animals

Female BalbC (7-8 weeks old) mice were purchased from Harlan Laboratories Italy (San Pietro al Natisone, Udine, Italy). Female congenic C57BL/6J WT and gut-corrected $CFTR^{tm1UNC}$ (8-10 weeks old) mice were purchased from Cystic Fibrosis animal Core facility (San Raffaele Hospital, Milan, Italy). Animals were maintained under conventional housing conditions. Prior to use, animals were acclimatized for at least 5-7 days to the local vivarium conditions, having free access to standard rodent chow and tap water.

In vivo gene delivery

In vivo JetPEI (Polyplus Transfection) was used as carrier for delivering bIL-8-Luc construct to lung tissue. DNA and JetPEI were mixed with a final N/P ratio of 7-7.5 following manufacturer's instructions. Briefly, 38-42 µg DNA and 5.3-6.3 µl JetPEI were separately diluted in 200 µl 5% glucose, mixed, and incubated at room temperature for 15 minutes. 400 µl/mouse of the mixture were intravenously injected through the tail vein after warming the animals for 5 minutes under a heating lamp. Expression and inactivation of the reporter were monitored by in vivo imaging after 24 hours and 7 days, respectively.

Intratracheal challenge

Starting 7-10 days and until 30 days after in vivo gene delivery, bIL-8-Luc transiently transgenic mice were intratracheally challenged with TSB culture supernatant. Briefly, mice were anesthetized with 2.5% isoflurane and placed on an intubation platform hanging by their incisor teeth. After visualization of the opening of the trachea using a laryngoscope, 50 µl supernatant were instilled by an intubation tube connected to a pressure control system. After 4, 24 and 48 hours, reporter activation was monitored by in vivo imaging.

In vivo bioluminescence imaging

Bioluminescence imaging of experimental animals was performed using IVIS Lumina imaging system (Caliper Life Sciences, Alameda, CA). 10 minutes prior to bioluminescence recording, mice were anesthetized with 2.5% isoflurane and intraperitoneally injected with 150 mg/kg D-Luciferin (Perkin Elmer). After 5 minutes-long luminescence recording, photons emitted from chest region were quantified using Living Image software (Caliper Life Sciences, Alameda, CA).

Bronchoalveolar lavage fluid analysis

Trachea was cannulated with an 18-gauge catheter. 5 ml sterile phosphate buffer saline were instilled in the bronchial tree and collected. After red blood cells lysis (in 0.2% sodium chloride for 20 seconds followed by addition of 1.2% sodium chloride) and centrifugation at 400 g for 10 minutes, supernatant was frozen at −80 °C for quantification of multiple cytokines/chemokines using a Bio-Plex™ Cytokine Assay Kit (Bio-Rad Laboratories, Segrate, Milan, Italy), and the cell pellet was resuspended in PBS. After cells count, 50.000 cells were cytocentrifuged and stained with May-Grunwald and Giemsa for differential count. The number of cells per animal was calculated as the number of cells per ml of BALF multiplied for the volume used for the resuspension of the cells pellet.

Statistical analysis

Statistical analysis was performed using GraphPad Prism software. Virulence factors concentration and LA-4 cells bioluminescence emission were analyzed by t-test or 1way ANOVA, and mice bioluminescence, cell counts and cytokines were analyzed by 1way or 2way ANOVA.

6.2. Results

P. aeruginosa virulence factors induce bovine IL-8 promoter activation

To set up a convenient, non-invasive method for in vivo imaging of lung inflammation, we evaluated the expression of a construct containing a luciferase reporter gene under control of bovine IL-8 promoter (bIL-8-Luc). Culture supernatant containing *P. aeruginosa* exoproducts, collected from the virulent CF clinical isolate VR1, was used to verify the activation of the exogenous IL-8 promoter both in vitro and in vivo. LA-4 murine lung adenoma cells were transfected with bIL-8-Luc construct, and treated with different concentrations of VR1 culture supernatant. The treatment induced a concentration-dependent bioluminescence emission, significantly higher in comparison to the control (tryptic soy broth culture medium, TSB) when using 10X-concentrated supernatant (Fig. 12A). As a vitality marker, cells were co-transfected with a construct containing enhanced Green Fluorescent Protein (GFP) gene under the control of a constitutive promoter. After challenge with culture supernatant, fluorescence emission was similar in treated and non-treated cells, confirming the same cellular vitality among the different treatment conditions (Fig. 12B).

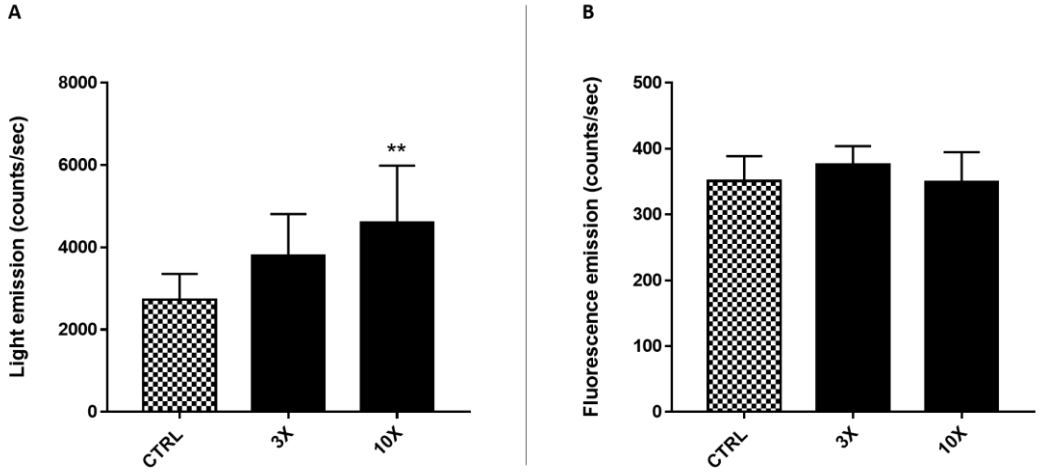

Figure 12. Light (A) and fluorescence (B) emission from bIL-8-Luc:eGFP co-transfected LA-4 cells treated with 3X and 10X concentrated VR1 culture supernatant. TSB was used as control. Each value represents the mean ± SD of 3 experiments. Statistical analysis was performed by 1way ANOVA followed by Dunnett's multiple comparisons test, ** $p<0.01$ vs. control.

In bIL-8-Luc-transgenic BalbC mice, intratracheal instillation with different concentrations of VR1 culture supernatant induced bioluminescence emission in the lungs area (Fig. 13A). The photon emission was concentration-dependent and the maximal increase was reached with the 10X-concentrated supernatant (Fig. 13B). Indeed, 30X-concentrated supernatant did not induce a further increase, indicating a saturation of the system with the 10X concentration, which was selected to be used for the following experiments.

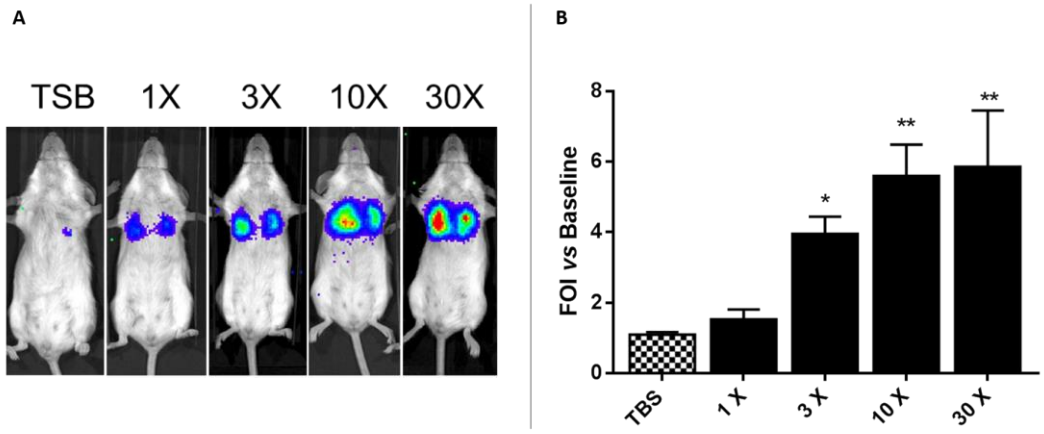

Figure 13. Representative images of bIL-8-Luc-mediated bioluminescence emission in BalbC mice 24 hs after instillation with increasing concentrations of VR1 culture supernatant (A). TSB was used as control. Photons emission expressed as folds of increase (FOI) over baseline (B). Each value represents the mean ± SEM of 3 animals. Statistical analysis was performed by 1way ANOVA followed by Dunnett's multiple comparisons test, * $p<0.05$ and ** $p<0.01$ vs. control.

Inhibition of P. aeruginosa virulence factors by azithromycin decreases mice lung inflammation

VR1 strain was grown in presence of 8 µg/ml azithromycin, a sub-inhibitory dose consistent with the range reported in the lungs of CF patients undergoing azithromycin therapy [305]. Growth of bacteria in presence of the macrolide reduced pyocyanin, pyoverdine and proteases levels in VR1 culture supernatant (Fig. 14A), confirming the known inhibitory effect of azithromycin on the synthesis of virulence factors. Particularly, inhibition of metalloprotease activity and alkaline protease (AprA) expression was detected in both culture supernatant and bacterial lysate (Fig. 14B), supporting that azithromycin interferes with metalloproteases synthesis. On the contrary, another *P. aeruginosa* CF clinical isolate, named VR2, was characterized by low levels of secreted virulence factors (Fig. 14A), and no metalloprotease activity/expression was detectable in its supernatant nor in the lysate (Fig. 14B). No significant difference in pyocyanin, pyoverdine and proteases levels was detected between supernatants from VR2 grown in absence or presence of 8 µg/ml azithromycin (VR2+AZM).

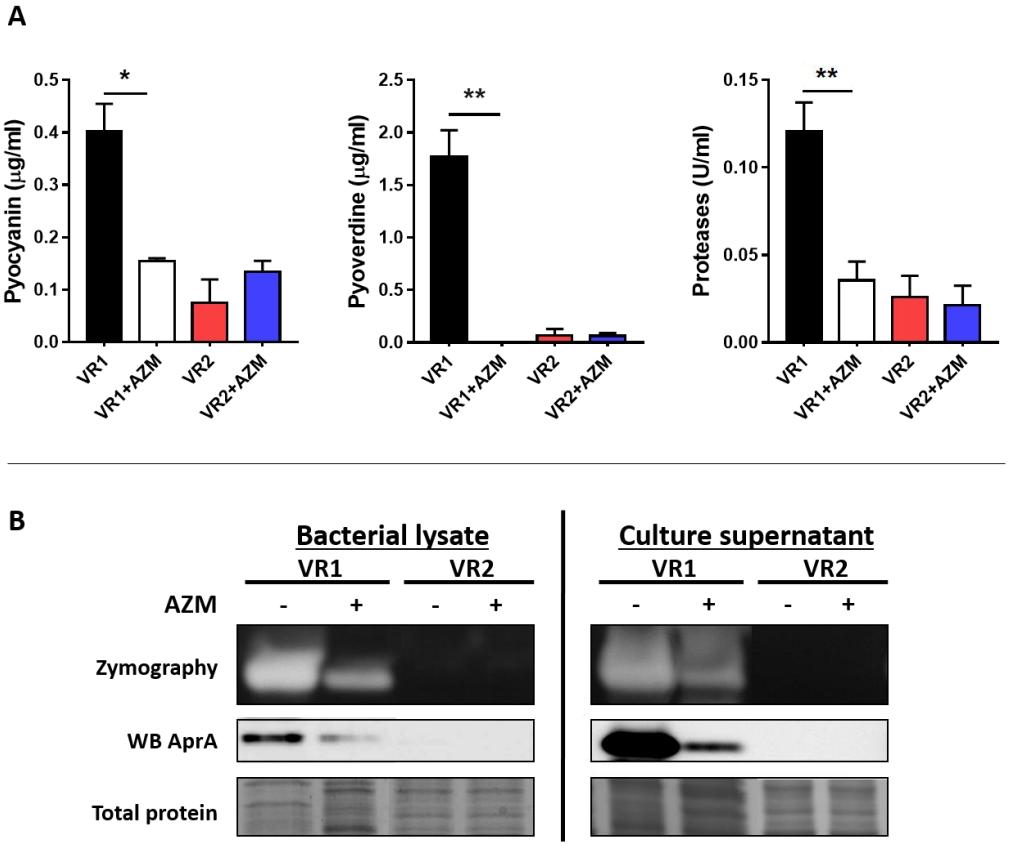

Figure 14. Pyocyanin, pyoverdine and proteases concentration in culture supernatants from VR1 and VR2 isolates grown in presence/absence of azithromycin (AZM) (A). Each value represents the mean ± SEM of 3 experiments. Statistical analysis was performed by 2-tailed t test, * $p<0.05$ and ** $p<0.01$. In both bacterial lysates and culture supernatants, metalloprotease activity and AprA expression were measured by zymography and western blot, respectively (B). Total proteins were quantified by electrophoretic separation on polyacrylamide gel.

In LA-4 cells transfected with bIL-8-Luc construct, treatment with culture supernatant collected after VR1 growth in presence of azithromycin (VR1+AZM) induced a significantly lower bioluminescence emission in comparison to supernatant from non-treated VR1 (Fig. 15). This preliminary in vitro result suggests that the anti-virulence activity of azithromycin might be involved in its anti-inflammatory effect.

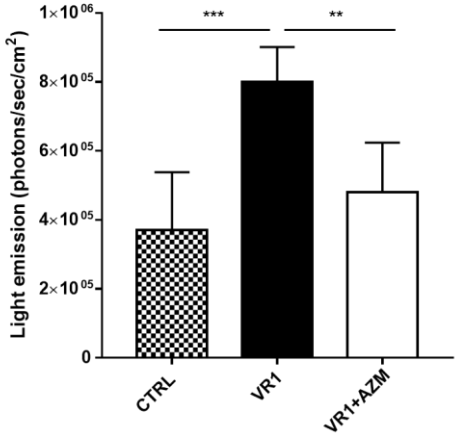

Figure 15. Light emission from bIL-8-Luc transfected LA-4 cells treated with 10X concentrated culture supernatant from VR1 isolate grown in presence/absence of 8 µg/ml azithromycin (AZM). TSB was used as control. Luminescence emission was recorded by IVIS Lumina system after addition of luciferin. Each value represents the mean ± SD of 3 experiments. Statistical analysis was performed by 1way ANOVA followed by Dunnett's multiple comparisons test, ** $p<0.01$ and *** $p<0.001$.

In bIL-8-Luc-transgenic BalbC mice challenged with 10X-concentrated VR1 supernatant, a strong bioluminescence emission was detectable already 4 hours after instillation and reached the highest peak after 24 hours. On the contrary, supernatant from VR1+AZM induced a low bioluminescence emission, comparable to that induced by VR2 supernatant, containing low levels of virulence factors (Fig. 16). No significant difference in bioluminescence emission was detected between mice treated with VR2 and VR2+AZM supernatants.

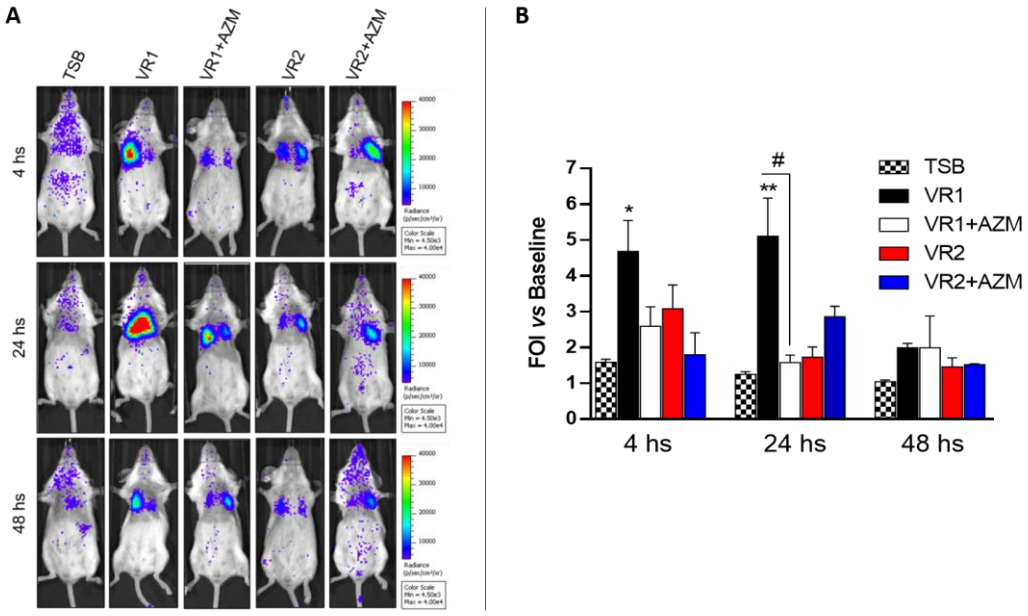

Figure 16. Representative images of bIL-8-Luc-mediated bioluminescence emission in BalbC mice 4, 24 and 48 hs after instillation with 10X concentrated culture supernatants from VR1 and VR2 isolates grown in presence or absence of sub-MIC azithromycin (AZM). TSB was used as control (A). Photons emission is expressed as folds of increase (FOI) over baseline. Each value represents the mean ± SEM of 8 animals. Statistical

analysis was performed by 1way ANOVA followed by Dunnett's multiple comparisons test, * $p<0.05$ and ** $p<0.01$ vs. control, # $p<0.05$ vs. treatment (B).

Immune cells recruitment (Fig. 17A) and cytokines expression (Fig. 17B) were evaluated in BALF at 24 hours after challenge. VR1 supernatant significantly stimulated total white blood cells (WBC) and neutrophils recruitment, and the expression of IL-1β, TNF-α, IL-17, RANTES, KC, IL-12 (p70) and IL-12 (p40) cytokines. Inflammatory cells and expression of many cytokines were lower in mice treated with VR1+AZM supernatant, except for TNF-α and IL-12 (p40), or VR2 supernatant, except for RANTES and IL-12 (p40). No significant difference between the stimulation caused by VR2 and VR2+AZM supernatants was observed, except for RANTES and IL-12 (p40) levels.

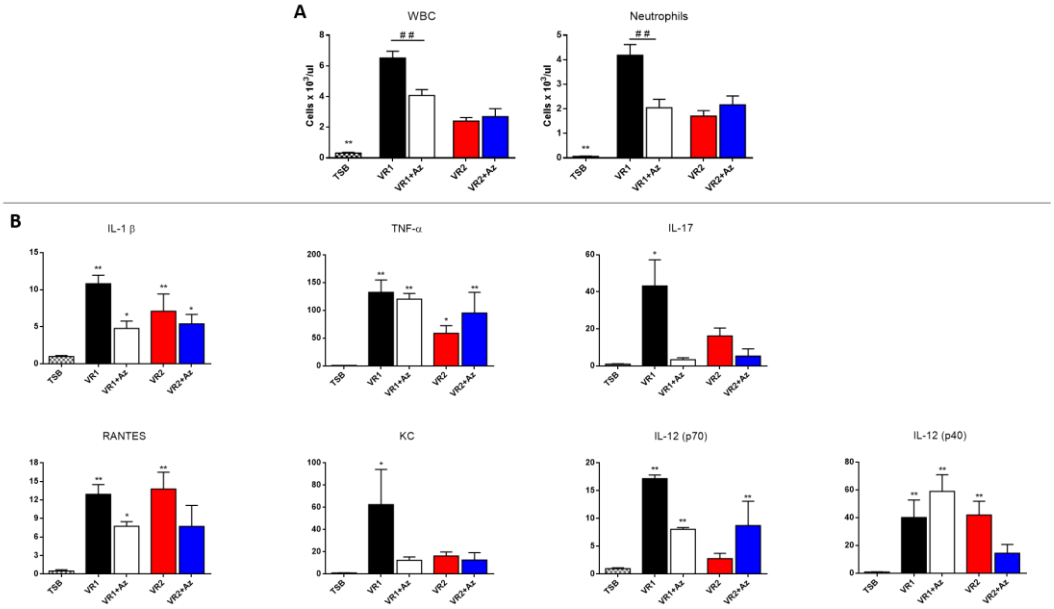

Figure 17. Immune cells recruitment (A) and cytokines expression (B) in BalbC mice 24 hs after instillation with 10X concentrated culture supernatants from VR1 and VR2 isolates grown in presence or absence of sub-MIC azithromycin (Az). TSB was used as control. The amount of white blood cells and neutrophils found in BALF was expressed as number of cells per µl. Cytokines concentration was expressed as folds of increase (FOI) over control. The experiment was repeated 3 times and each point represents the mean ± standard deviation of 8 animals. Results are reported as mean ± SEM. Statistical analysis was performed by 1way ANOVA followed by Dunnett's multiple comparisons test, * $p<0.05$ and ** $p<0.01$ vs control, ## $p<0.01$ vs. treatment.

P. aeruginosa protease inhibition decreases mice lung inflammation

Since *P. aeruginosa* proteases contribute to inflammatory exacerbation, their inhibition might result in the reduction of lung inflammatory response. Hydroxamate-based broad spectrum human metalloprotease inhibitor Ilomastat was previously reported to inhibit *P. aeruginosa* elastase. To confirm this finding, we tested its inhibitory activity against VR1 secreted proteases, and observed that Ilomastat could inactivate *P. aeruginosa* proteases in 1X and even 10X-concentrated culture supernatant (Fig. 18).

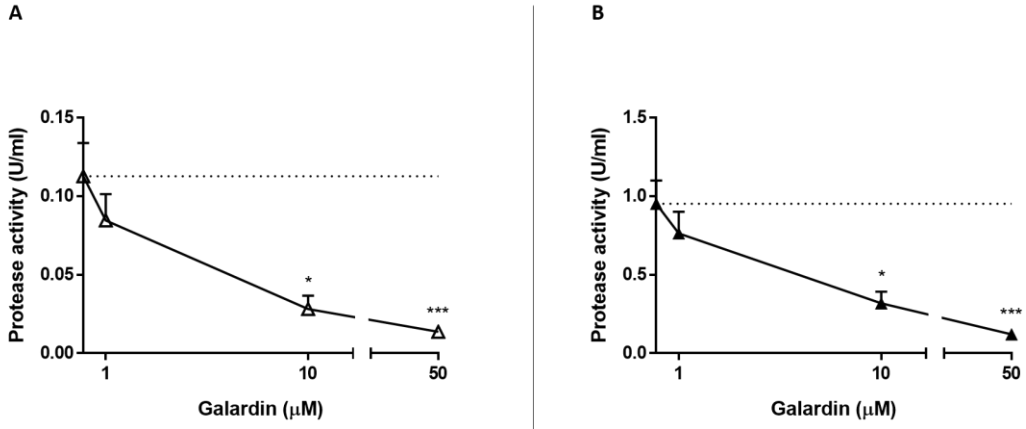

Figure 18. Protease activity in 1X (A) and 10X-concentrated (B) VR1 culture supernatant was measured in presence of increasing concentrations of Ilomastat (Galardin). Each value represents the mean ± SEM of 3 experiments. Statistical analysis was performed by Kruskal-Wallis test and Dunn's multiple comparisons test for non-parametric data, * $p<0.05$ and *** $p<0.001$ vs non-treated supernatant.

To verify whether inhibition of *P. aeruginosa* metalloproteases can influence and possibly reduce lung inflammation, bIL-8-Luc-transgenic BalbC mice were intratracheally challenged with VR1 supernatant pre-treated with Ilomastat: a reduced bioluminescence emission in comparison to non-pretreated supernatant was recorded at 24 hours after the challenge. The lower bIL-8 activation was similar to that previously observed with VR1+AZM challenge (Fig. 19A). Imaging data were supported by immune cells count in bronchoalveolar lavage fluid: total white blood cells and neutrophils recruitment was reduced when VR1 supernatant was pre-treated with Ilomastat (Fig. 19B).

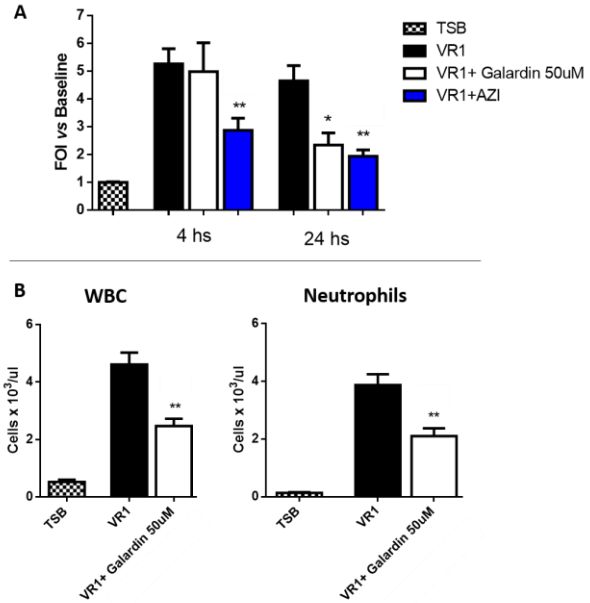

Figure 19. bIL-8-Luc-mediated bioluminescence emission in BalbC mice 4 and 24 hs after instillation with 10X concentrated VR1 culture supernatant non-treated or pre-

treated with 50 µM Ilomastat (Galardin), or from VR1 grown in presence or absence of 8 µg/ml azithromycin (AZI). Photons emission is expressed as folds of increase (FOI) over baseline (A). Total white blood cells and neutrophils recruitment in BalbC mice 24 hs after instillation with 10X concentrated VR1 culture supernatant non-treated or pre-treated with 50 uM galardin. The amount of immune cells found in BALF was expressed as number of cells per µl (B). TSB was used as control. Each point represents the mean ± SEM of 4 animals. Statistical analysis was performed by 1way ANOVA followed by Dunnett's multiple comparisons test, * $p<0.05$ and ** $p<0.01$ vs. VR1.

Adaptation of bIL-8-Luc model in CFTR-knockout mice

In order to carry on anti-inflammatory molecules testing by in vivo imaging in a CF background, bIL-8-Luc model was adapted to C57BL/6J Cftr^{tm1Unc} (KO) mice. Exogenous IL-8 promoter activation by *P. aeruginosa* exoproducts was verified after challenge with known *P. aeruginosa* pro-inflammatory stimuli, such as LPS and VR1 culture supernatant. After determining the optimal transfection conditions for this mouse strain, bIL-8-Luc congenic CFTR-KO and wild-type (WT) mice were intratracheally challenged with *P. aeruginosa* LPS (6.25 µg/mouse). LPS was previously resuspended in EMEM (Eagle's Minimum Essential Medium), which was used as control treatment. Both KO and WT mice responded to LPS reaching the maximum bioluminescence signal between 4 and 24 hours after the challenge (Fig. 20). Moreover, lungs were excised and their imaging was performed: as clearly shown in ex vivo pictures, the bioluminescence signal was well localized in the lung (Fig. 20). Immune cells recruitment and cytokines expression were evaluated in BALF at 24 hours after the intratracheal challenge. White blood cells (WBC) and neutrophils recruitment increased in both mouse strains when treated with LPS, and eight pro-inflammatory cytokines (IL-1β, IL-5, KC, IL-6, G-CSF, IFN-γ, MIP-1α, TNF-α) resulted up-regulated (Fig. 21).

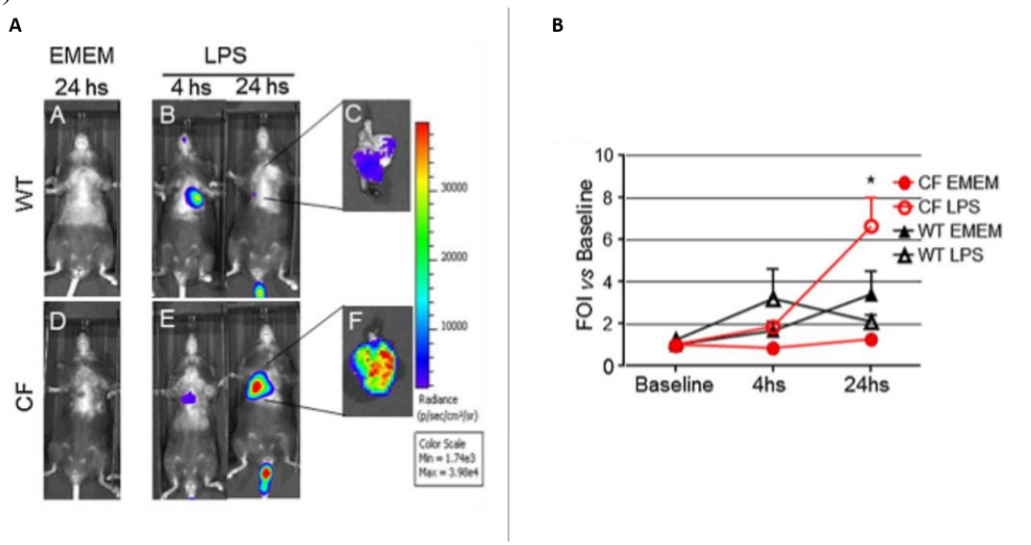

Figure 20. Representative in vivo images of bIL-8-Luc-trasgenic WT and CFTR-KO (CF) mice intratracheally treated with *P. aeruginosa* LPS (6.25 µg/mouse) (A). EMEM was used as control (a, d). Bioluminescence images were recorded at 4 and 24 hours after intratracheal instillation with LPS (b, e). Lungs were excised and imaged 24 hs after LPS challenge (c, f). Time-course of IL-8-luc activation (B). Results are reported as folds of increase (FOI) over baseline. Each value represents the mean ± SEM of 6 animals.

Statistical analysis was performed by 1way ANOVA followed by Dunnett's multiple comparisons test, * $p<0.05$ vs. control.

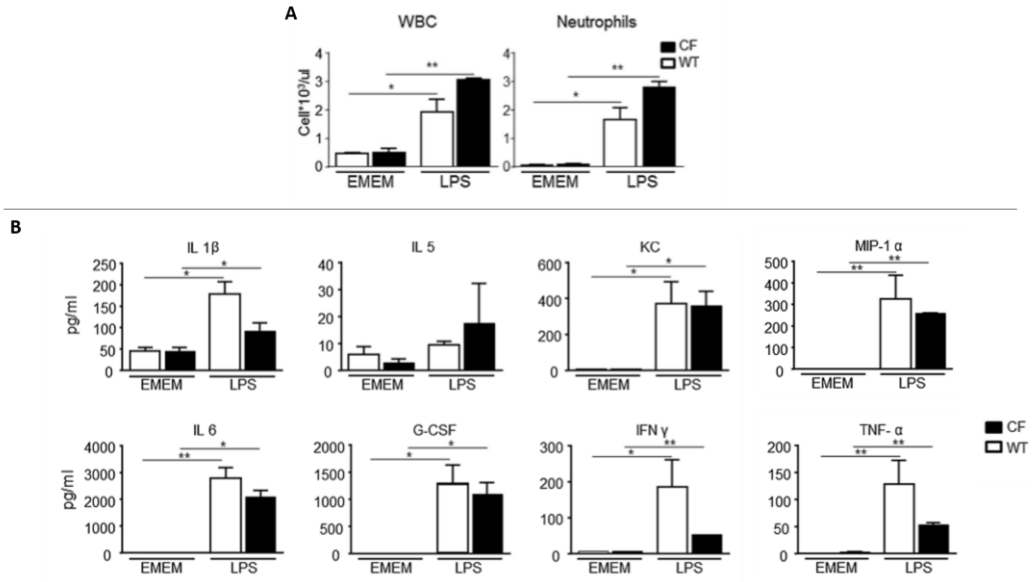

Figure 21. Immune cells recruitment (A) and cytokines expression (B) in WT and CFTR-KO (CF) mice 24 hours after instillation with *P. aeruginosa* LPS. EMEM was used as control. The amount of immune cells found in BALF was expressed as number of cells per µl (A). Cytokines concentration was expressed as pg/ml (B). Three mice were used for every time point and the experiment was replicated three times. Values are expressed as mean ± SEM of the three different experiments. Statistical analysis was performed by 1way ANOVA followed by Dunnett's multiple comparisons test, * $p<0.05$ and ** $p<0.01$ vs control.

In another set of experiments, WT and KO mice were challenged with 10X-concentrated VR1 culture supernatant, which activated the exogenous IL-8 promoter. Both mouse strains responded to the stimulus reaching the maximum BLI signal between 4 and 24 hours after the challenge (Fig. 22). Increase in total WBC and neutrophils in BALF was observed at 24 hours after VR1 culture supernatant treatment, as well as up-regulation of pro-inflammatory cytokines (Fig. 23). Thus, two different pro-inflammatory stimuli derived from *P. aeruginosa* had a similar behavior on bIL-8 activation in both WT and KO mice.

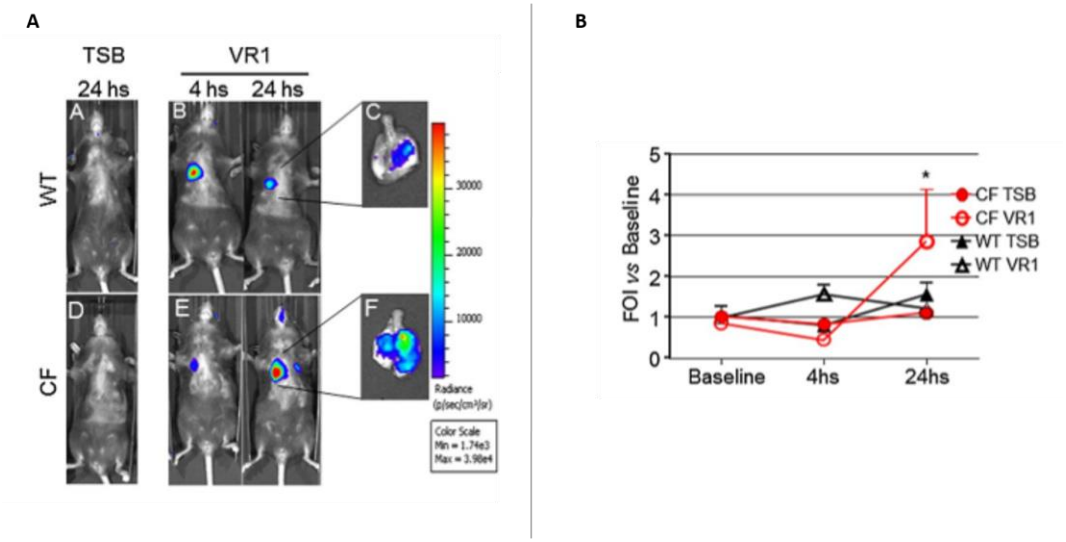

Figure 22. Representative in vivo images of bIL-8-Luc-trasgenic WT and CFTR-KO (CF) mice intratracheally treated with *P. aeruginosa* VR1 10X-concentrated culture supernatant (A). TSB was used as control (a, d). Bioluminescence images were recorded at 4 and 24 hours after intratracheal instillation with LPS (b, e). Lungs were excised and imaged 24 hs after LPS challenge (c, f). Time-course of IL-8-luc activation (B). Results are reported as folds of increase (FOI) over baseline. Each point represents the mean ± SEM of 6 animals. Statistical analysis was performed by 1way ANOVA followed by Dunnett's multiple comparisons test, * $p<0.05$ vs. control.

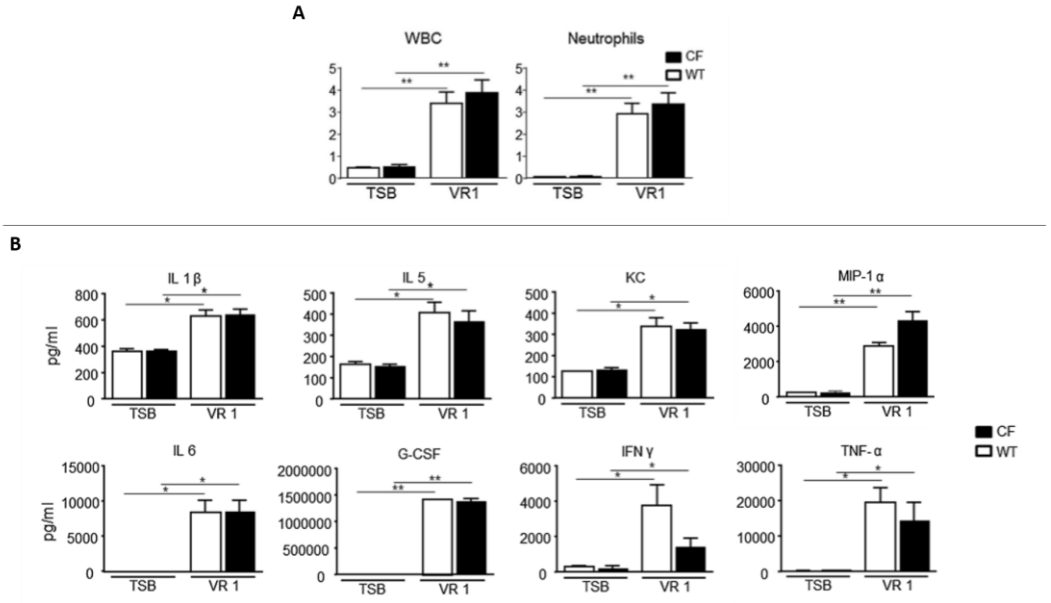

Figure 23. Immune cells recruitment (A) and cytokines expression (B) in WT and CFTR-KO (CF) mice 24 hours after instillation with *P. aeruginosa* VR1 10X-concentrated culture supernatant. TSB was used as control. The amount of immune cells found in BALF was expressed as number of cells per µl (A). Cytokines concentration was expressed as pg/ml (B). Three mice were used for every time point and the experiment was replicated three times. Values are expressed as mean ± SEM of the three different experiments. Statistical analysis was performed by 1way ANOVA followed by Dunnett's multiple comparisons test, * $p<0.05$ and ** $p<0.01$ vs control.

Inhibition of P. aeruginosa virulence by clarithromycin decreases lung inflammation in CF mice

We extended the investigation about connection between anti-virulence and anti-inflammatory effects to other molecules, like the macrolide clarithromycin. Performing minimum inhibitory concentration (MIC) assay, we established that doses up to 128 µg/ml clarithromycin has no bacteriostatic activity against VR1. Growth of VR1 in presence of 45 µg/ml (sub-MIC dose) clarithromycin caused a significant reduction in the synthesis of pyocyanin, pyoverdine and proteases (Fig. 24), similar to what previously observed with azithromycin, further supporting that macrolides interfere with protein synthesis. By inhibiting the production of *P. aeruginosa* exoproducts, clarithromycin could undermine bacterial virulence and indirectly modulate virulence-induced host inflammatory response.

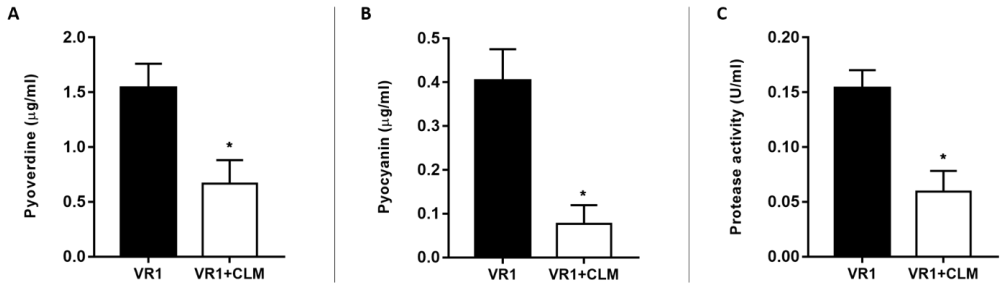

Figure 24. Pyocyanin, pyoverdine and proteases concentration was measured in culture supernatants from VR1 isolate grown in presence/absence of sub-MIC clarithromycin (CLM). Each value represents the mean ± SEM of 3 experiments. Statistical analysis was performed by 2-tailed t test, * $p<0.05$ vs. VR1.

Using the newly-developed CF bIL-8-Luc-transgenic mouse model, we extended the investigation to other molecules of interest, like clarithromycin. In both WT and KO animals the challenge with VR1 culture supernatant induced after 24 hours a strong inflammatory response in terms of IL-8 reporter activation (Fig. 25, 26). The bioluminescence signal lasted longer in KO mice, whose emission after 48 hours was still significantly higher than in mice challenged with TSB control medium (Fig. 25). In both WT and KO animals, the supernatant from VR1+CLM provoked only a minor response: the average of photons emitted was significantly lower than in mice challenged with VR1 supernatant, and comparable to the bioluminescence signal induced by TSB (Fig. 25, 26). These results resemble those obtained with azithromycin, supporting that the inhibitory action of clarithromycin on *P. aeruginosa* virulence might decrease the immune response in the lungs, with beneficial effects for the animals in terms of reduced inflammation, especially in CF-like mice.

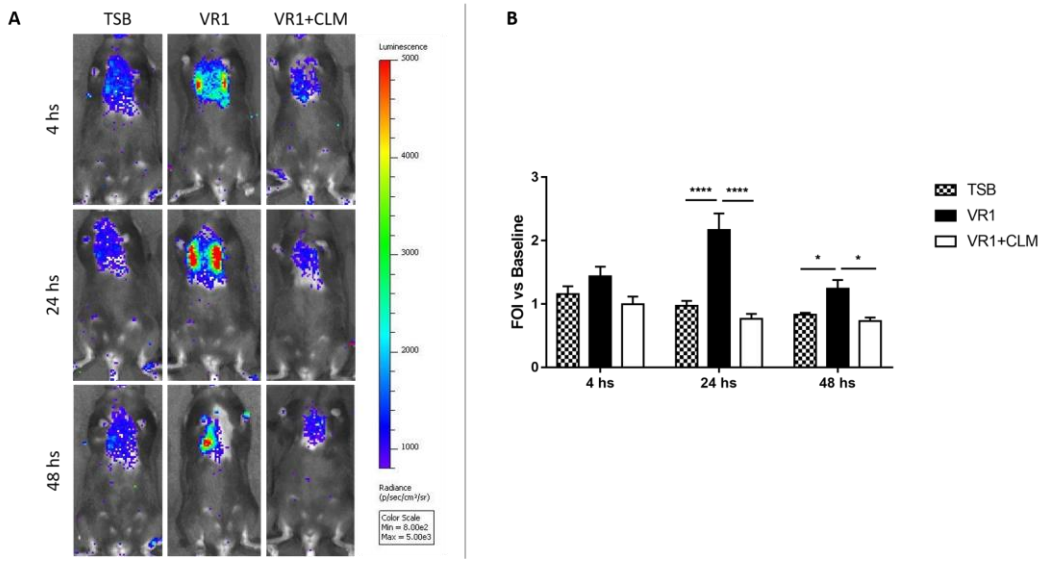

Figura 25. Representative images (A) and photons measurement (B) of bioluminescence emission in KO mice challenged with culture supernatant from VR1 ± 45 µg/ml clarithromycin (CLM). Control mice were treated with TSB. Photons emission is expressed as folds of increase (FOI) over baseline. Each point represents the mean ± SEM of 6 animals. Statistical analysis was performed by 2way ANOVA followed by Dunnett's multiple comparisons test, *p<0.05 and **** p<0.0001.

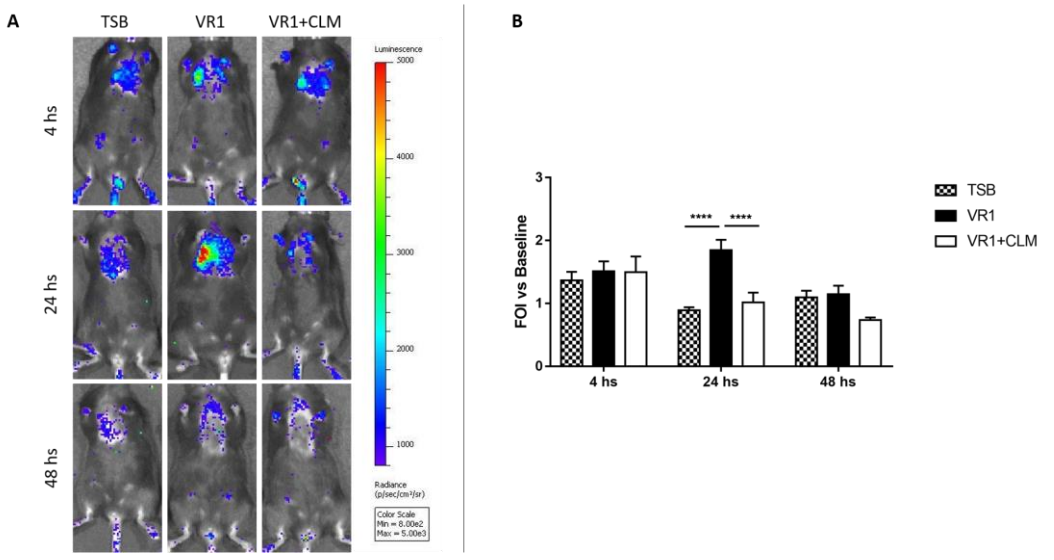

Figure 26. Representative images (A) and photons measurement (B) of bioluminescence emission in WT mice challenged with 10X-concentrated culture supernatant from VR1 ± 45 µg/ml clarithromycin (CLM). Control mice were treated with TSB. Photons emission is expressed as folds of increase (FOI) over baseline. Each point represents the mean ± SEM of 6 animals. Statistical analysis was performed by 2way ANOVA followed by Dunnett's multiple comparisons test, **** p<0.0001.

P. aeruginosa protease inhibition decreases lung inflammation in mice

We carried on the investigation on the inflammatory role of *P. aeruginosa* proteases testing more molecules chemically similar to Ilomastat, belonging to the hydroxamate-based group of metalloprotease inhibitors. We evaluated the effects of Marimastat and Batimastat; to our knowledge, the effect of these molecules on bacterial proteases has never been studied. Protease activity in VR1 culture supernatant was inhibited by Marimastat, but not by its chemical analogue Batimastat (Fig. 27). Thus, along with Ilomastat, we continued testing only Marimastat in vivo in bIL-8-Luc KO and WT mice.

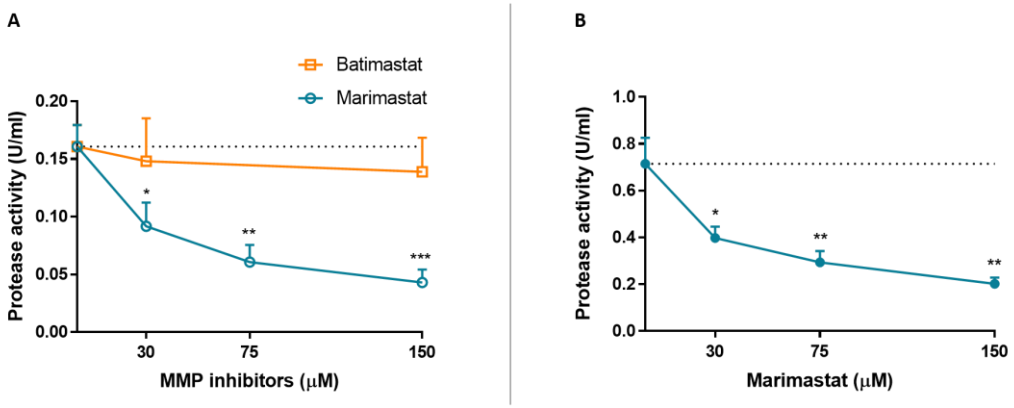

Figure 27. Protease activity in 1X (A) and 10X-concentrated (B) VR1 culture supernatant was measured in presence of increasing concentrations of MMP inhibitors Marimastat and Batimastat. Each value represents the mean ± SEM of 3 experiments. Statistical analysis was performed by 1way ANOVA followed by Dunnett's multiple comparisons test, * $p<0.05$, ** $p<0.01$ and *** $p<0.001$ vs. non-treated supernatant.

In bIL-8-Luc-transgenic KO mice intratracheally instilled with VR1 culture supernatant pre-treated with 50 µM Ilomastat, there was no significant reduction of the bioluminescence signal in comparison to animals challenged with non-pretreated supernatant (Fig. 28), differently to what previously observed in BalbC mice. But increasing the dose to 150 µM Ilomastat, a reduced bioluminescence was observed. The same concentration of Marimastat was even more effective in reducing lung inflammation in KO mice in terms of exogenous IL-8 promoter activation; indeed, bioluminescence emission was still significantly reduced at 48 hours after the intratracheal challenge with VR1 supernatant pre-treated with Marimastat, in comparison to non-treated supernatant (Fig. 28). We observed comparable results in WT mice challenged with VR1 pre-treated with 150 µM Ilomastat or Marimastat (Fig. 29). Thereby, Ilomastat and Marimastat might be good candidates for further in vivo studies in models of infection with virulent strains expressing high metalloprotease levels.

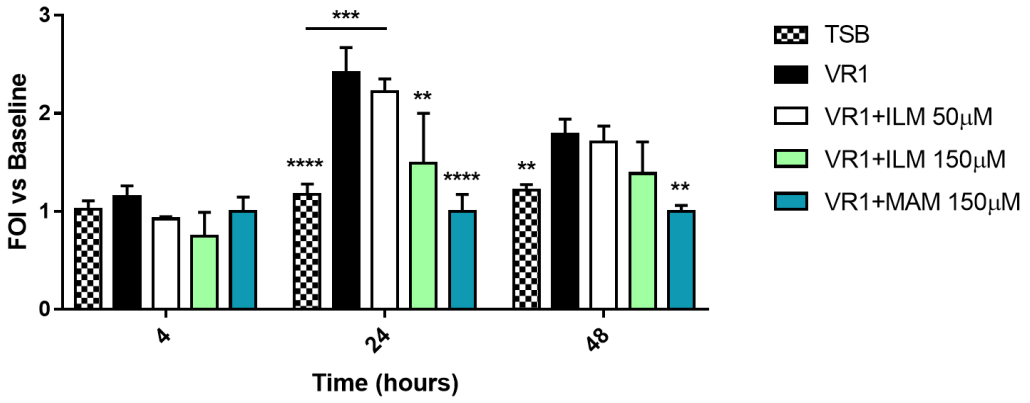

Figure 28. IL-8-mediated bioluminescence emission in C57BL/6J KO mice after instillation with 10X-concentrated VR1 culture supernatant untreated or pre-treated with 50 or 150 μM Ilomastat (ILM) or 150 μM Marimastat (MAM). TSB was used as control. Photons emission recorded after 4, 24 and 48 hs is expressed as folds of increase (FOI) over baseline. Each value represents the mean ± SEM of 6 animals. Statistical analysis was performed by 2way ANOVA followed by Dunnett's multiple comparisons test, ** $p<0.01$, *** $p<0.001$ and **** $p<0.0001$ vs. VR1.

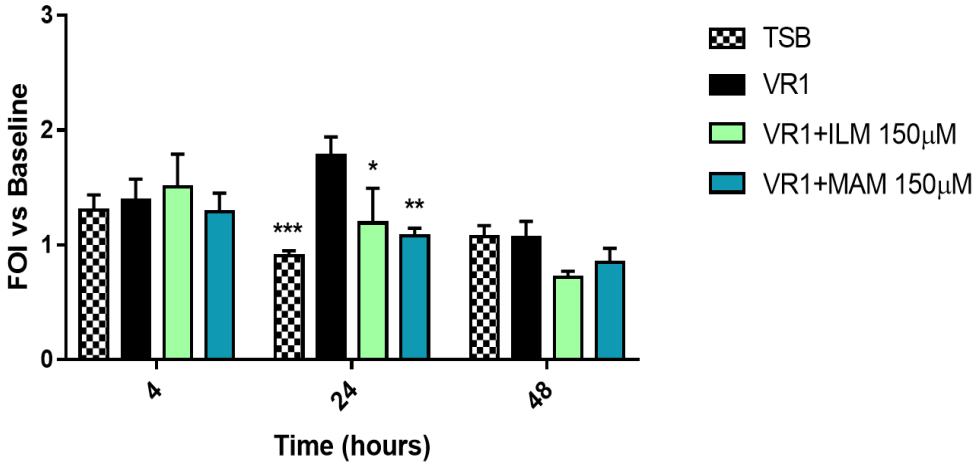

Figure 29. IL-8-mediated bioluminescence emission in C57BL/6J WT mice after instillation with 10X-concentrated VR1 culture supernatant untreated or pre-treated with 150 μM Ilomastat (ILM) or Marimastat (MAM). TSB was used as control. Photons emission recorded after 4, 24 and 48 hs is expressed as folds of increase (FOI) over baseline. Each value represents the mean ± SEM of 6 animals. Statistical analysis was performed by 2way ANOVA followed by Dunnett's multiple comparisons test, *$p<0.05$, ** $p<0.01$, and *** $p<0.001$ vs. VR1.

6.3. Discussion

P. aeruginosa is considered the main airway pathogen in cystic fibrosis, affecting a high percentage of patients, particularly adults. Especially during early colonization, *P. aeruginosa* releases a multitude of virulence factors which contribute to lung damage and trigger airways immune defenses, promoting final lung failure [30]. We studied the effects of *P. aeruginosa* virulence on lung inflammation using a transgenic mouse model which allows in vivo bioluminescence imaging of an exogenous bovine interleukin-8 promoter activation. Although mouse cells do not express a clear homologous IL-8 gene, the murine transcriptional apparatus can activate or repress the exogenous promoter driving a luciferase reporter gene [302]. The non-invasive nature of this mouse model and the possibility for bIL-8-luc-transgenic mice to be stimulated for long time enables the monitoring of the inflammatory process longitudinally in the same mouse. This represents an obvious advance for functional as well as pharmacological studies, reducing the number of sacrificed animals and the costs of housing, and increasing the data quality by lowering the inter-animal variability, since each mouse represents its own control. IL-8 promoter activation by *P. aeruginosa* virulence factors was verified in vitro, and in vivo in BalbC mice. In both systems, the treatment induced a strong, concentration-dependent bioluminescence emission, indicating activation of the exogenous bIL-8 promoter. In mice, the emission was limited to the lungs area, thereby confirming the correct transfection of lung tissue and the effectiveness of intratracheal challenge. Furthermore, the model was successfully applied to $Cftr^{tm1Unc}$ knockout (KO) mice into C57Bl/6J background, a CF mouse model reported to develop lung disease [303]. Moreover, post-bronchiolar hyperinflation of alveoli reported in this model is consistent with obstructive small airway disease, which is a characteristic early feature of the human disease [304]. In bIL-8-Luc-transgenic KO mice, intratracheal challenge with *P. aeruginosa* pro-inflammatory products such as LPS and the products released in culture supernatant induced bioluminescence emission in the lungs area, immune cells recruitment and inflammatory cytokines expression, indicating a local inflammatory response. Although IL-8 activation in KO mice resulted in a stronger and longer-lasting bioluminescence signal as compared to WT animals, the other lung inflammatory markers such as immune cells, cytokines and histology did not show significant differences between the two mouse strains at 24 hours after the challenge. Though surprising at a first glance, a differential degree of strain sensitivity to pro-inflammatory stimuli has been reported [323]. Indeed, the same stimulus in BalbC mice induced a higher number of recruited inflammatory cells than in the C57Bl/6 mouse strain, supporting this interpretation. Moreover, the reporter gene relies on bIL-8 promoter, which responds mainly to NF-κB while additional master genes, like AP-1 (Fos/Jun), NFATs, and STATs, control the expression of several cytokines [324]. Such additional pathways might bypass the need of full NF-κB recruitment, and can be activated in different mouse strains. In this specific case, the differential response to agonists further highlight the critical role of CF background in controlling inflammatory response, and support the notion that differential responses in CFTR-defective mice may occur, in line with the pro-inflammatory phenotypes recognized in humans.

Patients with chronic *P. aeruginosa* lung infection are often treated with azithromycin, a macrolide antibiotic known to interact with the 50S ribosomal subunit and affect specific genes and transcriptional factors involved in the regulation of virulence [202]. Azithromycin has no bactericidal activity against P. aeruginosa, but could inhibit the synthesis of secreted virulence factors such as pyocyanin, pyoverdine and proteases. Particularly, we observed that metalloprotease activity and alkaline protease expression were inhibited in both culture supernatant and bacterial lysate, confirming the macrolide inhibitory effect on metalloprotease synthesis. The observed anti-virulence activity is likely to be involved in the clinical benefits associated with azithromycin treatment. Supernatant collected after growth in presence of azithromycin induced lower bioluminescence emission, immune cells recruitment and cytokines expression in bIL-8-Luc BalbC mice in comparison to supernatant from non-treated bacteria. A similarly low pro-inflammatory effect was shown by the supernatant from a lowly-virulent *P. aeruginosa* isolate. These data support the involvement of bacterial virulence down-regulation in the beneficial effects of azithromycin in the first year of therapy, while the reduced efficacy associated with longer treatment duration might be due to development of bacterial resistance to azithromycin anti-virulence activity. Thereby, evaluation of molecules with similar antibacterial mechanisms is important to find alternative treatments for patients not responding to azithromycin or for whom the treatment lost efficacy [208, 325]. A candidate might be macrolide clarithromycin, which showed clinical effectiveness in treating DPB and has been studied as therapy for other respiratory diseases [231-236]. Clarithromycin effects in CF patients were also evaluated in different studies, although with contrasting outcomes [237-240]. Like azithromycin, clarithromycin has no bactericidal activity against *P. aeruginosa*, but could down-regulate synthesis of *P. aeruginosa* virulence factors [217, 241]. In bIL-8-Luc KO and WT $Cftr^{tm1Unc}$ mice, supernatant collected after growth in presence of clarithromycin induced lower bioluminescence emission in comparison to supernatant from non-treated bacteria. From these results, we conclude that clarithromycin acts similarly to azithromycin on *P. aeruginosa* by reducing the synthesis of various exoproducts involved in bacterial virulence and the associated host inflammatory response. The inhibitory action of clarithromycin on *P. aeruginosa* virulence seems to decrease the immune response in the lungs, with beneficial effects for the animals in terms of reduced inflammation, especially in KO mice. Our results support the possible efficacy of clarithromycin for treating CF patients and encourage more clinical trials to assess the effectiveness of this therapy, which gain particular interest when considering the possibility of aerosol administration; indeed, its formulation as dry powder inhaler is currently under investigation [250, 251]. Thus, local administration in the airways might represent an option for the treatment of chronic *P. aeruginosa*-infected patients, especially for those not responding to other therapies. To our knowledge, clarithromycin treatment has never been tested in patients that already showed no improvement under azithromycin therapy. A clinical study in this group of patients might clarify the possible use of clarithromycin as an alternative therapy, and help to understand the involvement of *P. aeruginosa* resistance in azithromycin long-treatment ineffectiveness.

Among many factors, proteases from both host and bacteria play a critical role in CF lung disease, contributing to lung tissue damage and exacerbation of host inflammatory response. *P. aeruginosa* exogenous proteases such as AprA and LasB can alter mucociliary clearance, degrade lung tissue and dysregulate host immune system, thus strongly contributing to lung disease [156]. We showed that downregulation of protease production is part of the anti-virulence effects of macrolides azithromycin and clarithromycin, and it might be involved in their anti-inflammatory effect associated with virulence inhibition. Thus, molecules targeting proteases might represent an alternative anti-inflammatory therapy. Broad spectrum hydroxamates are attractive candidates, since many members entered clinical trials as cancer therapeutics, although with disappointing results as regards their effectiveness in delaying disease progression [263, 264]. Hydroxamate-based broad spectrum human matrix metalloprotease inhibitor Ilomastat had previously been reported to inhibit *P. aeruginosa* elastase [255]; indeed, treatment of *P. aeruginosa* culture supernatant resulted in a strong reduction of protease activity. We also tested proteases inhibition by two more of these molecules, Batimastat and Marimastat: only the latter could decrease bacterial protease activity. In order to evaluate *P. aeruginosa* secreted proteases as possible targets of anti-inflammatory therapy, we tested in vivo the effect of their inhibition on lung inflammation. In bIL-8-Luc-transgenic BalbC mice challenged with Ilomastat-pretreated supernatant, we observed a strong reduction of bioluminescence and immune cells recruitment in comparison to non-pretreated supernatant. Differently, in KO $Cftr^{tm1Unc}$ mice the same Ilomastat concentration was not able to down-regulate the inflammatory response, probably due to a differential degree of strain sensitivity to the pro-inflammatory stimuli [323], but we found that a higher dose could reduce IL-8 promoter activation in both WT and KO mice. Similar to Ilomastat, inactivation of *P. aeruginosa* secreted proteases by Marimastat showed a beneficial effect on lung inflammation in bIL-8-Luc-transgenic WT and KO mice in terms of lower bioluminescence emission in comparison to non-pretreated supernatant, thereby reducing lung inflammatory response. These results highlight the key role played by *P. aeruginosa* proteases in host inflammatory response, since the inhibition of the sole bacterial proteases determined a significantly milder lung inflammation. Thus, anti-protease strategies to dampen the inflammatory response and concomitant airways damage might be an interesting additional therapy for CF lung disease. We tested two candidate molecules with interesting characteristics: while Marimastat is orally available, Ilomastat is under evaluation as inhaled therapy [262], which would allow local airways treatment. Furthermore, anti-protease therapy might avoid the limitations due to resistance development, a typical feature of antibiotic treatments [252].

7. PROJECT 2 - ADAPTIVE MICROBIAL INTERACTIONS BETWEEN *PSEUDOMONAS AERUGINOSA* AND *ACHROMOBACTER XYLOSOXIDANS*

In the present study, we observed the evolution of *P. aeruginosa* and *A. xylosoxidans* strains during chronic co-infection of CF lungs, and evaluated possible inter-species interactions that might have been engaged during this time, while the two microorganisms were neighbors sharing the same environment. Although the occurrence of close microbial interactions within the CF lung is not yet clear, our study might help to understand the role of bacterial interactions on survival and persistence in the human host.

7.1. Materials & Methods

Bacterial strains

P. aeruginosa and *A. xylosoxidans* clinical strains were longitudinally collected from sputum samples of a chronically co-infected patient followed at Rigshospitalet, Copenhagen, Denmark (kind gift of Dr. Helle Krogh Johansen). Isolates were collected in 2005 and 2008, and stored in 20% glycerol at -80°C.

Colony morphology

Bacterial strains were plated on LB agar and incubated at 37°C for 24-48 hours. Single colonies were observed and photographed. Different features were observed and reported: size, shape, color, edge, and mucoidy.

Growth curves

Bacterial strains were plated on LB agar and incubated at 37°C for 24-48 hours. 1-2 colonies were inoculated in 10 ml LB medium shaking at 37°C overnight. OD_{600} was measured using a spectrophotometer, cultures were diluted to 0.05 OD/ml in LB medium and 150 µl/well were incubated in a 96-well plate for 20-24 hours shaking at 37°C. Using an automated plate reader, A_{600} was measured every 20 minutes. Growth rate was calculated using GraphPad Prism software.

Culture supernatant collection

A. xylosoxidans strains were plated on LB agar and incubated at 37°C for 24-48 hours. 1-2 colonies were inoculated in 10 ml LB medium shaking at 37°C for 16 hours. OD_{600} was measured and cultures were diluted to 0.1 OD/ml in 10 ml of LB medium. After shaking at 37°C for 16 hours, cultures were diluted to 1 OD/ml and centrifuged at 7000 g for 30 min at 4°C. Supernatants were collected and sterile-filtered.

Adhesion assay

Bacterial strains were plated on LB agar and incubated at 37°C for 24-48 hours. 1-2 colonies were inoculated in 10 ml LB medium shaking at 37°C overnight. OD_{600} was measured using a spectrophotometer, cultures were diluted to 0.05 OD/ml in LB medium and 150 µl/well were incubated in a 96-well plate for 20-24 hours at 37°C. After measuring A_{600}, wells were washed twice with water to remove unattached cells, and surface-attached cells were stained with 0.1% crystal violet

solution for 15 minutes. Wells were rinsed and washed 3 times with water, then dried for 1-2 hours. 30% acetic acid was added, incubated at room temperature for 15 minutes, and A_{590} was measured. 30% acetic acid was used as blank. In competition assays, *P. aeruginosa* adhesion was measured in presence/absence of 10% *A. xylosoxidans* culture supernatant.

Protease assay

Protease activity in culture supernatants was determined by azocasein assay. Briefly, 350 µl reaction mixture containing 0.1 M Tris-HCl, pH 8.0, and 1% azocasein (Sigma-Aldrich, previously resuspended in 0.5% $NaHCO_3$) was added to 150 µl supernatant and incubated at 37°C for 20 minutes shaking. After addition of 1 ml 7% ice-cold perchloric acid, the solution was centrifuged. 150 µl of 10 N sodium hydroxide were added to the clear supernatant and OD_{430} was measured. One protease unit was calculated as the amount of enzyme producing an increase of 0.1 OD per hour.

Pulse field gel electrophoresis

Bacterial suspensions were prepared from individual bacterial colonies directly obtained from cultures incubated overnight on Blood Columbia agar plates. The suspensions were adjusted to a concentration of 10^9 CFU/ml, in EDTA-saline buffer (75 mmol/L NaCl and 25 mmol/L EDTA, pH 7.5). The cell suspension was mixed with an equal volume of 1% low-melting point agarose and was allowed to solidify in a 100 µL plug mould. The agarose plug was incubated for 24 h at 37 °C in 500 µL of lysis buffer (6 mmol/L Tris–HCl (pH 7.6), 0.1 mol/L EDTA, 1 mol/L NaCl, 0.5% Brij®58 (polyoxyethylene (20) cetyl ether; Sigma), 0.4% sodium deoxycholate, 0.5% sodium lauryl sarcosine and 1 mg/mL lysozyme). The lysis buffer was replaced with 500 µL of proteinase K buffer (1% sodium lauryl sarcosine, 0.5 mol/L EDTA (pH 9) and proteinase K (50 µg/mL; Sigma)) and this solution was incubated with gentle shaking at 50 °C for 20 h. The plugs were then washed four times for 30 min at 37 °C with 10 mL of Tris–EDTA buffer (10 mmol/L Tris–HCl (pH 8) and 1 mmol/L EDTA). One-third of a slice of each plug was cut and incubated for 18-20 h with 30 U of *SpeI* (Bio-Rad Laboratories) in the restriction buffer (Promega Buffer). DNA restriction fragments were separated in a PFGE apparatus at 14 °C, 6 V/cm, for 20 hours with a time switch of 2-40 s. The gel was stained with gel-red and visualized with a UV system. According to the criteria by Tenover et al., isolates were considered to be genetically indistinguishable or identical if the restriction fragments differed in no more than 3 bands and the corresponding bands had identical apparent size [306].

GFP reporter construct

P. aeruginosa strains were tagged with a mini-Tn7 construct carrying gentamycin resistance and green fluorescent protein GFPmut3b gene under the control of the growth-dependent E. coli ribosomal promoter *rrnB* P1 (kind gift of Prof. Søren Molin, Technical University of Denmark). The construct can be introduced in *P. aeruginosa* by conjugative transfer.

Bacterial conjugation

Recipient *P. aeruginosa* strains were grown overnight in 10 ml LB medium at 42°C shaking. *E. coli* donor strain and *E. coli* helper strains pRK2013 and pNTS2 were grown overnight at 30°C shaking in 10 ml LB medium added with 100 µg/ml gentamycin, 100 µg/ml ampicillin or 25 µg/ml kanamycin, respectively. Bacterial cultures were centrifuged at 7.000 rpm for 10 minutes and pellet was resuspended in 10 ml LB medium. 3 ml recipient were mixed with 1 ml of each E.coli strain. A 200 µl drop was put in the center of a LB agar plate, dried for 1-2 hours and incubated at 37°C overnight. Bacteria were retrieved with a sterile loop, resuspended in LB medium and plated on LB agar containing gentamycin and trimethoprim, to select for transconjugants. Single colonies were checked for fluorescence emission and mini-Tn7 insertion, streaked on LB agar and stored in 20% glycerol at -80°C.

Colony PCR verification of mini-Tn7 insertion

Single transconjugant colonies were picked and mixed with the following reagents: 2.5 µl DMSO, 1 µl 10 mM dNTPs, 5 µl 10x Taq buffer (containing $MgCl_2$), 1 µl 30 pmol/ µl PTn7R primer, 1 µl 30 pmol/ µl PglmS Fw primer, 0.5 µl 5 U/ µl Taq polymerase, and water up to 50 µl. PTn7R and PglmSF primers sequences are reported by Choi and Schweizer. PCR was performed as follows: 95 °C for 5 min; 95 °C for 45 s, 59 °C for 30 s, 72 °C for 20 s, repeat for 30 cycles; 72 °C for 10 min. An aliquot of the PCR reaction was analyzed by gel electrophoresis on 2% agarose gel in TAE buffer (run at a constant 100 V for 1 h). A single PCR fragment of approximately 272 bp should be observed.

Fluorescence production curves

P. aeruginosa GFP-tagged strains and *A. xylosoxidans* strains were plated on LB agar and incubated at 37°C for 24-48 hours. 1-2 colonies were inoculated in 10 ml LB medium shaking at 37°C overnight. OD_{600} was measured using a spectrophotometer, cultures were diluted to 0.05 OD/ml in LB medium and 150 µl/well were incubated in a 96-well plate for 20-24 hours shaking at 37°C. For competition experiments, 75 µl/well of *P. aeruginosa* and *A. xylosoxidans* were mixed. Using an automated plate reader, fluorescence (excitation 475 nm, emission 520 nm) and A_{600} were measured every 20 minutes. Fluorescence rate was calculated using GraphPad Prism software.

Flow-chamber biofilm

Flow-chamber system was assembled and sterilized following the protocol from M. W. Nielsen and colleagues. Bacterial strains were plated on LB agar and incubated at 37°C for 24-48 hours. 1-2 colonies were inoculated in 10 ml LB medium shaking at 37°C overnight. OD_{600} was measured using a spectrophotometer, cultures were diluted to 0.05 OD/ml in saline solution. 250 µl of bacterial culture were injected in each flow-cell channel. Flow cells were left upside-down for an hour without flow, to let bacteria attach on the cover glass. Flow cells were turned and the system was incubated at 30°C up to 5 days with flow. Biofilms were grown in A10 minimal medium added with $MgCl_2$, $CaCl_2$ and trace metals.

Confocal microscopy

Biofilm formation was observed every day by confocal laser scanning microscopy of GFP-tagged *P. aeruginosa* strains and Syto62 staining of total cells. For statistical analysis, at least 7 pictures/channel were taken, homogeneously distributed along the channel. Pictures were visualized and elaborated using Imaris 7.4 software. Biomass was calculated using Comstat software.

Statistical analysis

Statistical analysis was performed using GraphPad Prism software. Growth rates, fluorescence rates, adhesion and protease activity were analyzed by unpaired t test. Biofilm biomass was analyzed by Mann-Whitney test for non-parametric data.

7.2. Results

Phenotypic and genotypic characterization of longitudinal isolates

P. aeruginosa and *A. xylosoxidans* strains were longitudinally collected from a chronically co-infected CF patient twice, in 2005 and 2008. Pulse field gel electrophoresis profiles (PFGE) of longitudinal isolates showed high similarity: *P. aeruginosa* profiles were identical, while *A. xylosoxidans* profiles differed in 2 bands (Fig. 30). According to the criteria by Tenover and collegues [306], the longitudinal isolates can be considered genetically indistinguishable. Thus, PFGE analysis confirmed that the patient was colonized with the same *P. aeruginosa* and *A. xylosoxidans* genotypes for 3 years.

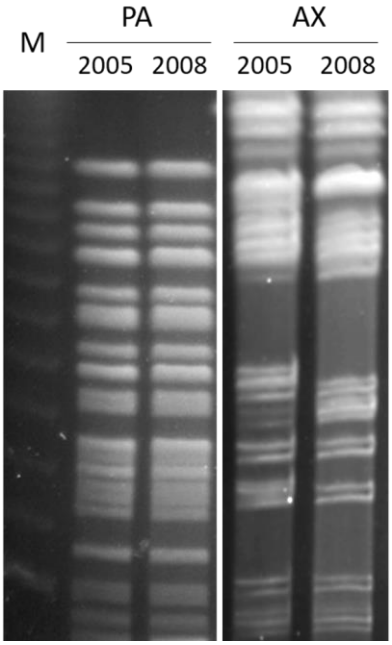

Figure 30. Representative image of PFGE profiles of *P. aeruginosa* (PA) and *A. xylosoxidans* (AX) longitudinal isolates collected in 2005 and 2008.

During the 3 years long co-infection, *P. aeruginosa* underwent phenotypic evolution known to occur during chronic infection. Colony morphology showed a

switch towards the mucoid phenotype, characterized by the overproduction of alginate, typical of late infection isolates (Fig. 31A). The morphology of the first isolate was already different from the typical environmental *P. aeruginosa* strains, usually forming green, swarming colonies, indicating that probably a partial evolution might have happened before 2005. Other phenotypic features observed were growth and adhesion. Growth rate diminished over time, while adhesion on plastic surfaces increased (Fig. 32). Both changes were expected and confirm evolution towards a typical CF *P. aeruginosa* late infection isolate. On the contrary, *A. xylosoxidans* does not show major changes in any of the observed features: colony morphology was similar between longitudinal isolates, while growth rate and adhesion capability did not present significant differences (Fig. 31B, 32). Particularly, *A. xylosoxidans* isolates showed very low adhesion ability on plastic surfaces (Fig. 32B).

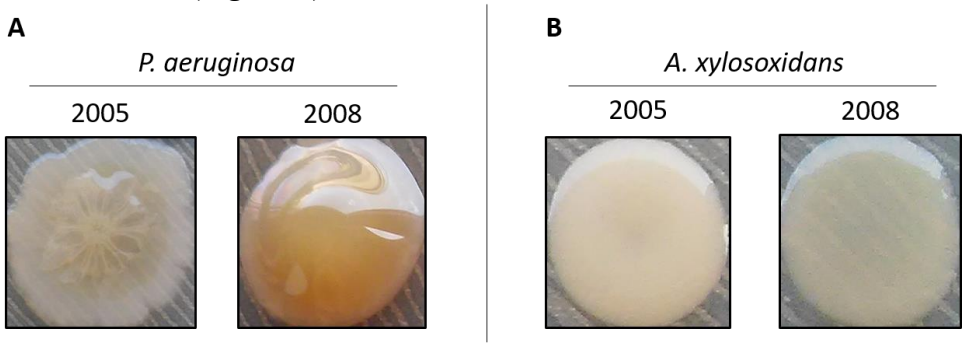

Figure 31. Representative images of *P. aeruginosa* (A) and *A. xylosoxidans* (B) longitudinal isolates colony morphology. Single colonies were photographed after growth for 24-48 hours at 37°C on LB agar.

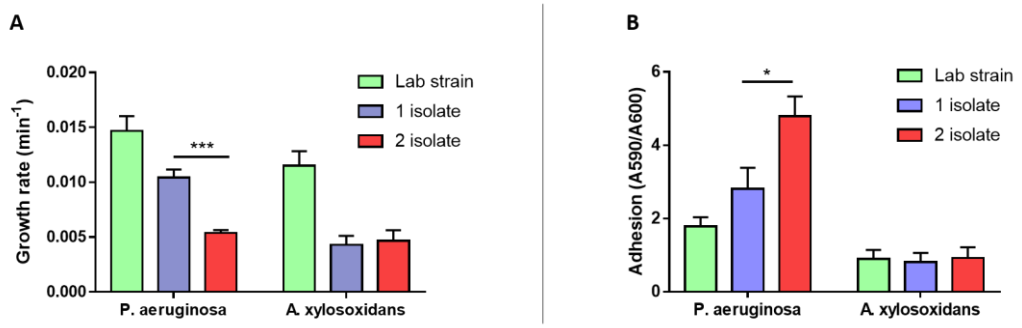

Figure 32. Growth rate (A) and adhesion (B) ability of *P. aeruginosa* and *A. xylosoxidans* isolates. Lab strains *P. aeruginosa* PAO1 and *A. xylosoxidans* CIP71.32 were used as controls. Growth rate was calculated from 24 hours growth curves in LB medium. Each value represents the mean ± SD of 3 experiments. Statistical analysis was performed by t test, *** $p<0.001$ (A). Adhesion was measured by crystal violet staining of surface-attached bacteria divided by A_{600} of non-attached bacteria. Each value represents the mean ± SEM of 3 experiments. Statistical analysis was performed by t test, * $p<0.05$ (B).

A. xylosoxidans initially interferes with P. aeruginosa growth

To observe possible synergistic/competitive interactions between the co-isolated *P. aeruginosa* and *A. xylosoxidans* strains, mixed planktonic cultures were grown.

P. aeruginosa isolates were previously tagged with a construct containing GFP gene under the control of a growth-dependent promoter, thus fluorescence emission increases during bacterial growth, as shown in figure 33A. The fluorescence rate was then used as a read-out of bacterial growth rate.
P. aeruginosa fluorescence emission was measured during growth in presence/absence of *A. xylosoxidans*: a lower fluorescence rate was observed when the first *P. aeruginosa* isolate was cultured in the presence of the first *A. xylosoxidans* isolate. On the contrary, this inhibitory effect was not observed when the late isolates were co-cultured (Fig. 33B).

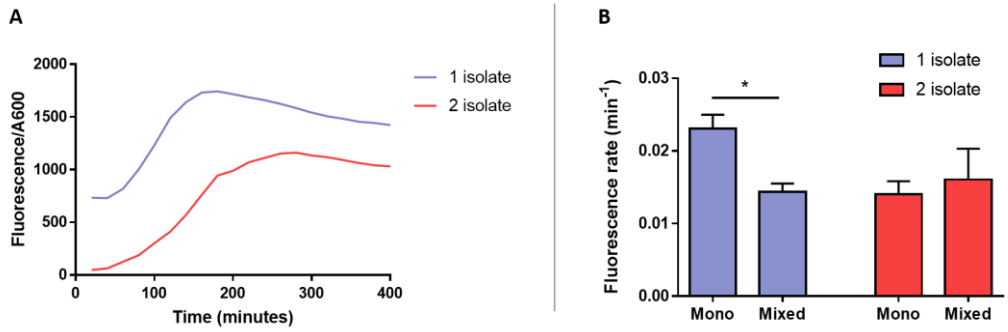

Figure 33. Effects of *A. xylosoxidans* on *P. aeruginosa* growth-dependent fluorescence rate. Fluorescence emission curves of GFP-tagged *P. aeruginosa* isolates (A). Fluorescence rate of GFP-tagged *P. aeruginosa* strains cultured in presence/absence of the co-isolated *A. xylosoxidans* strain. Fluorescence rate was calculated from 24 hours fluorescence emission curves in LB medium. Each value represents the mean ± SEM of 3 experiments. Statistical analysis was performed by t test, * $p<0.001$.

A. xylosoxidans initially interferes with P. aeruginosa biofilm formation

Mono-species and multi-species biofilms were grown in flow-chamber system up to 5 days. As shown in figure 34A, *P. aeruginosa* isolates could form big, stable aggregates firmly attached on the glass surface. On the contrary, *A. xylosoxidans* strains confirmed their poor adhesion ability on abiotic surfaces like plastic and glass, forming sporadic, unstable, small aggregates characterized by scattering and dispersal of planktonic cells (Fig. 34B).

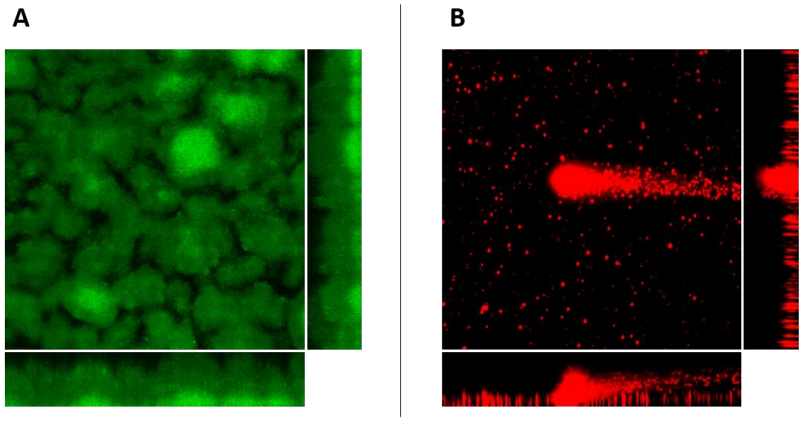

Figure 34. Representative images of *P. aeruginosa* (A) and *A. xylosoxidans* (B) biofilm structures. Biofilms were grown in flow-chambers system for 5 days and monitored by confocal microscopy. *P. aeruginosa* strains were previously tagged with GFP (green), *A. xylosoxidans* was stained with Syto62 (red).

Interestingly, when cultured together the two microbes could form mixed biofilms, suggesting that *A. xylosoxidans* adhesion is probably enhanced on biotic surfaces. In mixed biofilms, we observed a difference between the two stages of infection: in the early stage, *A. xylosoxidans* interferes with *P. aeruginosa* biofilm formation. As shown in figure 35, *P. aeruginosa* aggregates are smaller in presence of *A. xylosoxidans*; this observation is confirmed by the quantification of *P. aeruginosa* biomass, which is reduced in mixed biofilms (Fig. 35C). As previously observed for *P. aeruginosa* growth, the inhibitory effect of *A. xylosoxidans* on *P. aeruginosa* biofilm formation is visible only at the beginning of co-infection, while 3 years later the two species can form mixed aggregates without any visible interference (Fig. 36A-B). *P. aeruginosa* biomass quantification confirmed this observation (Fig. 36C).

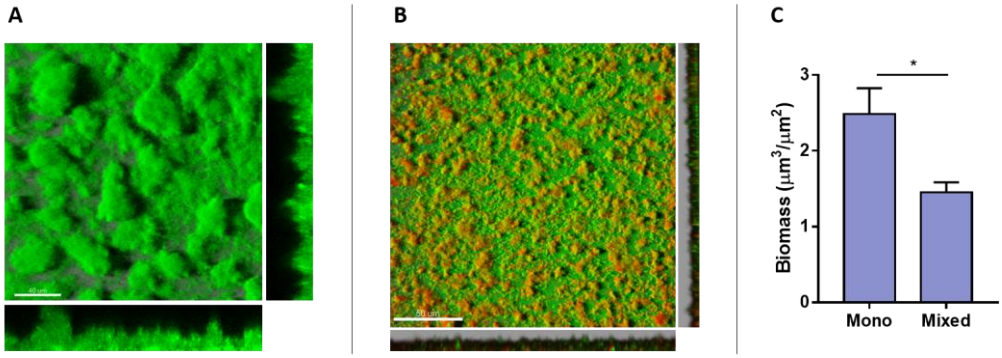

Figure 35. Representative biofilm images of the first *P. aeruginosa* strain in absence (A)/presence (B) of the co-isolated *A. xylosoxidans*. Biofilms were grown in flow-chambers system for 5 days and monitored by confocal microscopy. *P. aeruginosa* strains were previously tagged with GFP (green), *A. xylosoxidans* was counterstained with Syto62 (red). *P. aeruginosa* biomass was calculated using Comstat2 software. Each value represents the mean ± SEM of 3 experiments. Statistical analysis was performed by Mann-Whitney test for non-parametric data, * $p<0.05$ (C).

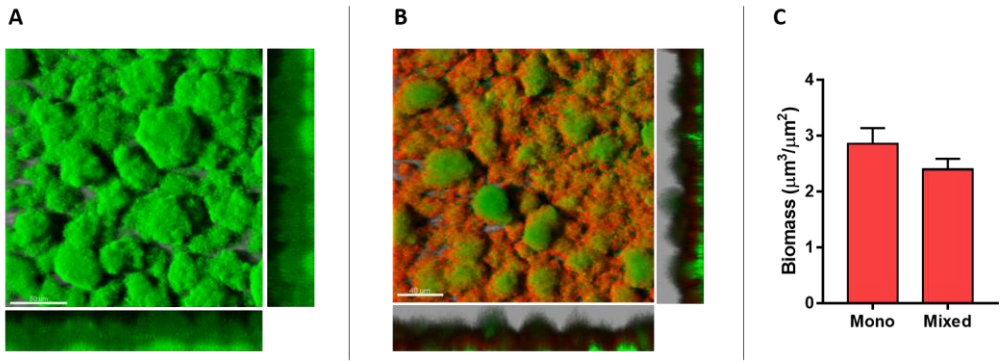

Figure 36. Representative biofilm images of the second *P. aeruginosa* strain in absence (A)/presence (B) of the co-isolated *A. xylosoxidans*. Biofilms were grown in flow-chambers system for 5 days and monitored by confocal microscopy. *P. aeruginosa* strains were previously tagged with GFP (green), *A. xylosoxidans* was counterstained with Syto62 (red). *P. aeruginosa* biomass was calculated using Comstat2 software. Each value represents the mean ± SEM of 3 experiments (C).

A. xylosoxidans exoproducts initially interfere with P. aeruginosa adhesion

P. aeruginosa early isolate showed a significantly lower adhesion ability when grown in presence of the co-isolated *A. xylosoxidans* culture supernatant, containing all the exoproducts released during bacterial growth, including possible virulence factors; again, this effect was not observed between the late isolates, suggesting a competitive effect in the initial stages of co-infection, probably due to virulence factors secreted by *A. xylosoxidans* (Fig. 37).

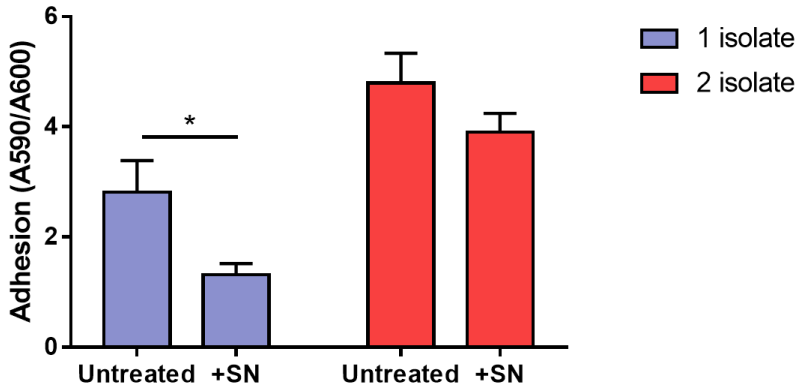

Figura 37. *P. aeruginosa* adhesion in absence (untreated) or presence of the co-isolated *A. xylosoxidans* culture supernatant (SN). Adhesion was measured by crystal violet staining of surface-attached bacteria divided by A_{600} of non-attached bacteria. Each value represents the mean ± SEM of 3 experiments. Statistical analysis was performed by t test, * $p<0.05$.

A. xylosoxidans down-regulates protease secretion over time

To identify possible factors involved in the initial inhibitory effect of *A. xylosoxidans* against *P. aeruginosa*, we searched for the presence of secreted virulence factors in *A. xylosoxidans* culture supernatant. We measured secreted proteases, which are virulence factors typical of many bacterial species and one of the few reported in *A. xylosoxidans* strains. We detected high protease activity in the culture supernatant of the early isolate, while the activity was significantly lower in the late strain (Fig. 38). This finding might help to explain the inhibitory effects observed only at the beginning of the co-infection.

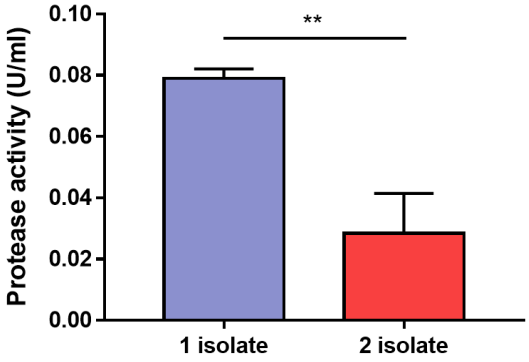

Figure 38. Protease activity in *A. xylosoxidans* culture supernatant measured by azocasein assay. Protease activity is expressed as U/ml. Each value represents the mean ± SEM of 3 experiments. Statistical analysis was performed by t test, ** $p<0.01$.

P. aeruginosa develops resistance against A. xylosoxidans exoproducts

To verify weather *A. xylosoxidans* virulence down-regulation is the only responsible for the apparent reciprocal adaptation of the two microbes, we evaluated the effect of virulence factors secreted by the first *A. xylosoxidans* isolate also against the second *P. aeruginosa* isolate: this late strain did not show a lower adhesion ability when grown in presence of the early *A. xylosoxidans* culture supernatant, containing proteases (Fig. 39). This observation suggests that the adaptation of *P. aeruginosa* in CF airways helps the bacterium to withstand *A. xylosoxidans* virulence.

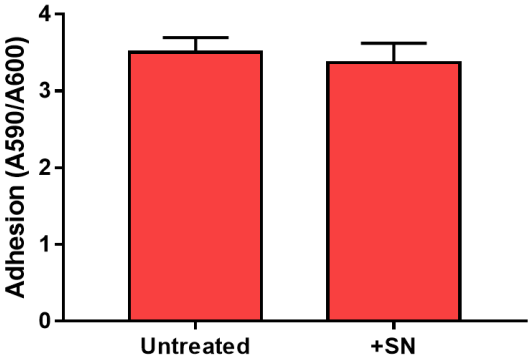

Figura 39. *P. aeruginosa* adhesion in absence (untreated) or presence of culture supernatant (SN) from the first *A. xylosoxidans* isolate. Adhesion was measured by crystal violet staining of surface-attached bacteria divided by A600 of non-attached bacteria. Each value represents the mean ± SEM of 3 experiments.

7.3. Discussion

For long time CF lung infection has been studied and treated as a disease caused by a single pathogen, while nowadays we are aware of its polymicrobial nature. Both pathogens and commensals are isolated from CF airways, leading to consider the whole microbial community as participant in the disease [88, 89]. Within communities, intra- and inter-species interactions can take place and potentially influence the course of the infection [90, 91]. *P. aeruginosa* interactions with other well-known CF pathogens such as *Burkholderia spp.* and *S. aureus* have extensively been studied [125-134]. On the contrary, *P. aeruginosa* interactions with emerging pathogens such as *S. maltophilia* and *A. xylosoxidans* have not been clearly evaluated yet, probably because the clinical relevance of these microorganisms became evident only recently. In the present investigation, we focused on *A. xylosoxidans*, which lately gained attention as an important pathogen that can cause chronic lung infection, further complicated by its innate and acquired multidrug resistance [308]. Despite the increasing number of patients becoming chronically infected with this microorganism, and the frequent co-isolation of *A. xylosoxidans* and *P. aeruginosa* from the same sputum samples, studies about their possible interactions still lack. We investigated the behavior and evolution of *P. aeruginosa* and *A. xylosoxidans* clinical isolates sharing the same CF airway environment for three years.

P. aeruginosa is known to evolve at both genotypic and phenotypic level during chronic infection of CF airways. Particularly, the appearance of mucoid morphology is the most typical feature of late chronic isolates, due to mutations in *mucA* gene leading to overproduction of alginate [101]. This evolution was evident from the first non-mucoid strain isolated in 2005 to the second mucoid strain collected in 2008. We also observed reduction in the growth rate over time, probably due to down-regulation of central metabolism usually associated with *mucA* mutations [115], as well as increase in adhesion ability. Adhesion is another typical feature of chronic *P. aeruginosa*, allowing the bacteria to grow in biofilm communities. Indeed, both *P. aeruginosa* isolates could form large and stable aggregates. On the contrary, *A. xylosoxidans* did not show any of these phenotypic changes. Both isolates grew slowly, showed poor adhesion and could form only sporadic, loosely-attached biofilm structures characterized by dispersal of planktonic cells. This difference in adaptation between the two microorganisms suggests that *A. xylosoxidans* survival and successful lung colonization relies on different mechanisms than *P. aeruginosa*. Thus, further studies about this bacterium might unveil new features involved in microbial persistence within CF airways.

As regards the interaction between the two pathogens, in the early stage of co-infection *A. xylosoxidans* showed inhibitory effects against *P. aeruginosa*, indicating an initial competition. This inhibitory activity was observed at various levels, interfering with *P. aeruginosa* growth, adhesion and biofilm formation. Interestingly, the nature of this interplay changed with time: in the late stage of co-infection the inhibitory effects disappeared, in favor of a more indolent cohabitation or even cooperation, which might represent a survival advantage. In the late stage, the two microbes could also grow together in mixed biofilm

communities, supporting that close microbial interactions might occur between them. Indeed, bacterial proximity within biofilm communities can favor social exchanges of signal molecules and genetic elements, influencing many aspects of the community itself, like microbial composition, nutrients availability, and antibiotic resistance [92, 93]. Although the occurrence of close microbial interactions within the CF airway has not been demonstrated yet, in this particular case their relevance should be considered: *A. xylosoxidans* is rich in mobile genetic elements carrying antibiotic resistance [313], whose exchange and acquisition by other microbes like *P. aeruginosa* might influence the course of infection and the outcome of antibiotic therapies.

Trying to elucidate the mechanisms underlying the initial competition observed between *A. xylosoxidans* and *P. aeruginosa*, we evaluated proteases secretion by *A. xylosoxidans*. Proteases are common bacterial virulence factors involved in infectivity and directed against both host and other microorganisms. The early *A. xylosoxidans* isolate showed strong protease secretion. Although genes related to protease regulation were previously found in *A. xylosoxidans* genome [316], to our knowledge the actual presence of extracellular proteases had never been reported yet. Interestingly, proteases secretion decreased in the late stage of infection. This is the first adaptive change that we could observe between the two *A. xylosoxidans* isolates, suggesting virulence modulation as a mechanism involved in long-term colonization of CF airways by this pathogen. Along with protease down-regulation in *A. xylosoxidans*, we observed an increase of *P. aeruginosa* resistance to these virulence factors, probably resulting from adaptation towards the mucoid phenotype. Thereby, the evolution from initial competition to co-habitation observed between the two pathogens probably depends on adaptive changes involving both microbes and represents a survival advantage in CF airways.

8. Conclusions

Understanding which mechanisms are primarily involved in successful colonization of CF lungs by *P. aeruginosa* and other pathogens is essential to find new therapeutic approaches and develop appropriate treatment regimens. In this thesis, two studies were described, that contributed to this knowledge and pointed at bacterial virulence and microbial interactions as critical players.

We demonstrated that *P. aeruginosa* virulence is strongly involved in host inflammatory response by monitoring in vivo the activation of an exogenous IL-8 promoter. Although this method does not permit to study the molecular and cellular mechanisms underlying immune activation, it gives an appropriate read-out of the inflammatory CF response and is suitable for the evaluation of treatments to dampen lung inflammation. We identified macrolides and protease inhibitors as candidates for anti-inflammatory therapy, thanks to their anti-virulence action on *P. aeruginosa*. As for clarithromycin, we encourage more clinical trials to assess the effectiveness of this therapy, while further in vivo studies about protease inhibitors are needed to better understand the specificity of their action and find appropriate formulations and doses in view of a possible clinical usage.

We added new insights to the mechanisms underlying the colonization of CF airways by the pathogen *A. xylosoxidans* and to its interplay with *P. aeruginosa*. We reported the secretion of proteases by *A. xylosoxidans*, and identified protease down-regulation as an adaptive mechanism of this bacterium in the lung environment. Although further studies to characterize more *A. xylosoxidans* virulence factors are needed, we speculate that virulence down-regulation might have a key role in long-term colonization. As regards its interaction with *P. aeruginosa*, we observed an initial competition evolving towards co-habitation in mixed biofilm communities, suggesting that close social interactions and genetic exchanges might happen. Further studies are needed to clarify the occurrence of these inter-species events and their impact on lung disease.

These studies lead to the following scientific contributions:

- Stellari F., Bergamini G., Sandri A., Donofrio G., Sorio C., Ruscitti F., Villetti G., Asseal B.M., Melotti P., Lleò M.M. *In vivo imaging of the lung inflammatory response to Pseudomonas aeruginosa and its modulation by azithromycin.* Journal of Translational Medicine. 2015, 13:251.

- Stellari F.*, Bergamini G.*, Ruscitti F., Sandri A., Ravanetti F., Donofrio G., Boschi F., Villetti G., Sorio C., Assael B.M., Melotti P., Lleò M.M. *In vivo monitoring of lung inflammation in CFTR-deficient mice.* Journal of Translational Medicine. 2016, 14:226.

- Bergamini G.*, Stellari F.*, Sandri A.*, Lleò M.M., Donofrio G., Ruscitti F., Boschi F., Sbarbati A., Villetti G., Melotti P., Sorio C. *IL-8 transiently transgenized mouse model for the in vivo long-term monitoring of the*

inflammatory response. Journal of Visualized Experiments. 2017 (in-press), e55499, doi:10.3791/55499. *equal contribution

- Sandri A., Haagensen J.A.J., Jimenez Fernandez A., Molin S., Krogh Johansen H., Lleò M.M. *Adaptive microbial interactions between Pseudomonas aeruginosa and Achromobacter xylosoxidans* [abstract]. In: 14th ECFS Basic Science Conference; 2017 Mar 29-Apr 1; Albufeira, Portugal. Journal of Cystic Fibrosis, in-press. Abstract n. 68.

- Sandri A., Stellari F., Boschi F., Ortombina A., Bergamini G.*, Lleò M.M.*. *Matrix metalloprotease inhibitors as anti-inflammatory therapy in Pseudomonas aeruginosa lung infection* [abstract]. In: 14th ECFS Basic Science Conference; 2017 Mar 29-Apr 1; Albufeira, Portugal. Journal of Cystic Fibrosis, in-press. Abstract n. 69.

9. Bibliography

1. O'Sullivan, B.P. and S.D. Freedman, *Cystic fibrosis.* Lancet, 2009. **373**(9678): p. 1891-904.
2. Tsui, L.C., et al., *Cystic fibrosis locus defined by a genetically linked polymorphic DNA marker.* Science, 1985. **230**(4729): p. 1054-7.
3. Wainwright, B.J., et al., *Localization of cystic fibrosis locus to human chromosome 7cen-q22.* Nature, 1985. **318**(6044): p. 384-5.
4. Rowntree, R.K. and A. Harris, *The phenotypic consequences of CFTR mutations.* Ann Hum Genet, 2003. **67**(Pt 5): p. 471-85.
5. Zielenski, J., *Genotype and phenotype in cystic fibrosis.* Respiration, 2000. **67**(2): p. 117-33.
6. Denning, G.M., et al., *Localization of cystic fibrosis transmembrane conductance regulator in chloride secretory epithelia.* J Clin Invest, 1992. **89**(1): p. 339-49.
7. Nagel, G., et al., *The protein kinase A-regulated cardiac Cl- channel resembles the cystic fibrosis transmembrane conductance regulator.* Nature, 1992. **360**(6399): p. 81-4.
8. Michoud, M.C., et al., *Role of the cystic fibrosis transmembrane conductance channel in human airway smooth muscle.* Am J Respir Cell Mol Biol, 2009. **40**(2): p. 217-22.
9. Sprague, R.S., et al., *Deformation-induced ATP release from red blood cells requires CFTR activity.* Am J Physiol, 1998. **275**(5 Pt 2): p. H1726-32.
10. Di, A., et al., *CFTR regulates phagosome acidification in macrophages and alters bactericidal activity.* Nat Cell Biol, 2006. **8**(9): p. 933-44.
11. Painter, R.G., et al., *CFTR Expression in human neutrophils and the phagolysosomal chlorination defect in cystic fibrosis.* Biochemistry, 2006. **45**(34): p. 10260-9.
12. Ford, R.C., et al., *CFTR three-dimensional structure.* Methods Mol Biol, 2011. **741**: p. 329-46.
13. Gadsby, D.C., P. Vergani, and L. Csanady, *The ABC protein turned chloride channel whose failure causes cystic fibrosis.* Nature, 2006. **440**(7083): p. 477-83.
14. Randak, C. and M.J. Welsh, *An intrinsic adenylate kinase activity regulates gating of the ABC transporter CFTR.* Cell, 2003. **115**(7): p. 837-50.
15. Hwang, T.C. and D.N. Sheppard, *Gating of the CFTR Cl- channel by ATP-driven nucleotide-binding domain dimerisation.* J Physiol, 2009. **587**(Pt 10): p. 2151-61.

16. Vergani, P., et al., *CFTR channel opening by ATP-driven tight dimerization of its nucleotide-binding domains.* Nature, 2005. **433**(7028): p. 876-80.
17. Stutts, M.J., et al., *CFTR as a cAMP-dependent regulator of sodium channels.* Science, 1995. **269**(5225): p. 847-50.
18. McNicholas, C.M., et al., *Sensitivity of a renal K+ channel (ROMK2) to the inhibitory sulfonylurea compound glibenclamide is enhanced by coexpression with the ATP-binding cassette transporter cystic fibrosis transmembrane regulator.* Proc Natl Acad Sci U S A, 1996. **93**(15): p. 8083-8.
19. Schwiebert, E.M., et al., *CFTR regulates outwardly rectifying chloride channels through an autocrine mechanism involving ATP.* Cell, 1995. **81**(7): p. 1063-73.
20. Wei, L., et al., *The C-terminal part of the R-domain, but not the PDZ binding motif, of CFTR is involved in interaction with Ca(2+)-activated Cl- channels.* Pflugers Arch, 2001. **442**(2): p. 280-5.
21. Schreiber, R., et al., *Cystic fibrosis transmembrane conductance regulator activates water conductance in Xenopus oocytes.* Pflugers Arch, 1997. **434**(6): p. 841-7.
22. Quinton, P.M., *Cystic fibrosis: impaired bicarbonate secretion and mucoviscidosis.* Lancet, 2008. **372**(9636): p. 415-7.
23. Reisin, I.L., et al., *The cystic fibrosis transmembrane conductance regulator is a dual ATP and chloride channel.* J Biol Chem, 1994. **269**(32): p. 20584-91.
24. Jouret, F., et al., *Cystic fibrosis is associated with a defect in apical receptor-mediated endocytosis in mouse and human kidney.* J Am Soc Nephrol, 2007. **18**(3): p. 707-18.
25. Barasch, J., et al., *Defective acidification of intracellular organelles in cystic fibrosis.* Nature, 1991. **352**(6330): p. 70-3.
26. Bergamini, G., et al., *Effects of azithromycin on glutathione S-transferases in cystic fibrosis airway cells.* Am J Respir Cell Mol Biol, 2009. **41**(2): p. 199-206.
27. Vandivier, R.W., et al., *Dysfunctional cystic fibrosis transmembrane conductance regulator inhibits phagocytosis of apoptotic cells with proinflammatory consequences.* Am J Physiol Lung Cell Mol Physiol, 2009. **297**(4): p. L677-86.
28. Quinton, P.M., *Cystic fibrosis: lessons from the sweat gland.* Physiology (Bethesda), 2007. **22**: p. 212-25.
29. Derichs, N., *Targeting a genetic defect: cystic fibrosis transmembrane conductance regulator modulators in cystic fibrosis.* Eur Respir Rev, 2013. **22**(127): p. 58-65.

30. Lubamba, B., et al., *Cystic fibrosis: insight into CFTR pathophysiology and pharmacotherapy.* Clin Biochem, 2012. **45**(15): p. 1132-44.
31. Radpour, R., et al., *Genetic investigations of CFTR mutations in congenital absence of vas deferens, uterus, and vagina as a cause of infertility.* J Androl, 2008. **29**(5): p. 506-13.
32. Chan, H.C., et al., *The cystic fibrosis transmembrane conductance regulator in reproductive health and disease.* J Physiol, 2009. **587**(Pt 10): p. 2187-95.
33. Rowe, S.M., S. Miller, and E.J. Sorscher, *Cystic fibrosis.* N Engl J Med, 2005. **352**(19): p. 1992-2001.
34. Engelhardt, J.F., et al., *Submucosal glands are the predominant site of CFTR expression in the human bronchus.* Nat Genet, 1992. **2**(3): p. 240-8.
35. Kreda, S.M., et al., *Characterization of wild-type and deltaF508 cystic fibrosis transmembrane regulator in human respiratory epithelia.* Mol Biol Cell, 2005. **16**(5): p. 2154-67.
36. Derichs, N., et al., *Hyperviscous airway periciliary and mucous liquid layers in cystic fibrosis measured by confocal fluorescence photobleaching.* FASEB J, 2011. **25**(7): p. 2325-32.
37. Boucher, R.C., *Airway surface dehydration in cystic fibrosis: pathogenesis and therapy.* Annu Rev Med, 2007. **58**: p. 157-70.
38. Mall, M. and R. Boucher, *Pathogenesis of Pulmonary Disease in Cystic Fibrosis.* Prog Respir Res, 2006. **34**: p. 116-121.
39. Weber, A.J., et al., *Activation of NF-kappaB in airway epithelial cells is dependent on CFTR trafficking and Cl- channel function.* Am J Physiol Lung Cell Mol Physiol, 2001. **281**(1): p. L71-8.
40. Perez, A., et al., *CFTR inhibition mimics the cystic fibrosis inflammatory profile.* Am J Physiol Lung Cell Mol Physiol, 2007. **292**(2): p. L383-95.
41. Saadane, A., J. Soltys, and M. Berger, *Role of IL-10 deficiency in excessive nuclear factor-kappaB activation and lung inflammation in cystic fibrosis transmembrane conductance regulator knockout mice.* J Allergy Clin Immunol, 2005. **115**(2): p. 405-11.
42. Parker, D., et al., *Induction of type I interferon signaling by Pseudomonas aeruginosa is diminished in cystic fibrosis epithelial cells.* Am J Respir Cell Mol Biol, 2012. **46**(1): p. 6-13.

43. Kelley, T.J. and H.L. Elmer, *In vivo alterations of IFN regulatory factor-1 and PIAS1 protein levels in cystic fibrosis epithelium.* J Clin Invest, 2000. **106**(3): p. 403-10.
44. Roussel, L., R. Farias, and S. Rousseau, *IL-33 is expressed in epithelia from patients with cystic fibrosis and potentiates neutrophil recruitment.* J Allergy Clin Immunol, 2013. **131**(3): p. 913-6.
45. Bonfield, T.L., et al., *Inflammatory cytokines in cystic fibrosis lungs.* Am J Respir Crit Care Med, 1995. **152**(6 Pt 1): p. 2111-8.
46. Moser, C., et al., *Serum concentrations of GM-CSF and G-CSF correlate with the Th1/Th2 cytokine response in cystic fibrosis patients with chronic Pseudomonas aeruginosa lung infection.* APMIS, 2005. **113**(6): p. 400-9.
47. Tiringer, K., et al., *Differential expression of IL-33 and HMGB1 in the lungs of stable cystic fibrosis patients.* Eur Respir J, 2014. **44**(3): p. 802-5.
48. Khan, T.Z., et al., *Early pulmonary inflammation in infants with cystic fibrosis.* Am J Respir Crit Care Med, 1995. **151**(4): p. 1075-82.
49. Tan, H.L. and M. Rosenthal, *IL-17 in lung disease: friend or foe?* Thorax, 2013. **68**(8): p. 788-90.
50. Balfour-Lynn, I.M., A. Laverty, and R. Dinwiddie, *Reduced upper airway nitric oxide in cystic fibrosis.* Arch Dis Child, 1996. **75**(4): p. 319-22.
51. Bonfield, T.L., M.W. Konstan, and M. Berger, *Altered respiratory epithelial cell cytokine production in cystic fibrosis.* J Allergy Clin Immunol, 1999. **104**(1): p. 72-8.
52. Grasemann, H., et al., *Decreased concentration of exhaled nitric oxide (NO) in patients with cystic fibrosis.* Pediatr Pulmonol, 1997. **24**(3): p. 173-7.
53. Karp, C.L., et al., *Defective lipoxin-mediated anti-inflammatory activity in the cystic fibrosis airway.* Nat Immunol, 2004. **5**(4): p. 388-92.
54. Moss, R.B., et al., *Reduced IL-10 secretion by CD4+ T lymphocytes expressing mutant cystic fibrosis transmembrane conductance regulator (CFTR).* Clin Exp Immunol, 1996. **106**(2): p. 374-88.
55. Sato, Y., et al., *Nitric oxide reduces the sequestration of polymorphonuclear leukocytes in lung by changing deformability and CD18 expression.* Am J Respir Crit Care Med, 1999. **159**(5 Pt 1): p. 1469-76.
56. Painter, R.G., et al., *The role of chloride anion and CFTR in killing of Pseudomonas aeruginosa by normal and CF neutrophils.* J Leukoc Biol, 2008. **83**(6): p. 1345-53.

57. Painter, R.G., et al., *CFTR-mediated halide transport in phagosomes of human neutrophils.* J Leukoc Biol, 2010. **87**(5): p. 933-42.
58. Colombo, C., et al., *Analysis of inflammatory and immune response biomarkers in sputum and exhaled breath condensate by a multi-parametric biochip array in cystic fibrosis.* Int J Immunopathol Pharmacol, 2011. **24**(2): p. 423-32.
59. Liu, G., et al., *High mobility group protein-1 inhibits phagocytosis of apoptotic neutrophils through binding to phosphatidylserine.* J Immunol, 2008. **181**(6): p. 4240-6.
60. Nichols, D.P. and J.F. Chmiel, *Inflammation and its genesis in cystic fibrosis.* Pediatr Pulmonol, 2015. **50 Suppl 40**: p. S39-56.
61. Kirk, K.L. and D.C. Dawson, *The Cystic Fibrosis Transmembrane Conductance Regulator*. Molecular Biology Intelligence Unit. 2003: Springer US.
62. Bartling, T.R. and M.L. Drumm, *Oxidative stress causes IL8 promoter hyperacetylation in cystic fibrosis airway cell models.* Am J Respir Cell Mol Biol, 2009. **40**(1): p. 58-65.
63. Smallman, L.A., S.L. Hill, and R.A. Stockley, *Reduction of ciliary beat frequency in vitro by sputum from patients with bronchiectasis: a serine proteinase effect.* Thorax, 1984. **39**(9): p. 663-7.
64. Park, J.A., et al., *Human neutrophil elastase induces hypersecretion of mucin from well-differentiated human bronchial epithelial cells in vitro via a protein kinase C{delta}-mediated mechanism.* Am J Pathol, 2005. **167**(3): p. 651-61.
65. Caldwell, R.A., R.C. Boucher, and M.J. Stutts, *Neutrophil elastase activates near-silent epithelial Na+ channels and increases airway epithelial Na+ transport.* Am J Physiol Lung Cell Mol Physiol, 2005. **288**(5): p. L813-9.
66. Nakamura, H., et al., *Neutrophil elastase in respiratory epithelial lining fluid of individuals with cystic fibrosis induces interleukin-8 gene expression in a human bronchial epithelial cell line.* J Clin Invest, 1992. **89**(5): p. 1478-84.
67. Tosi, M.F., H. Zakem, and M. Berger, *Neutrophil elastase cleaves C3bi on opsonized pseudomonas as well as CR1 on neutrophils to create a functionally important opsonin receptor mismatch.* J Clin Invest, 1990. **86**(1): p. 300-8.
68. Vandivier, R.W., et al., *Elastase-mediated phosphatidylserine receptor cleavage impairs apoptotic cell clearance in cystic fibrosis and bronchiectasis.* J Clin Invest, 2002. **109**(5): p. 661-70.

69. Le Gars, M., et al., *Neutrophil elastase degrades cystic fibrosis transmembrane conductance regulator via calpains and disables channel function in vitro and in vivo.* Am J Respir Crit Care Med, 2013. **187**(2): p. 170-9.
70. Mayer-Hamblett, N., et al., *Association between pulmonary function and sputum biomarkers in cystic fibrosis.* Am J Respir Crit Care Med, 2007. **175**(8): p. 822-8.
71. Sagel, S.D., et al., *Induced sputum inflammatory measures correlate with lung function in children with cystic fibrosis.* J Pediatr, 2002. **141**(6): p. 811-7.
72. Sly, P.D., et al., *Risk factors for bronchiectasis in children with cystic fibrosis.* N Engl J Med, 2013. **368**(21): p. 1963-70.
73. Brennan, S., et al., *Alveolar macrophages and CC chemokines are increased in children with cystic fibrosis.* Eur Respir J, 2009. **34**(3): p. 655-61.
74. Meyer, M., et al., *Azithromycin reduces exaggerated cytokine production by M1 alveolar macrophages in cystic fibrosis.* Am J Respir Cell Mol Biol, 2009. **41**(5): p. 590-602.
75. Bruscia, E.M., et al., *Macrophages directly contribute to the exaggerated inflammatory response in cystic fibrosis transmembrane conductance regulator-/- mice.* Am J Respir Cell Mol Biol, 2009. **40**(3): p. 295-304.
76. Deriy, L.V., et al., *Disease-causing mutations in the cystic fibrosis transmembrane conductance regulator determine the functional responses of alveolar macrophages.* J Biol Chem, 2009. **284**(51): p. 35926-38.
77. Pillarisetti, N., et al., *Infection, inflammation, and lung function decline in infants with cystic fibrosis.* Am J Respir Crit Care Med, 2011. **184**(1): p. 75-81.
78. Ciofu, O., C.R. Hansen, and N. Hoiby, *Respiratory bacterial infections in cystic fibrosis.* Curr Opin Pulm Med, 2013. **19**(3): p. 251-8.
79. Aanaes, K., et al., *Decreased mucosal oxygen tension in the maxillary sinuses in patients with cystic fibrosis.* J Cyst Fibros, 2011. **10**(2): p. 114-20.
80. Hansen, C.R., et al., *Inflammation in Achromobacter xylosoxidans infected cystic fibrosis patients.* J Cyst Fibros, 2010. **9**(1): p. 51-8.
81. Lambiase, A., et al., *Achromobacter xylosoxidans respiratory tract infection in cystic fibrosis patients.* Eur J Clin Microbiol Infect Dis, 2011. **30**(8): p. 973-80.
82. Hu, Y., et al., *Genomic insights into intrinsic and acquired drug resistance mechanisms in Achromobacter xylosoxidans.* Antimicrob Agents Chemother, 2015. **59**(2): p. 1152-61.

83. Traglia, G.M., et al., *Achromobacter xylosoxidans: an emerging pathogen carrying different elements involved in horizontal genetic transfer.* Curr Microbiol, 2012. **65**(6): p. 673-8.
84. Lynch, J.P., 3rd, *Burkholderia cepacia complex: impact on the cystic fibrosis lung lesion.* Semin Respir Crit Care Med, 2009. **30**(5): p. 596-610.
85. Ulrich, M., et al., *Relative contribution of Prevotella intermedia and Pseudomonas aeruginosa to lung pathology in airways of patients with cystic fibrosis.* Thorax, 2010. **65**(11): p. 978-84.
86. Tunney, M.M., et al., *Detection of anaerobic bacteria in high numbers in sputum from patients with cystic fibrosis.* Am J Respir Crit Care Med, 2008. **177**(9): p. 995-1001.
87. Lebecque, P., et al., *ABPA in adulthood: a CFTR-related disorder.* Thorax, 2011. **66**(6): p. 540-1.
88. Rabin, H.R. and M.G. Surette, *The cystic fibrosis airway microbiome.* Curr Opin Pulm Med, 2012. **18**(6): p. 622-7.
89. Lim, Y.W., et al., *Clinical insights from metagenomic analysis of sputum samples from patients with cystic fibrosis.* J Clin Microbiol, 2014. **52**(2): p. 425-37.
90. McGuigan, L. and M. Callaghan, *The evolving dynamics of the microbial community in the cystic fibrosis lung.* Environ Microbiol, 2015. **17**(1): p. 16-28.
91. Tashiro, Y., et al., *Interspecies interaction between Pseudomonas aeruginosa and other microorganisms.* Microbes Environ, 2013. **28**(1): p. 13-24.
92. De Oliveira, R.V.D., *Interactions among cariogenic bacterial species in oral biofilm* in *The Battle Against Microbial Pathogens: Basic Science, Technological Advances and Educational Programs*, A. Méndez-Vilas, Editor. 2015, Formatex Research Center. p. 438-444.
93. Kuramitsu, H.K., et al., *Interspecies interactions within oral microbial communities.* Microbiol Mol Biol Rev, 2007. **71**(4): p. 653-70.
94. Hall-Stoodley, L. and P. Stoodley, *Evolving concepts in biofilm infections.* Cell Microbiol, 2009. **11**(7): p. 1034-43.
95. Lieleg, O., et al., *Mechanical robustness of Pseudomonas aeruginosa biofilms.* Soft Matter, 2011. **7**(7): p. 3307-3314.
96. Bjarnsholt, T., *The role of bacterial biofilms in chronic infections.* APMIS Suppl, 2013(136): p. 1-51.
97. Hart, C.A. and C. Winstanley, *Persistent and aggressive bacteria in the lungs of cystic fibrosis children.* Br Med Bull, 2002. **61**: p. 81-96.

98. Vonberg, R.P. and P. Gastmeier, *Isolation of infectious cystic fibrosis patients: results of a systematic review.* Infect Control Hosp Epidemiol, 2005. **26**(4): p. 401-9.

99. Tramper-Stranders, G.A., et al., *Diagnostic value of serological tests against Pseudomonas aeruginosa in a large cystic fibrosis population.* Thorax, 2006. **61**(8): p. 689-93.

100. Johansen, H.K. and N. Hoiby, *Seasonal onset of initial colonisation and chronic infection with Pseudomonas aeruginosa in patients with cystic fibrosis in Denmark.* Thorax, 1992. **47**(2): p. 109-11.

101. Hansen, S.K., et al., *Evolution and diversification of Pseudomonas aeruginosa in the paranasal sinuses of cystic fibrosis children have implications for chronic lung infection.* ISME J, 2012. **6**(1): p. 31-45.

102. Johansen, H.K., et al., *Colonisation and infection of the paranasal sinuses in cystic fibrosis patients is accompanied by a reduced PMN response.* J Cyst Fibros, 2012. **11**(6): p. 525-31.

103. Bjarnsholt, T., et al., *Pseudomonas aeruginosa biofilms in the respiratory tract of cystic fibrosis patients.* Pediatr Pulmonol, 2009. **44**(6): p. 547-58.

104. de Jong, P.A., et al., *Progressive damage on high resolution computed tomography despite stable lung function in cystic fibrosis.* Eur Respir J, 2004. **23**(1): p. 93-7.

105. Ulrich, M., et al., *Alveolar inflammation in cystic fibrosis.* J Cyst Fibros, 2010. **9**(3): p. 217-27.

106. Hoiby, N. and H.K. Johansen, *Isolation measures for prevention of infection with respiratory pathogens in cystic fibrosis: a systematic review?* J Hosp Infect, 2007. **65**(4): p. 374-5; author reply 375-6.

107. Ciofu, O., et al., *Genetic adaptation of Pseudomonas aeruginosa during chronic lung infection of patients with cystic fibrosis: strong and weak mutators with heterogeneous genetic backgrounds emerge in mucA and/or lasR mutants.* Microbiology, 2010. **156**(Pt 4): p. 1108-19.

108. Rau, M.H., et al., *Early adaptive developments of Pseudomonas aeruginosa after the transition from life in the environment to persistent colonization in the airways of human cystic fibrosis hosts.* Environ Microbiol, 2010. **12**(6): p. 1643-58.

109. Boucher, J.C., et al., *Mucoid Pseudomonas aeruginosa in cystic fibrosis: characterization of muc mutations in clinical isolates and analysis of clearance in a mouse model of respiratory infection.* Infect Immun, 1997. **65**(9): p. 3838-46.
110. Martin, D.W., et al., *Mechanism of conversion to mucoidy in Pseudomonas aeruginosa infecting cystic fibrosis patients.* Proc Natl Acad Sci U S A, 1993. **90**(18): p. 8377-81.
111. Chitnis, C.E. and D.E. Ohman, *Genetic analysis of the alginate biosynthetic gene cluster of Pseudomonas aeruginosa shows evidence of an operonic structure.* Mol Microbiol, 1993. **8**(3): p. 583-93.
112. Deretic, V., et al., *Conversion of Pseudomonas aeruginosa to mucoidy in cystic fibrosis: environmental stress and regulation of bacterial virulence by alternative sigma factors.* J Bacteriol, 1994. **176**(10): p. 2773-80.
113. DeVries, C.A. and D.E. Ohman, *Mucoid-to-nonmucoid conversion in alginate-producing Pseudomonas aeruginosa often results from spontaneous mutations in algT, encoding a putative alternate sigma factor, and shows evidence for autoregulation.* J Bacteriol, 1994. **176**(21): p. 6677-87.
114. Ramsey, D.M. and D.J. Wozniak, *Understanding the control of Pseudomonas aeruginosa alginate synthesis and the prospects for management of chronic infections in cystic fibrosis.* Mol Microbiol, 2005. **56**(2): p. 309-22.
115. Wood, L.F. and D.E. Ohman, *Identification of genes in the sigma(2)(2) regulon of Pseudomonas aeruginosa required for cell envelope homeostasis in either the planktonic or the sessile mode of growth.* MBio, 2012. **3**(3).
116. Hauser, A.R., et al., *Clinical significance of microbial infection and adaptation in cystic fibrosis.* Clin Microbiol Rev, 2011. **24**(1): p. 29-70.
117. Wood, L.F., A.J. Leech, and D.E. Ohman, *Cell wall-inhibitory antibiotics activate the alginate biosynthesis operon in Pseudomonas aeruginosa: Roles of sigma (AlgT) and the AlgW and Prc proteases.* Mol Microbiol, 2006. **62**(2): p. 412-26.
118. Wood, L.F. and D.E. Ohman, *Use of cell wall stress to characterize sigma 22 (AlgT/U) activation by regulated proteolysis and its regulon in Pseudomonas aeruginosa.* Mol Microbiol, 2009. **72**(1): p. 183-201.
119. Pedersen, S.S., et al., *Pseudomonas aeruginosa alginate in cystic fibrosis sputum and the inflammatory response.* Infect Immun, 1990. **58**(10): p. 3363-8.
120. Winnie, G.B. and R.G. Cowan, *Respiratory tract colonization with Pseudomonas aeruginosa in cystic fibrosis: correlations between anti-Pseudomonas aeruginosa*

antibody levels and pulmonary function. Pediatr Pulmonol, 1991. **10**(2): p. 92-100.

121. Breidenstein, E.B., C. de la Fuente-Nunez, and R.E. Hancock, *Pseudomonas aeruginosa: all roads lead to resistance.* Trends Microbiol, 2011. **19**(8): p. 419-26.

122. Strateva, T. and D. Yordanov, *Pseudomonas aeruginosa - a phenomenon of bacterial resistance.* J Med Microbiol, 2009. **58**(Pt 9): p. 1133-48.

123. Oliver, A., et al., *High frequency of hypermutable Pseudomonas aeruginosa in cystic fibrosis lung infection.* Science, 2000. **288**(5469): p. 1251-4.

124. Ren, C.L., et al., *Multiple antibiotic-resistant Pseudomonas aeruginosa and lung function decline in patients with cystic fibrosis.* J Cyst Fibros, 2012. **11**(4): p. 293-9.

125. Chattoraj, S.S., et al., *Pseudomonas aeruginosa alginate promotes Burkholderia cenocepacia persistence in cystic fibrosis transmembrane conductance regulator knockout mice.* Infect Immun, 2010. **78**(3): p. 984-93.

126. Bragonzi, A., et al., *Modelling co-infection of the cystic fibrosis lung by Pseudomonas aeruginosa and Burkholderia cenocepacia reveals influences on biofilm formation and host response.* PLoS One, 2012. **7**(12): p. e52330.

127. El-Halfawy, O.M. and M.A. Valvano, *Chemical communication of antibiotic resistance by a highly resistant subpopulation of bacterial cells.* PLoS One, 2013. **8**(7): p. e68874.

128. Bakkal, S., et al., *Role of bacteriocins in mediating interactions of bacterial isolates taken from cystic fibrosis patients.* Microbiology, 2010. **156**(Pt 7): p. 2058-67.

129. Waite, R.D. and M.A. Curtis, *Pseudomonas aeruginosa PAO1 pyocin production affects population dynamics within mixed-culture biofilms.* J Bacteriol, 2009. **191**(4): p. 1349-54.

130. Smith, K., et al., *Activity of pyocin S2 against Pseudomonas aeruginosa biofilms.* Antimicrob Agents Chemother, 2012. **56**(3): p. 1599-601.

131. Lowery, C.A., et al., *Defining the mode of action of tetramic acid antibacterials derived from Pseudomonas aeruginosa quorum sensing signals.* J Am Chem Soc, 2009. **131**(40): p. 14473-9.

132. Yang, L., et al., *Pattern differentiation in co-culture biofilms formed by Staphylococcus aureus and Pseudomonas aeruginosa.* FEMS Immunol Med Microbiol, 2011. **62**(3): p. 339-47.

133. Hoffman, L.R., et al., *Selection for Staphylococcus aureus small-colony variants due to growth in the presence of Pseudomonas aeruginosa.* Proc Natl Acad Sci U S A, 2006. **103**(52): p. 19890-5.
134. Hubert, D., et al., *Association between Staphylococcus aureus alone or combined with Pseudomonas aeruginosa and the clinical condition of patients with cystic fibrosis.* J Cyst Fibros, 2013. **12**(5): p. 497-503.
135. Pompilio, A., et al., *Cooperative pathogenicity in cystic fibrosis: Stenotrophomonas maltophilia modulates Pseudomonas aeruginosa virulence in mixed biofilm.* Front Microbiol, 2015. **6**: p. 951.
136. De Baets, F., et al., *Achromobacter xylosoxidans in cystic fibrosis: prevalence and clinical relevance.* J Cyst Fibros, 2007. **6**(1): p. 75-8.
137. Hansen, C.R., *Chronic infection with Achromobacter xylosoxidans in cystic fibrosis patients; a retrospective case control study.* J Cyst Fibros, 2006. **5**(4): p. 245-251.
138. Hogardt, M. and J. Heesemann, *Adaptation of Pseudomonas aeruginosa during persistence in the cystic fibrosis lung.* Int J Med Microbiol, 2010. **300**(8): p. 557-62.
139. Miao, E.A., et al., *TLR5 and Ipaf: dual sensors of bacterial flagellin in the innate immune system.* Semin Immunopathol, 2007. **29**(3): p. 275-88.
140. Wolfgang, M.C., et al., *Pseudomonas aeruginosa regulates flagellin expression as part of a global response to airway fluid from cystic fibrosis patients.* Proc Natl Acad Sci U S A, 2004. **101**(17): p. 6664-8.
141. Kohler, T., et al., *Swarming of Pseudomonas aeruginosa is dependent on cell-to-cell signaling and requires flagella and pili.* J Bacteriol, 2000. **182**(21): p. 5990-6.
142. Yeung, A.T., et al., *Swarming of Pseudomonas aeruginosa is controlled by a broad spectrum of transcriptional regulators, including MetR.* J Bacteriol, 2009. **191**(18): p. 5592-602.
143. Craig, L., M.E. Pique, and J.A. Tainer, *Type IV pilus structure and bacterial pathogenicity.* Nat Rev Microbiol, 2004. **2**(5): p. 363-78.
144. Sriramulu, D.D., et al., *Microcolony formation: a novel biofilm model of Pseudomonas aeruginosa for the cystic fibrosis lung.* J Med Microbiol, 2005. **54**(Pt 7): p. 667-76.

145. Kelly, N.M., et al., *Pseudomonas aeruginosa pili as ligands for nonopsonic phagocytosis by fibronectin-stimulated macrophages.* Infect Immun, 1989. **57**(12): p. 3841-5.
146. King, J.D., et al., *Review: Lipopolysaccharide biosynthesis in Pseudomonas aeruginosa.* Innate Immun, 2009. **15**(5): p. 261-312.
147. Ernst, R.K., et al., *Unique lipid a modifications in Pseudomonas aeruginosa isolated from the airways of patients with cystic fibrosis.* J Infect Dis, 2007. **196**(7): p. 1088-92.
148. Hancock, R.E., et al., *Pseudomonas aeruginosa isolates from patients with cystic fibrosis: a class of serum-sensitive, nontypable strains deficient in lipopolysaccharide O side chains.* Infect Immun, 1983. **42**(1): p. 170-7.
149. Sadikot, R.T., et al., *Pathogen-host interactions in Pseudomonas aeruginosa pneumonia.* Am J Respir Crit Care Med, 2005. **171**(11): p. 1209-23.
150. Hauser, A.R., *The type III secretion system of Pseudomonas aeruginosa: infection by injection.* Nat Rev Microbiol, 2009. **7**(9): p. 654-65.
151. Miyata, S., et al., *Use of the Galleria mellonella caterpillar as a model host to study the role of the type III secretion system in Pseudomonas aeruginosa pathogenesis.* Infect Immun, 2003. **71**(5): p. 2404-13.
152. Shaver, C.M. and A.R. Hauser, *Relative contributions of Pseudomonas aeruginosa ExoU, ExoS, and ExoT to virulence in the lung.* Infect Immun, 2004. **72**(12): p. 6969-77.
153. Neeld, D., et al., *Pseudomonas aeruginosa injects NDK into host cells through a type III secretion system.* Microbiology, 2014. **160**(Pt 7): p. 1417-26.
154. Deep, A., U. Chaudhary, and V. Gupta, *Quorum sensing and Bacterial Pathogenicity: From Molecules to Disease.* J Lab Physicians, 2011. **3**(1): p. 4-11.
155. Heeb, S., et al., *Quinolones: from antibiotics to autoinducers.* FEMS Microbiol Rev, 2011. **35**(2): p. 247-74.
156. Kipnis, E., T. Sawa, and J. Wiener-Kronish, *Targeting mechanisms of Pseudomonas aeruginosa pathogenesis.* Med Mal Infect, 2006. **36**(2): p. 78-91.
157. Pearson, J.P., et al., *Pseudomonas aeruginosa cell-to-cell signaling is required for virulence in a model of acute pulmonary infection.* Infect Immun, 2000. **68**(7): p. 4331-4.
158. Fleiszig, S.M. and D.J. Evans, *The pathogenesis of bacterial keratitis: studies with Pseudomonas aeruginosa.* Clin Exp Optom, 2002. **85**(5): p. 271-8.

159. Hobden, J.A., *Pseudomonas aeruginosa proteases and corneal virulence.* DNA Cell Biol, 2002. **21**(5-6): p. 391-6.
160. Laarman, A.J., et al., *Pseudomonas aeruginosa alkaline protease blocks complement activation via the classical and lectin pathways.* J Immunol, 2012. **188**(1): p. 386-93.
161. Horvat, R.T. and M.J. Parmely, *Pseudomonas aeruginosa alkaline protease degrades human gamma interferon and inhibits its bioactivity.* Infect Immun, 1988. **56**(11): p. 2925-32.
162. Krunkosky, T.M., et al., *Inhibition of tumor necrosis factor-alpha-induced RANTES secretion by alkaline protease in A549 cells.* Am J Respir Cell Mol Biol, 2005. **33**(5): p. 483-9.
163. Leidal, K.G., et al., *Metalloproteases from Pseudomonas aeruginosa degrade human RANTES, MCP-1, and ENA-78.* J Interferon Cytokine Res, 2003. **23**(6): p. 307-18.
164. Parmely, M., et al., *Proteolytic inactivation of cytokines by Pseudomonas aeruginosa.* Infect Immun, 1990. **58**(9): p. 3009-14.
165. Matsumoto, T., et al., *Efficacies of alkaline protease, elastase and exotoxin A toxoid vaccines against gut-derived Pseudomonas aeruginosa sepsis in mice.* J Med Microbiol, 1998. **47**(4): p. 303-8.
166. Bardoel, B.W., et al., *Pseudomonas evades immune recognition of flagellin in both mammals and plants.* PLoS Pathog, 2011. **7**(8): p. e1002206.
167. Butterworth, M.B., et al., *Activation of the epithelial sodium channel (ENaC) by the alkaline protease from Pseudomonas aeruginosa.* J Biol Chem, 2012. **287**(39): p. 32556-65.
168. de Kievit, T.R. and B.H. Iglewski, *Bacterial quorum sensing in pathogenic relationships.* Infect Immun, 2000. **68**(9): p. 4839-49.
169. Toder, D.S., et al., *lasA and lasB genes of Pseudomonas aeruginosa: analysis of transcription and gene product activity.* Infect Immun, 1994. **62**(4): p. 1320-7.
170. Mariencheck, W.I., et al., *Pseudomonas aeruginosa elastase degrades surfactant proteins A and D.* Am J Respir Cell Mol Biol, 2003. **28**(4): p. 528-37.
171. Azghani, A.O., T. Bedinghaus, and R. Klein, *Detection of elastase from Pseudomonas aeruginosa in sputum and its potential role in epithelial cell permeability.* Lung, 2000. **178**(3): p. 181-9.

172. Dulon, S., et al., *Pseudomonas aeruginosa elastase disables proteinase-activated receptor 2 in respiratory epithelial cells.* Am J Respir Cell Mol Biol, 2005. **32**(5): p. 411-9.
173. Leduc, D., et al., *The Pseudomonas aeruginosa LasB metalloproteinase regulates the human urokinase-type plasminogen activator receptor through domain-specific endoproteolysis.* Infect Immun, 2007. **75**(8): p. 3848-58.
174. Kuang, Z., et al., *Pseudomonas aeruginosa elastase provides an escape from phagocytosis by degrading the pulmonary surfactant protein-A.* PLoS One, 2011. **6**(11): p. e27091.
175. Matsumoto, K., *Role of bacterial proteases in pseudomonal and serratial keratitis.* Biol Chem, 2004. **385**(11): p. 1007-16.
176. Malloy, J.L., et al., *Pseudomonas aeruginosa protease IV degrades surfactant proteins and inhibits surfactant host defense and biophysical functions.* Am J Physiol Lung Cell Mol Physiol, 2005. **288**(2): p. L409-18.
177. Hall, S., et al., *Cellular Effects of Pyocyanin, a Secreted Virulence Factor of Pseudomonas aeruginosa.* Toxins (Basel), 2016. **8**(8).
178. Suntres, Z.E., A. Omri, and P.N. Shek, *Pseudomonas aeruginosa-induced lung injury: role of oxidative stress.* Microb Pathog, 2002. **32**(1): p. 27-34.
179. Gloyne, L.S., et al., *Pyocyanin-induced toxicity in A549 respiratory cells is causally linked to oxidative stress.* Toxicol In Vitro, 2011. **25**(7): p. 1353-8.
180. Allen, L., et al., *Pyocyanin production by Pseudomonas aeruginosa induces neutrophil apoptosis and impairs neutrophil-mediated host defenses in vivo.* J Immunol, 2005. **174**(6): p. 3643-9.
181. Prince, L.R., et al., *Subversion of a lysosomal pathway regulating neutrophil apoptosis by a major bacterial toxin, pyocyanin.* J Immunol, 2008. **180**(5): p. 3502-11.
182. Bianchi, S.M., et al., *Impairment of apoptotic cell engulfment by pyocyanin, a toxic metabolite of Pseudomonas aeruginosa.* Am J Respir Crit Care Med, 2008. **177**(1): p. 35-43.
183. Denning, G.M., et al., *Pseudomonas pyocyanin increases interleukin-8 expression by human airway epithelial cells.* Infect Immun, 1998. **66**(12): p. 5777-84.
184. Leidal, K.G., K.L. Munson, and G.M. Denning, *Small molecular weight secretory factors from Pseudomonas aeruginosa have opposite effects on IL-8*

and RANTES expression by human airway epithelial cells. Am J Respir Cell Mol Biol, 2001. **25**(2): p. 186-95.

185. Nutman, J., et al., *Studies on the mechanism of T cell inhibition by the Pseudomonas aeruginosa phenazine pigment pyocyanine.* J Immunol, 1987. **138**(10): p. 3481-7.

186. Rada, B., et al., *Reactive oxygen species mediate inflammatory cytokine release and EGFR-dependent mucin secretion in airway epithelial cells exposed to Pseudomonas pyocyanin.* Mucosal Immunol, 2011. **4**(2): p. 158-71.

187. Hao, Y., et al., *Pseudomonas aeruginosa pyocyanin causes airway goblet cell hyperplasia and metaplasia and mucus hypersecretion by inactivating the transcriptional factor FoxA2.* Cell Microbiol, 2012. **14**(3): p. 401-15.

188. Lau, G.W., B.E. Britigan, and D.J. Hassett, *Pseudomonas aeruginosa OxyR is required for full virulence in rodent and insect models of infection and for resistance to human neutrophils.* Infect Immun, 2005. **73**(4): p. 2550-3.

189. Vinckx, T., et al., *The Pseudomonas aeruginosa oxidative stress regulator OxyR influences production of pyocyanin and rhamnolipids: protective role of pyocyanin.* Microbiology, 2010. **156**(Pt 3): p. 678-86.

190. Britigan, B.E., M.A. Railsback, and C.D. Cox, *The Pseudomonas aeruginosa secretory product pyocyanin inactivates alpha1 protease inhibitor: implications for the pathogenesis of cystic fibrosis lung disease.* Infect Immun, 1999. **67**(3): p. 1207-12.

191. Das, T. and M. Manefield, *Pyocyanin promotes extracellular DNA release in Pseudomonas aeruginosa.* PLoS One, 2012. **7**(10): p. e46718.

192. Jimenez, P.N., et al., *The multiple signaling systems regulating virulence in Pseudomonas aeruginosa.* Microbiol Mol Biol Rev, 2012. **76**(1): p. 46-65.

193. Hunt, T.A., et al., *The Pseudomonas aeruginosa alternative sigma factor PvdS controls exotoxin A expression and is expressed in lung infections associated with cystic fibrosis.* Microbiology, 2002. **148**(Pt 10): p. 3183-93.

194. Meyer, J.M., et al., *Pyoverdin is essential for virulence of Pseudomonas aeruginosa.* Infect Immun, 1996. **64**(2): p. 518-23.

195. Takase, H., et al., *Impact of siderophore production on Pseudomonas aeruginosa infections in immunosuppressed mice.* Infect Immun, 2000. **68**(4): p. 1834-9.

196. Llamas, M.A., et al., *Cell-surface signaling in Pseudomonas: stress responses, iron transport, and pathogenicity.* FEMS Microbiol Rev, 2014. **38**(4): p. 569-97.

197. Visaggio, D., et al., *Cell aggregation promotes pyoverdine-dependent iron uptake and virulence in Pseudomonas aeruginosa.* Front Microbiol, 2015. **6**: p. 902.
198. Schultz, M.J., et al., *The effect of pseudomonas exotoxin A on cytokine production in whole blood exposed to Pseudomonas aeruginosa.* FEMS Immunol Med Microbiol, 2000. **29**(3): p. 227-32.
199. Wolf, P. and U. Elsasser-Beile, *Pseudomonas exotoxin A: from virulence factor to anti-cancer agent.* Int J Med Microbiol, 2009. **299**(3): p. 161-76.
200. Du, X., et al., *Pseudomonas exotoxin A-mediated apoptosis is Bak dependent and preceded by the degradation of Mcl-1.* Mol Cell Biol, 2010. **30**(14): p. 3444-52.
201. Holm, B.A., et al., *Inhibition of pulmonary surfactant function by phospholipases.* J Appl Physiol (1985), 1991. **71**(1): p. 317-21.
202. Retsema, J. and W. Fu, *Macrolides: structures and microbial targets.* Int J Antimicrob Agents, 2001. **18 Suppl 1**: p. S3-10.
203. Jaffe, A. and A. Bush, *Anti-inflammatory effects of macrolides in lung disease.* Pediatr Pulmonol, 2001. **31**(6): p. 464-73.
204. Rubin, B.K., *Immunomodulatory properties of macrolides: overview and historical perspective.* Am J Med, 2004. **117 Suppl 9A**: p. 2S-4S.
205. Clement, A., et al., *Long term effects of azithromycin in patients with cystic fibrosis: A double blind, placebo controlled trial.* Thorax, 2006. **61**(10): p. 895-902.
206. Equi, A., et al., *Long term azithromycin in children with cystic fibrosis: a randomised, placebo-controlled crossover trial.* Lancet, 2002. **360**(9338): p. 978-84.
207. Wolter, J., et al., *Effect of long term treatment with azithromycin on disease parameters in cystic fibrosis: a randomised trial.* Thorax, 2002. **57**(3): p. 212-6.
208. Saiman, L., et al., *Azithromycin in patients with cystic fibrosis chronically infected with Pseudomonas aeruginosa: a randomized controlled trial.* JAMA, 2003. **290**(13): p. 1749-56.
209. Ratjen, F., et al., *Effect of azithromycin on systemic markers of inflammation in patients with cystic fibrosis uninfected with Pseudomonas aeruginosa.* Chest, 2012. **142**(5): p. 1259-66.
210. Saiman, L., et al., *Open-label, follow-on study of azithromycin in pediatric patients with CF uninfected with Pseudomonas aeruginosa.* Pediatr Pulmonol, 2012. **47**(7): p. 641-8.

211. Steel, H.C., et al., *Pathogen- and host-directed anti-inflammatory activities of macrolide antibiotics.* Mediators Inflamm, 2012. **2012**: p. 584262.
212. Wagner, T., et al., *Effects of azithromycin on clinical isolates of Pseudomonas aeruginosa from cystic fibrosis patients.* Chest, 2005. **128**(2): p. 912-9.
213. Favre-Bonte, S., T. Kohler, and C. Van Delden, *Biofilm formation by Pseudomonas aeruginosa: role of the C4-HSL cell-to-cell signal and inhibition by azithromycin.* J Antimicrob Chemother, 2003. **52**(4): p. 598-604.
214. Gillis, R.J. and B.H. Iglewski, *Azithromycin retards Pseudomonas aeruginosa biofilm formation.* J Clin Microbiol, 2004. **42**(12): p. 5842-5.
215. Ichimiya, T., et al., *The influence of azithromycin on the biofilm formation of Pseudomonas aeruginosa in vitro.* Chemotherapy, 1996. **42**(3): p. 186-91.
216. Kita, E., et al., *Suppression of virulence factors of Pseudomonas aeruginosa by erythromycin.* J Antimicrob Chemother, 1991. **27**(3): p. 273-84.
217. Molinari, G., et al., *Inhibition of Pseudomonas aeruginosa virulence factors by subinhibitory concentrations of azithromycin and other macrolide antibiotics.* J Antimicrob Chemother, 1993. **31**(5): p. 681-8.
218. Molinari, G., P. Paglia, and G.C. Schito, *Inhibition of motility of Pseudomonas aeruginosa and Proteus mirabilis by subinhibitory concentrations of azithromycin.* Eur J Clin Microbiol Infect Dis, 1992. **11**(5): p. 469-71.
219. Nagino, K. and H. Kobayashi, *Influence of macrolides on mucoid alginate biosynthetic enzyme from Pseudomonas aeruginosa.* Clin Microbiol Infect, 1997. **3**(4): p. 432-439.
220. Kai, T., et al., *A low concentration of azithromycin inhibits the mRNA expression of N-acyl homoserine lactone synthesis enzymes, upstream of lasI or rhlI, in Pseudomonas aeruginosa.* Pulm Pharmacol Ther, 2009. **22**(6): p. 483-6.
221. Nalca, Y., et al., *Quorum-sensing antagonistic activities of azithromycin in Pseudomonas aeruginosa PAO1: a global approach.* Antimicrob Agents Chemother, 2006. **50**(5): p. 1680-8.
222. Skindersoe, M.E., et al., *Effects of antibiotics on quorum sensing in Pseudomonas aeruginosa.* Antimicrob Agents Chemother, 2008. **52**(10): p. 3648-63.
223. Imamura, Y., et al., *Azithromycin exhibits bactericidal effects on Pseudomonas aeruginosa through interaction with the outer membrane.* Antimicrob Agents Chemother, 2005. **49**(4): p. 1377-80.

224. Sugimura, M., et al., *Macrolide antibiotic-mediated downregulation of MexAB-OprM efflux pump expression in Pseudomonas aeruginosa.* Antimicrob Agents Chemother, 2008. **52**(11): p. 4141-4.

225. Tateda, K., et al., *Effects of sub-MICs of erythromycin and other macrolide antibiotics on serum sensitivity of Pseudomonas aeruginosa.* Antimicrob Agents Chemother, 1993. **37**(4): p. 675-80.

226. Tateda, K., et al., *Profiles of outer membrane proteins and lipopolysaccharide of Pseudomonas aeruginosa grown in the presence of sub-MICs of macrolide antibiotics and their relation to enhanced serum sensitivity.* J Antimicrob Chemother, 1994. **34**(6): p. 931-42.

227. Tateda, K., et al., *Direct evidence for antipseudomonal activity of macrolides: exposure-dependent bactericidal activity and inhibition of protein synthesis by erythromycin, clarithromycin, and azithromycin.* Antimicrob Agents Chemother, 1996. **40**(10): p. 2271-5.

228. Southern, K.W., et al., *Macrolide antibiotics for cystic fibrosis.* Cochrane Database Syst Rev, 2012. **11**: p. CD002203.

229. Fleet, J.E., et al., *A retrospective analysis of the impact of azithromycin maintenance therapy on adults attending a UK cystic fibrosis clinic.* J Cyst Fibros, 2013. **12**(1): p. 49-53.

230. Shinkai, M., et al., *Clarithromycin delays progression of bronchial epithelial cells from G1 phase to S phase and delays cell growth via extracellular signal-regulated protein kinase suppression.* Antimicrob Agents Chemother, 2006. **50**(5): p. 1738-44.

231. Fouka, E., et al., *Low-dose clarithromycin therapy modulates Th17 response in non-cystic fibrosis bronchiectasis patients.* Lung, 2014. **192**(6): p. 849-55.

232. Kadota, J., et al., *Long-term efficacy and safety of clarithromycin treatment in patients with diffuse panbronchiolitis.* Respir Med, 2003. **97**(7): p. 844-50.

233. Sandrini, A., M.S. Balter, and K.R. Chapman, *Diffuse panbronchiolitis in a Caucasian man in Canada.* Can Respir J, 2003. **10**(8): p. 449-51.

234. Kudoh, S., *Erythromycin treatment in diffuse panbronchiolitis.* Curr Opin Pulm Med, 1998. **4**(2): p. 116-21.

235. Yalcin, E., et al., *Effects of claritromycin on inflammatory parameters and clinical conditions in children with bronchiectasis.* J Clin Pharm Ther, 2006. **31**(1): p. 49-55.

236. Tagaya, E., et al., *Effect of a short course of clarithromycin therapy on sputum production in patients with chronic airway hypersecretion.* Chest, 2002. **122**(1): p. 213-8.
237. Pukhalsky, A.L., et al., *Anti-inflammatory and immunomodulating effects of clarithromycin in patients with cystic fibrosis lung disease.* Mediators Inflamm, 2004. **13**(2): p. 111-7.
238. Ordonez, C.L., et al., *Effect of clarithromycin on airway obstruction and inflammatory markers in induced sputum in cystic fibrosis: a pilot study.* Pediatr Pulmonol, 2001. **32**(1): p. 29-37.
239. Robinson, P., et al., *Clarithromycin therapy for patients with cystic fibrosis: a randomized controlled trial.* Pediatr Pulmonol, 2012. **47**(6): p. 551-7.
240. Dogru, D., et al., *Long-term clarithromycin in cystic fibrosis: effects on inflammatory markers in BAL and clinical status.* Turk J Pediatr, 2009. **51**(5): p. 416-23.
241. Alhajlan, M., M. Alhariri, and A. Omri, *Efficacy and safety of liposomal clarithromycin and its effect on Pseudomonas aeruginosa virulence factors.* Antimicrob Agents Chemother, 2013. **57**(6): p. 2694-704.
242. Wozniak, D.J. and R. Keyser, *Effects of subinhibitory concentrations of macrolide antibiotics on Pseudomonas aeruginosa.* Chest, 2004. **125**(2 Suppl): p. 62S-69S; quiz 69S.
243. Kobayashi, H., *Biofilm disease: its clinical manifestation and therapeutic possibilities of macrolides.* Am J Med, 1995. **99**(6A): p. 26S-30S.
244. Yanagihara, K., et al., *Effect of clarithromycin on chronic respiratory infection caused by Pseudomonas aeruginosa with biofilm formation in an experimental murine model.* J Antimicrob Chemother, 2002. **49**(5): p. 867-70.
245. Elkhatib, W. and A. Noreddin, *Efficacy of ciprofloxacin-clarithromycin combination against drug-resistant Pseudomonas aeruginosa mature biofilm using in vitro experimental model.* Microb Drug Resist, 2014. **20**(6): p. 575-82.
246. Tre-Hardy, M., et al., *Efficacy of the combination of tobramycin and a macrolide in an in vitro Pseudomonas aeruginosa mature biofilm model.* Antimicrob Agents Chemother, 2010. **54**(10): p. 4409-15.
247. Tre-Hardy, M., et al., *In vitro activity of antibiotic combinations against Pseudomonas aeruginosa biofilm and planktonic cultures.* Int J Antimicrob Agents, 2008. **31**(4): p. 329-36.

248. Saiman, L., et al., *Synergistic activities of macrolide antibiotics against Pseudomonas aeruginosa, Burkholderia cepacia, Stenotrophomonas maltophilia, and Alcaligenes xylosoxidans isolated from patients with cystic fibrosis.* Antimicrob Agents Chemother, 2002. **46**(4): p. 1105-7.

249. Dimer, F., et al., *Inhalable Clarithromycin Microparticles for Treatment of Respiratory Infections.* Pharm Res, 2015. **32**(12): p. 3850-61.

250. Manniello, M.D., et al., *Aerodynamic properties, solubility and in vitro antibacterial efficacy of dry powders prepared by spray drying: Clarithromycin versus its hydrochloride salt.* Eur J Pharm Biopharm, 2016. **104**: p. 1-6.

251. Pilcer, G., et al., *New co-spray-dried tobramycin nanoparticles-clarithromycin inhaled powder systems for lung infection therapy in cystic fibrosis patients.* J Pharm Sci, 2013. **102**(6): p. 1836-46.

252. Travis, J. and J. Potempa, *Bacterial proteinases as targets for the development of second-generation antibiotics.* Biochim Biophys Acta, 2000. **1477**(1-2): p. 35-50.

253. Avidano, M.A., et al., *Analysis of protease activity in human otitis media.* Otolaryngol Head Neck Surg, 1998. **119**(4): p. 346-51.

254. Barletta, J.P., et al., *Inhibition of pseudomonal ulceration in rabbit corneas by a synthetic matrix metalloproteinase inhibitor.* Invest Ophthalmol Vis Sci, 1996. **37**(1): p. 20-8.

255. Grobelny, D., L. Poncz, and R.E. Galardy, *Inhibition of human skin fibroblast collagenase, thermolysin, and Pseudomonas aeruginosa elastase by peptide hydroxamic acids.* Biochemistry, 1992. **31**(31): p. 7152-4.

256. Hao, J.L., et al., *Effect of galardin on collagen degradation by Pseudomonas aeruginosa.* Exp Eye Res, 1999. **69**(6): p. 595-601.

257. Schmidtchen, A., et al., *Proteinases of common pathogenic bacteria degrade and inactivate the antibacterial peptide LL-37.* Mol Microbiol, 2002. **46**(1): p. 157-68.

258. Anderson, D.R., et al., *Sulfur mustard-induced neutropenia: treatment with granulocyte colony-stimulating factor.* Mil Med, 2006. **171**(5): p. 448-53.

259. Liesenfeld, B., *Protease inhibitors prevent microvesication in sulfur mustard wounds on human skin explants.* Wound Rep Reg, 2008. **16**(2): p. A14-A14.

260. Mazzoni, A., et al., *Role of dentin MMPs in caries progression and bond stability.* J Dent Res, 2015. **94**(2): p. 241-51.

261. Parkinson, G., et al., *Characterisation of ilomastat for prolonged ocular drug release.* AAPS PharmSciTech, 2012. **13**(4): p. 1063-72.

262. Pemberton, P.A., et al., *An inhaled matrix metalloprotease inhibitor prevents cigarette smoke-induced emphysema in the mouse.* COPD, 2005. **2**(3): p. 303-10.
263. Gialeli, C., A.D. Theocharis, and N.K. Karamanos, *Roles of matrix metalloproteinases in cancer progression and their pharmacological targeting.* FEBS J, 2011. **278**(1): p. 16-27.
264. Coussens, L.M., B. Fingleton, and L.M. Matrisian, *Matrix metalloproteinase inhibitors and cancer: trials and tribulations.* Science, 2002. **295**(5564): p. 2387-92.
265. Rasmussen, H.S., *Batimastat and Marimastat in Cancer*, in *Antiangiogenic Agents in Cancer Therapy*. 1999. p. 399-405.
266. Steward, W.P., *Marimastat (BB2516): current status of development.* Cancer Chemother Pharmacol, 1999. **43 Suppl**: p. S56-60.
267. Millar, A.W., et al., *Results of single and repeat dose studies of the oral matrix metalloproteinase inhibitor marimastat in healthy male volunteers.* Br J Clin Pharmacol, 1998. **45**(1): p. 21-6.
268. Rosemurgy, A., et al., *Marimastat in patients with advanced pancreatic cancer: a dose-finding study.* Am J Clin Oncol, 1999. **22**(3): p. 247-52.
269. Rasmussen, H.S. and P.P. McCann, *Matrix metalloproteinase inhibition as a novel anticancer strategy: a review with special focus on batimastat and marimastat.* Pharmacol Ther, 1997. **75**(1): p. 69-75.
270. Wilke, M., et al., *Mouse models of cystic fibrosis: Phenotypic analysis and research applications.* J Cyst Fibros, 2011. 10(2): p. 152-71.
271. Snouwaert, J.N., et al., *An animal model for cystic fibrosis made by gene targeting.* Science, 1992. **257**(5073): p. 1083-8.
272. Ratcliff, R., et al., *Production of a severe cystic fibrosis mutation in mice by gene targeting.* Nat Genet, 1993. **4**(1): p. 35-41.
273. O'Neal, W.K., et al., *A severe phenotype in mice with a duplication of exon 3 in the cystic fibrosis locus.* Hum Mol Genet, 1993. **2**(10): p. 1561-9.
274. Hasty, P., et al., *Severe phenotype in mice with termination mutation in exon 2 of cystic fibrosis gene.* Somat Cell Mol Genet, 1995. **21**(3): p. 177-87.
275. Rozmahel, R., et al., *Modulation of disease severity in cystic fibrosis transmembrane conductance regulator deficient mice by a secondary genetic factor.* Nat Genet, 1996. **12**(3): p. 280-7.
276. van Doorninck, J.H., et al., *A mouse model for the cystic fibrosis delta F508 mutation.* EMBO J, 1995. **14**(18): p. 4403-11.

277. Zeiher, B.G., et al., *A mouse model for the delta F508 allele of cystic fibrosis.* J Clin Invest, 1995. **96**(4): p. 2051-64.
278. Colledge, W.H., et al., *Generation and characterization of a delta F508 cystic fibrosis mouse model.* Nat Genet, 1995. **10**(4): p. 445-52.
279. Dickinson, P., et al., *The severe G480C cystic fibrosis mutation, when replicated in the mouse, demonstrates mistrafficking, normal survival and organ-specific bioelectrics.* Hum Mol Genet, 2002. **11**(3): p. 243-51.
280. Delaney, S.J., et al., *Cystic fibrosis mice carrying the missense mutation G551D replicate human genotype-phenotype correlations.* EMBO J, 1996. **15**(5): p. 955-63.
281. Mall, M., et al., *Increased airway epithelial Na^+ absorption produces cystic fibrosis-like lung disease in mice.* Nat Med, 2004. 10: p. 487–93.
282. Dorin, J.R., et al., *Cystic fibrosis in the mouse by targeted insertional mutagenesis.* Nature, 1992. **359**(6392): p. 211-5.
283. Clarke, L.L., et al., *Relationship of a non-cystic fibrosis transmembrane conductance regulator-mediated chloride conductance to organ-level disease in Cftr(-/-) mice.* Proc Natl Acad Sci U S A, 1994. **91**(2): p. 479-83.
284. Gosselin, D., et al., *Impaired ability of Cftr knockout mice to control lung infection with Pseudomonas aeruginosa.* Am J Respir Crit Care Med, 1998. **157**(4 Pt 1): p. 1253-62.
285. Sajjan, U., et al., *Enhanced susceptibility to pulmonary infection with Burkholderia cepacia in Cftr(-/-) mice.* Infect Immun, 2001. **69**(8): p. 5138-50.
286. van Heeckeren, A.M. and M.D. Schluchter, *Murine models of chronic Pseudomonas aeruginosa lung infection.* Lab Anim, 2002. **36**(3): p. 291-312.
287. Shah, V.S., et al., *Airway acidification initiates host defense abnormalities in cystic fibrosis mice.* Science, 2016. **351**(6272): p. 503-7.
288. Balloy, V., et al., *Azithromycin analogue CSY0073 attenuates lung inflammation induced by LPS challenge.* Br J Pharmacol, 2014. **171**(7): p. 1783-94.
289. Belessis, Y., et al., *Early cystic fibrosis lung disease detected by bronchoalveolar lavage and lung clearance index.* Am J Respir Crit Care Med, 2012. **185**(8): p. 862-73.
290. Hakansson, H.F., et al., *Altered lung function relates to inflammation in an acute LPS mouse model.* Pulm Pharmacol Ther, 2012. **25**(5): p. 399-406.

291. Mauffray, M., et al., *Neurturin influences inflammatory responses and airway remodeling in different mouse asthma models.* J Immunol, 2015. **194**(4): p. 1423-33.
292. Starkey, M.R., et al., *Murine models of infectious exacerbations of airway inflammation.* Curr Opin Pharmacol, 2013. **13**(3): p. 337-44.
293. Bianchi, A., et al., *Ultrashort-TE MRI longitudinal study and characterization of a chronic model of asthma in mice: inflammation and bronchial remodeling assessment.* NMR Biomed, 2013. **26**(11): p. 1451-9.
294. Lederlin, M., et al., *In vivo micro-CT assessment of airway remodeling in a flexible OVA-sensitized murine model of asthma.* PLoS One, 2012. **7**(10): p. e48493.
295. Ma, X., et al., *Assessment of asthmatic inflammation using hybrid fluorescence molecular tomography-x-ray computed tomography.* J Biomed Opt, 2016. **21**(1): p. 15009.
296. Stellari, F., et al., *Monitoring inflammation and airway remodeling by fluorescence molecular tomography in a chronic asthma model.* J Transl Med, 2015. **13**: p. 336.
297. Ble, F.X., et al., *Allergen-induced lung inflammation in actively sensitized mice assessed with MR imaging.* Radiology, 2008. **248**(3): p. 834-43.
298. Enright, H.A., et al., *Tracking retention and transport of ultrafine polystyrene in an asthmatic mouse model using positron emission tomography.* Exp Lung Res, 2013. **39**(7): p. 304-13.
299. Thomas, A.C., et al., *Effects of corticosteroid treatment on airway inflammation, mechanics, and hyperpolarized (3)He magnetic resonance imaging in an allergic mouse model.* J Appl Physiol (1985), 2012. **112**(9): p. 1437-44.
300. Crane, L.M., et al., *Intraoperative near-infrared fluorescence imaging for sentinel lymph node detection in vulvar cancer: first clinical results.* Gynecol Oncol, 2011. **120**(2): p. 291-5.
301. van Dam, G.M., et al., *Intraoperative tumor-specific fluorescence imaging in ovarian cancer by folate receptor-alpha targeting: first in-human results.* Nat Med, 2011. **17**(10): p. 1315-9.
302. Stellari, F.F., et al., *In vivo imaging of transiently transgenized mice with a bovine interleukin 8 (CXCL8) promoter/luciferase reporter construct*. PLoS One, 2012. **7**(6): p. e39716.

303. Guilbault, C., et al., *Distinct pattern of lung gene expression in the Cftr-KO mice developing spontaneous lung disease compared with their littermate controls*. Physiol Genomics, 2006. **25**(2): p. 179-93.
304. Kent, G., et al., *Lung disease in mice with cystic fibrosis.* J Clin Invest, 1997. **100**(12): p. 3060-9.
305. Di Paolo, A., et al., *Pharmacokinetics of azithromycin in lung tissue, bronchial washing, and plasma in patients given multiple oral doses of 500 and 1000 mg daily*. Pharmacol Res, 2002. **46**(6): p. 545-50.
306. Tenover, F.C., et al., *Interpreting chromosomal DNA restriction patterns produced by pulsed-field gel electrophoresis: criteria for bacterial strain typing*. J Clin Microbiol, 1995. **33**(9): p. 2233-9.
307. Zhou, L., et al., *Correction of lethal intestinal defect in a mouse model of cystic fibrosis by human CFTR.* Science, 1994. **266**: p. 1705–8.
308. Hansen, C.R., et al., *Inflammation in Achromobacter xylosoxidans infected cystic fibrosis patients*. J Cyst Fibros, 2010. **9**(1): p. 51-8.
309. Firmida, M.C., et al., *Clinical impact of Achromobacter xylosoxidans colonization/infection in patients with cystic fibrosis*. Braz J Med Biol Res, 2016. **49**(4): e5097.
310. Ridderberg, W., et al., *Multilocus sequence analysis of isolates of Achromobacter from patients with cystic fibrosis reveals infecting species other than Achromobacter xylosoxidans*. JCM, 2012. **50**(8): p. 2688-94.
311. Hansen, C.R., et al., *Achromobacter species in cystic fibrosis: Cross-infection caused by indirect patient-to-patient contact.* J Cyst Fibro, 2013. 12: p. 609-15.
312. Hu, Y., et al., *Genomic insights into intrinsic and acquired drug resistance mechanisms in Achromobacter xylosoxidans*. Antimicrob Agents Chemother, 2015. **59**(2): p. 1152-61.
313. Traglia, G.M., et al., *Achromobacter xylosoxidans: an emerging pathogen carrying different elements involved in horizontal genetic transfer*. Curr Microbiol, 2012. **65**: p. 673-8.
314. Li, X., et al., *Comparative genome characterization of Achromobacter members reveals potential genetic determinants facilitating the adaptation to a pathogenic lifestyle*. Appl Microbiol Biotechnol, 2013. **97**: p. 6413-25.
315. Hutchison, M.L., et al. *Endotoxic activity of lipopolysaccharides isolated from emergent potential cystic fibrosis pathogens*. FEMS Immunol Med Microbiol, 2000. **27**: p. 73–77.

316. Jakobsen, T.M., et al. *Complete genome sequence of the cystic fibrosis pathogen Achromobacter xylosoxidans NH44784-1996 complies with important pathogenic phenotypes*. PLoS ONE, 2013. **8**(7): e68484.

317. Ridderberg, W., et al., *Genetic adaptation of Achromobacter sp. during persistence in the lungs of cystic fibrosis patients*. PLoS ONE, 2015. **10**(8): e0136790.

318. Ivanov, A., et al., *Phosphatidylcholine-specific phospholipase C from Achromobacter xylosoxidans*. Acta Microbiol Bulg, 1993. **29**: p. 3–8.

319. Ye-Chen Soh, E., et al., *Biotic inactivation of the Pseudomonas aeruginosa quinolone signal molecule*. Environ Microbiol, 2015. **17**(11): p. 4352-65.

320. Mantovani, R., et al., *A heat-stable cytotoxic factor produced by Achromobacter xylosoxidans isolated from Brazilian patients with CF is associated with in vitro increased proinflammatory cytokines*. J Cyst Fibros, 2012. **11**: p. 305-11.

321. O'Toole, G.A., et al. *Flagellar and twitching motility are necessary for Pseudomonas aeruginosa biofilm development*. Mol Microbiol, 1998. **30**(2): p. 295-304.

322. Nielsen, S.M., et al., *Achromobacter species isolated from cystic fibrosis patients reveal distinctly different biofilm morphotypes*. Microorganisms, 2016. **4**: p. 33.

323. De Simone, M., et al., *Host genetic background influences the response to the opportunistic Pseudomonas aeruginosa infection altering cell-mediated immunity and bacterial replication*. PLoS One, 2014. **9**(9): e106873.

324. Schmeck, B., et al., *Pneumococci induced TLR- and Rac1-dependent NF-kappaB-recruitment to the IL-8 promoter in lung epithelial cells*. Am J Physiol Lung Cell Mol Physiol, 2006. **290**(4): p. 730–7.

325. Samson, C., Tamalet, A., Thien, H.V., Taytard, J., Perisson, C., Nathan, N., Clement, A., Boelle, P.Y., Corvol, H., *Long-term effects of azithromycin in patients with cystic fibrosis*. Respir Med, 2016. **117**: p. 1-6.

10. Scientific contributions

In vivo imaging of the lung inflammatory response to *Pseudomonas aeruginosa* and its modulation by azithromycin

Fabio Stellari, Gabriella Bergamini, **Angela Sandri**, Gaetano Donofrio, Claudio Sorio, Francesca Ruscitti, Gino Villetti, Barouk Maurice Assael, Paola Melotti*, Maria del Mar Lleò*

Journal of Translational Medicine (2015) 13:251

DOI 10.1186/s12967-015-0615-9

*Equal contribution

Stellari et al. J Transl Med (2015) 13:251
DOI 10.1186/s12967-015-0615-9

JOURNAL OF TRANSLATIONAL MEDICINE

RESEARCH Open Access

In vivo imaging of the lung inflammatory response to *Pseudomonas aeruginosa* and its modulation by azithromycin

Fabio Stellari[1*], Gabriella Bergamini[2], Angela Sandri[2], Gaetano Donofrio[3], Claudio Sorio[2], Francesca Ruscitti[4], Gino Villetti[1], Barouk M Assael[5], Paola Melotti[5†] and Maria M Lleo[2†]

Abstract

Background: Chronic inflammation of the airways is a central component in lung diseases and is frequently associated with bacterial infections. Monitoring the pro-inflammatory capability of bacterial virulence factors in vivo is challenging and usually requires invasive methods.

Methods: Lung inflammation was induced using the culture supernatants from two *Pseudomonas aeruginosa* clinical strains, VR1 and VR2, isolated from patients affected by cystic fibrosis and showing different phenotypes in terms of motility, colony characteristics and biofilm production as well as pyoverdine and pyocyanine release. More interesting, the strains differ also for the presence in supernatants of metalloproteases, a family of virulence factors with known pro-inflammatory activity. We have evaluated the benefit of using a mouse model, transiently expressing the luciferase reporter gene under the control of an heterologous IL-8 bovine promoter, to detect and monitoring lung inflammation.

Results: In vivo imaging indicated that VR1 strain, releasing in its culture supernatant metalloproteases and other virulence factors, induced lung inflammation while the VR2 strain presented with a severely reduced pro-inflammatory activity. The bioluminescence signal was detectable from 4 to 48 h after supernatant instillation. The animal model was also used to test the anti-inflammatory activity of azithromycin (AZM), an antibiotic with demonstrated inhibitory effect on the synthesis of bacterial exoproducts. The inflammation signal in mice was in fact significantly reduced when bacteria grew in the presence of a sub-lethal dose of AZM causing inhibition of the synthesis of metalloproteases and other bacterial elements. The in vivo data were further supported by quantification of immune cells and cytokine expression in mouse broncho-alveolar lavage samples.

Conclusions: This experimental animal model is based on the transient transduction of the bovine IL-8 promoter, a gene representing a major player during inflammation, essential for leukocytes recruitment to the inflamed tissue. It appears to be an appropriate molecular read-out for monitoring the activation of inflammatory pathways caused by bacterial virulence factors. The data presented indicate that the model is suitable to functionally monitor in real time the lung inflammatory response facilitating the identification of bacterial factors with pro-inflammatory activity and the evaluation of the anti-inflammatory activity of old and new molecules for therapeutic use.

Keywords: In vivo bioluminescence imaging, Lung inflammation mouse model, *Pseudomonas aeruginosa*, Azithromycin

*Correspondence: fb.stellari@chiesi.com
†Paola Melotti and Maria M Lleo contributed equally to this work
[1] Pharmacology and Toxicology Department Corporate Pre-Clinical R&D, Chiesi Farmaceutici S.p.A. Parma, Largo Belloli, 11/A, 43122 Parma, Italy
Full list of author information is available at the end of the article

Background

Airway inflammation is a central component of a number of chronic lung diseases such as asthma, chronic obstructive pulmonary disease (COPD), cystic fibrosis (CF) and bronchiectasis. Airway inflammation is characterized by edema, cellular infiltration, activated T lymphocytes and mast cells, increased airway secretions, and deposition of excess collagen [1, 2]. Frequently, the inflammation is associated with bacterial infections such as those caused by *Pseudomonas aeruginosa*, an opportunistic human pathogen involved in severe airway infections especially in patients suffering from CF and COPD [1, 3]. During the early onset of the lung infection, *P. aeruginosa* secretes a high number of virulence factors which are responsible for tissue damage and inflammation [4]. As the infection progresses, the bacterium switches off most of the virulence genes but synthesizes a biofilm matrix and becomes resistant to antibiotics causing a chronic disease frequently leading to respiratory failure and lung transplantation or death [4].

Therefore, it is mandatory to identify those factors and conditions causing lung cell damage and favoring the passage from an acute to a chronic bacterial infection by monitoring, for long times, the inflammation process. Furthermore, to avoid the onset of the chronic phase of the infection, it is important to treat *P. aeruginosa* infection during the acute phase using efficient antibiotic therapy and anti-inflammatory drugs.

By standard methods, the inflammation of the respiratory tract can be monitored by counting immunological markers recruited during the inflammatory process with sputum collection, a technique which provides poorly reliable results, or invasive sampling techniques such as bronchoscopy [5]. Animal models of acute and chronic lung infection have been used to study the bacterial behavior and for monitoring the host response in vivo [1, 6]. These models provide an important resource to identify essential bacterial genes for in vivo infection persistence and for the development and testing of new therapies [6, 7]. Recently, a mouse model, transiently expressing the luciferase reporter gene under the control of the bovine IL-8 promoter, has been described [8] and demonstrated to be suitable to functionally monitor in real time the lung inflammatory response [8–11]. This small size experimental animal model is based on the transient transduction of the IL-8 promoter, a gene representing a major player during inflammation, essential for leukocytes recruitment to the inflamed tissue and an appropriate molecular read-out for monitoring the activation of inflammatory pathways [8]. Although mice do not have an IL-8 (bIL-8) gene, mouse cell signaling and their transcriptional apparatus could specifically activate the bovine IL-8 gene promoter. Since lung disease manifestation in ruminants overlap with the majority of human lung disease manifestations, this model could be of great value to study human lung diseases too.

It has been shown that the *P. aeruginosa* strains isolated during the early phase of lung colonization had a pro-inflammatory capability higher than that induced by strains isolated during lung chronic colonization [12]. The pro-inflammatory effect, associated with the expression of IL-8 mRNA in CF airway epithelial cells, was shown to be associated to several *Pseudomonas* released proteins with proteolytic activity including members of the metalloprotease (MP) family [12]. Other virulence factors secreted by *Pseudomonas* such as exotoxins and exoenzymes, pyoverdine and pyocianine are also involved in tissue damage and inflammation. It has been suggested that azithromycin (AZM), an antibiotic used in CF patients, could elicit its anti-inflammatory activity by decreasing the synthesis of *Pseudomonas* exoproducts [13–15]. In fact, Molinari et al. [13] have shown that sub-lethal doses of AZM strongly suppressed the synthesis of elastase, lecithinase, proteases and DNase, while in another study it has been shown that AZM reduced the production of bacteria virulence factors by inhibiting quorum-sensing [15].

In the present study, we used the IL-8/luciferase transgenic mouse model for the in vivo monitoring of the IL-8 mediated lung inflammation induced by *P. aeruginosa* secreted pro-inflammatory virulence factors and their modulation by AZM.

Methods

Collection of bacterial cell-free supernatants

Two *P. aeruginosa* strains, VR1 and VR2, were isolated from sputum samples of CF patients followed at the Cystic Fibrosis Center in Verona, Italy and were characterized for their differential expression of known virulence factors (data summarized in Fig. 1). Written informed consent was obtained from the subjects enrolled in the study and approved by the Institutional Review Board of Azienda Ospedaliera Universitaria Integrata (AOUI) Verona as project 1612.

Bacterial strains were grown overnight at 37°C in Bacto™ Tryptic Soy Broth (TSB, Becton, Dickinson and Company) with continuous agitation. The day after, *P. aeruginosa* cells were diluted in TSB to the concentration of 1×10^8 CFU/mL (OD of 0.1 at 600 nm) and incubated in absence and in presence of 8 μg/mL of AZM, at 37°C for 16 h with continuous agitation. The concentration chosen for this antibiotic is in the sub-minimum inhibitory concentration (sub-MIC) range for *P. aeruginosa*, and is consistent with the concentrations found in lungs of patients treated with this drug [16]. By adding TSB, the cultures were normalized to an optical density of 0.2

Virulence factors and phenotypes		*P. aeruginosa* strain VR1	*P. aeruginosa* strain VR1 + AZM	*P. aeruginosa* strain VR2	*P. aeruginosa* strain VR2 + AZM
Metallo-proteases		+++	+	-	-
Pyocianin	µg/ml	0,29	0,16	0,12	0,13
	Relative conc. (OD550/OD600)	0,048	0,026	0,020	0,022
Pyoverdine	µg/ml	2,63	0,00	0,13	0,06
	Relative conc. (OD550/OD600)	0,103	0,00	0,005	0,002
Colony phenotype	Colour	Green	Light brown	Light brown	Light brown
	Mucoidy	No	No	Yes	Yes
	Edges	Jagged	Jagged	Regular	Regular
	Morphology	Swarming	Swarming	Round	Round
Biofilm production		+++	ND	++	ND
Twiching (⌀ cm)		0,8	0,7	0,6	0,8
Swimming (⌀ cm)		2,3	1,2	0,5	0,5
Swarming (⌀ cm)		1,6	1,2	0,3	0,4

Fig. 1 Phenotypic characteristics and virulence factors of the *P. aeruginosa* clinical strains.

OD at 600 nm. Culture supernatants (Sn) were collected by centrifugation (7,000×*g*, 30 min, 4°C) and filtered through a 0.22 µm Millipore filter to remove any remaining bacteria. Supernatants were concentrated to 30X using Amicon Ultra-15 30 K (Millipore, Billerica, USA), then centrifuged at 27,000×*g* for 1 h at 4°C to remove cellular debris and finally sterilized by filtration through a Millipore 0.22 µm filter.

Phenotype characterization

Colony characterization

P. aeruginosa VR1 and VR2 isolates were grown on Luria Bertani (LB) agar plates for 24–48 h at 37°C and colony morphotypes were visually inspected for color, shape, edges regularity, and mucoidy.

Motility assays

Swimming plates (1% tryptone, 0.5% NaCl and 0.3% (w/v) agar) were point-inoculated from an overnight culture with a sterile toothpick and incubated at 37°C for 24 h. The zone diameter was measured to assess swimming motility.

Swarming plates (0.5% peptone, 0.3% yeast extract, 0.5% NaCl, 0.5% D-glucose and 0.5% (w/v) agar) were point-inoculated from an overnight culture with a sterile toothpick and incubated at 37°C for 24 h. Swarming motility was assessed by measuring the circular turbid zones formed by the bacterial cells migrating away from the point of inoculation.

Twiching motility was evaluated on LB 1% (w/v) agar plates. Overnight cultures were stabbed with a sterile toothpick through the agar layer to the bottom of the Petri dish. The plates were then incubated at 37°C for 48 h. Twiching motility was examined by measuring the diameter of the halo formed in the plastic-agar interface.

Biofilm formation assay

Bacterial cells were grown at 37°C in TSB-1% glucose until they reached the exponentially growing phase ($OD_{650nm} = 0.4$). Exponentially growing cells were then diluted in TSB-1% glucose medium to reach 10^6 CFU/mL. Two hundred microliter of each cell suspension were used to inoculate sterile flat-bottomed polystyrene microtiter plates (CytoOne, Starlab) and plates were incubated aerobically at 37°C without agitation for 48 h to allow biofilm formation. After incubation, the planktonic cells were aseptically aspirated, washed with sterile physiological solution and dried. For biofilm quantification, 100 µL of 1% methylene blue were added to each well and the plate maintained for 15 min at room temperature. The wells were subsequently slowly washed once with sterile water and dried at 37°C. The methylene blue bound to the biofilm was extract using 100 µL of 70% ethanol and the absorbance measured at 570 nm using "A3 Plate Reader" microplate reader (DAS Srl, Italy). All the mentioned experiment were performed in triplicate.

Virulence factor assays

The presence of virulence factors in culture supernatants was evaluated after growth of the bacterial strains with and without AZM.

Gelatin-zymography for analysis of the protease profile

We used gelatin-zymography to investigate the presence of total metalloprotease activity, by visualization of clear bands (areas of gelatin digestion) over a deep blue background after Coomassie staining. Five millilitres of 5X SDS sample buffer (5% SDS, 0.5 M Tris–HCl pH 6.8, 25% glycerol) were added to 20 µL of culture supernatants. The sample was run on a SDS-PAGE gel containing 1 mg/mL gelatin (Sigma-Aldrich) as described [12]. In order to compare metalloproteases expression/release by the different strains, for each sample we loaded equal aliquots of culture supernatants normalized to a 0.2 final OD after overnight growth starting from 0.1 OD. The gel was washed twice (20 min per cycle) with 2.5% Triton X-100 at room temperature, then incubated in 200 mL of activation buffer (10 mM Tris–HCl, 1.25% Triton X-100, 5 mM $CaCl_2$, 1 mM $ZnCl_2$) overnight at 37°C and finally stained with Coomassie Brilliant Blue G-250 in 20% methanol/10% phosphoric acid/10% ammonium sulfate and destained in water. Gel images were captured by ImageQuant LAS 4000 (GE Healthcare Life Sciences, Milan, Italy).

Western blot analysis of alkaline metalloprotease AprA

Proteins were precipitated from 12 mL of culture supernatants by addition of 10% (final concentration) trichloroacetic acid with stirring at 4°C. The sample was then centrifuged at 3,000*g* for 30 min and washed 3 times with an excess of acetone:methanol (8:1). The pellet was air-dried, resuspended in SDS sample buffer, subjected to SDS-PAGE and Western blotting as described [12]. Briefly, protein bands were transferred from the 10% acrylamide gel onto a nitrocellulose membrane (HybondTM ECLTM, Amersham, NJ, USA), using a mini trans-blot apparatus (Bio-Rad, California, USA) following the manufacturer's instructions. The membrane was incubated with a 1:500 dilution of purified rabbit IgG against *P. aeruginosa* alkaline protease (AprA), a kind gift from G. Döring (University of Tübingen, Germany), in TBS-T with 1% BSA overnight at 4°C. The blot was washed four times in TBS-T and then incubated for 1 h at room temperature with donkey anti-rabbit IgG secondary antibody conjugated to horseradish peroxidase (Amersham, NJ, USA) diluted 1:15,000 in TBS-T with 1% BSA. Bound proteins were visualized using the ECL detection system (Millipore Corporation, Bedford, MA, USA).

In vitro imaging probe

A near infrared (NIR)-activatable "smart" probe (Perkin Elmer, Inc. Boston, MA, USA) was used for imaging protease activities. Specifically, MMPsense 750 FAST is a proteases activatable fluorescent in vivo imaging agent that is activated by key disease associated-proteinases such as MMPs including MMP-2, -3, -9 and -13 and bacterial proteases. Smart probes are optically silent in their inactivated state and becomes highly fluorescent following protease-mediated activation.

The MMPsense 750 FAST probe was added to 50 µL of culture supernatants at the final concentration of 0.02 nmoles in a 96-well plate and an imaging system (IVIS, Caliper Life Sciences, Alameda, CA, USA) was used to quantify the time course of the fluorescence every 30 s from 1 to 40 min.

Pyoverdine assay

The production of pyoverdine by *P. aeruginosa* was measured spectrophotometrically by a modification of a standard method. Overnight cultures of the strains were diluted to an optical density at 600 nm (OD_{600}) of 0.1 in 30 mL of King's B broth (low-iron medium) with and without 8 µg/mL AZM and grown at 37°C until they reached an OD_{600} of ≈2–3 (after 16 h). Cultures were normalized to OD_{600} of 0.2 in order to reproduce the conditions of supernatants used for mice stimulation. The absorbance of cell-free supernatants was measured at 405 nm. The concentration of pyoverdine was calculated by using the extinction coefficient ($1.9 \times 10^{-4}\,M^{-1}\,cm^{-1}$).

Pyocyanin assay

The pyocyanin assay is based on the absorbance of pyocyanin at 520 nm in acidic solution (Essar et al. 1990). Bacterial cultures were grown in LB medium with or without AZM following the same conditions described for pyoverdine assay. Five milliliters of cell-free supernatants were extracted with 3 mL of chloroform. The lower phase was mixed with 1 mL of 0.2 M HCl, and the absorbance of the resulting upper pink phase was measured at 520 nm (A_{520}). Concentration, expressed as µg of pyocyanin per millilitre of culture supernatant, was determined by multiplying the A520 value by 17.072.

Experimental animals

Female inbred BalbC (7–8 week-old) mice were purchased from Harlan Laboratories Italy (San Pietro al Natisone, Udine, Italy). Prior to use, animals were acclimatized for at least 5 days to the local vivarium conditions (room temperature: 20–24°C; relative humidity: 40–70%; 12-h light–dark cycle), having free access to standard rodent chow and softened tap water. Animal

experiments were conducted in compliance with national (Decreto Legislativo numero 26, 4 Marzo 2014) and international laws and policies (Guide for the Care and Use of Laboratory Animals) [17]. Animal studies were approved by the Institutional Animal Care and Use Committee at Chiesi Farmaceutici, Parma, Italy.

In vivo gene delivery

The bIL-8-Luc plasmid (Department of Medical Veterinary Science, University of Parma, Italy) was obtained by sub-cloning the 2,030 bp IL8 bovine promoter, amplified by PCR from Madin–Darby bovine kidney (MDBK; ATCC #CCL-22) genomic DNA and subcloned into the digested pGL3basic vector (Promega) as previously described [8]. We applied in vivo JetPEI (Polyplus Transfection) as a carrier for delivering DNA to lung tissues. The DNA and JetPEI mix was formulated according to the product manual with a final N/P ratio of 7. Briefly, 40 μg of bIL-8–luc and 7 μL of JetPEI were both diluted into 200 μL 5% glucose. The two solutions were then mixed and incubated for 15 min at room temperature. The entire mixture was injected intravenously into BalbC mice and the expression of bIL-8–Luc was monitored through imaging with an IVIS imaging system.

In vivo bioluminescence imaging

Transfection per se causes a mild lung inflammatory response and bIL-8 activation that is detectable by bioluminescence imaging (BLI) up to 3–4 days after DNA injection and disappears completely after 1 week [11].

One week after DNA delivery, the transient transgenic mice were injected intraperitoneally (i.p.) with luciferin (150 mg/kg) and BLI was recorded in order to check the baseline activation of the IL-8 pathway. Briefly, 10 and 15 min following luciferin injection, mice were lightly anesthetized with isoflurane and images were obtained using the IVIS imaging system: an average of photons emitted from the chest of the mice was quantified using Living Image® software (Caliper Life Sciences, Alameda, CA, USA). The following day, mice were intratracheally challenged with 10X supernatants and BLI was recorded at 4, 24, and 48 h. Data were expressed as mean folds of induction (FOI) over the baseline activation of each mouse.

Bronchoalveolar lavage and cytokine

Twenty-four hours after intratracheal challenge, animals were weighted, anaesthetized with isoflurane and sacrificed by bleeding from the abdominal aorta for bronchoalveolar lavage fluid (BALF) collection, performed as previously described [8]. BALF supernatants were frozen at −80°C for simultaneous quantitation of multiple cytokines/chemokines using a Bio-Plex™ Cytokine Assay Kit (Bio-Rad Laboratories, Segrate, Milano, Italy).

The cell pellet was suspended in 0.2 mL of PBS and total and differential cell counts were obtained using an automated cell counter (Dasit XT 1800J, Cornaredo; Milano, Italy).

Reagents

In vivo JetPEI DNA transfection reagent (Polyplus Transfection) was obtained from Euroclone (Milan, Italy), D-luciferin was obtained from Perkin Elmer Inc. (Boston, MA, USA). AZM was from Pfizer (Italy).

Data analysis

Experimental values were expressed as the mean and standard error of the mean (SEM). Statistical analysis was performed using one-way analysis of variance followed by Dunnett's t test (* $p < 0.05$, ** $p < 0.01$).

Results

Phenotypic characterization of *Pseudomonas aeruginosa* clinical isolates

We have previously characterized by large-scale proteomic analysis the proteins released by different *P. aeruginosa* strains and have demonstrated their different capability to induce pro-inflammatory factors in bronchial epithelial cells [12]. For this study, we selected two *P. aeruginosa* strains, VR1 and VR2, isolated from two patients affected by CF and showing significant differences as regards phenotypic characteristics and release of various established virulence factors. The phenotypic characterization of the two strains is shown in Fig. 1. VR1 and VR2 differentiate for the production of pyoverdin and pyocyanin which are released only in the VR1 supernatant, the capability of moving by swimming, swarming and twitching detectable in VR1 but non in VR2, the production of biofilm which is more evident in VR1 with respect to VR2 and by the level of protease activity, well detectable in the VR1 supernatant and very reduced in the VR2 one.

Culture supernatants were prepared from the bacterial strains by growing them in a culture medium in the absence (SnVR1 and SnVR2) and in the presence of a sub-MIC dose of AZM (SnVR1 + AZM and SnVR2 + AZM). The inhibitory action of AZM on the expression of virulence factors is clearly shown in Fig. 1. Culture supernatants were tested for the presence of proteolytic activity by a proteases activatable fluorescent probe (Fig. 2) and by zymography (Fig. 3b). The specific inhibitory effect of AZM on metalloprotease synthesis used as a marker of the efficacy of the treatment was also demonstrated by testing cell lysate and supernatants for the presence of proteolytic activity with a proteases activable fluorescent

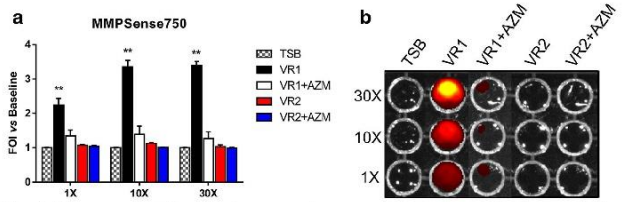

Fig. 2 Protease activity of cell-free supernatants from *Pseudomonas aeruginosa* grown in the presence and the absence of azithromycin. MMPsense 750 FAST was added to supernatants from VR1 and VR2 strains grown in presence or absence of AZM (SnVR1 ± AZM and SnVR2 ± AZM) concentrated 1X, 10X and 30X. IVIS imaging system has been used to quantify the time course of the fluorescence. Data were expressed as induction folds over baseline (bacterial growth medium TSB). Results are reported as mean ± SEM and significance attributed when $P < 0.05$ (*) or $P < 0.01$ (**).

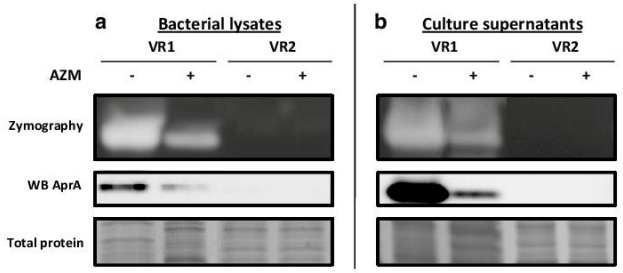

Fig. 3 Analysis of metalloproteases activity and synthesis in VR1 and VR2 bacterial lysates and culture supernatants. MPs activity and synthesis are downregulated in VR1 + AZM and absent in VR2, both in lysates (**a**) and supernatants (**b**), as shown by zymography and western blot specific for AprA.

probe (Fig. 2) and by zymography and western blotting specific for the *P. aeruginosa* metalloprotease, AprA (Fig. 3).

In vivo monitoring of lung inflammation induced by *P. aeruginosa* culture supernatants in IL-8 transiently transgenic mice

In vivo monitoring of lung inflammation after intratracheal challenge with *P. aeruginosa* SnVR1 and SnVR2 at 1X, 3X, 10X and 30X concentrations was carried out by in vivo imaging in bIL-8 luc transient transgenic mice. Administration of the 10X SN concentration was sufficient to induce the maximal increase in BLI signal. In fact, the use of the 30X Sn preparation did not translate into a higher inflammation signal, indicating a saturation of the system at lower concentration (10X) (Fig. 4a). For this reason, further experiments were conducted using 10X concentration.

SnVR1 pro-inflammatory activity was clearly detectable as soon as 4 h post instillation, although the BLI signal reached the highest peak at 24 h (FOI 5.11 ± 1.07) and was still detectable at 48 h even if there is no statistical difference among the different groups (Fig. 4b). On the contrary, the SnVR2 did not induce detectable inflammation in the mouse lung at any time point. The BLI signal induced by the challenge with SnVR1 + AZI was significantly lower (FOI 1.58 ± 0.21) after 24 h with respect to the response induced by SnVR1 obtained from the same bacterial strain grown without the antibiotic (Fig. 4b).

Recruitment of inflammatory cells and cytokine activation induced by *P. aeruginosa* culture supernatants

Twenty-four hours after mice stimulation with *P. aeruginosa* products, BALF was recovered from bIL-8 transgenic animals treated with both VR1 and VR2 supernatants in order to compare their effect on cell recruitment and cytokine expression. SnVR1, containing a series of important virulence factors, significantly stimulated total white blood cells (WBC) and neutrophils recruitment (respectively $6.52 \times 10^3 \pm 0.44$

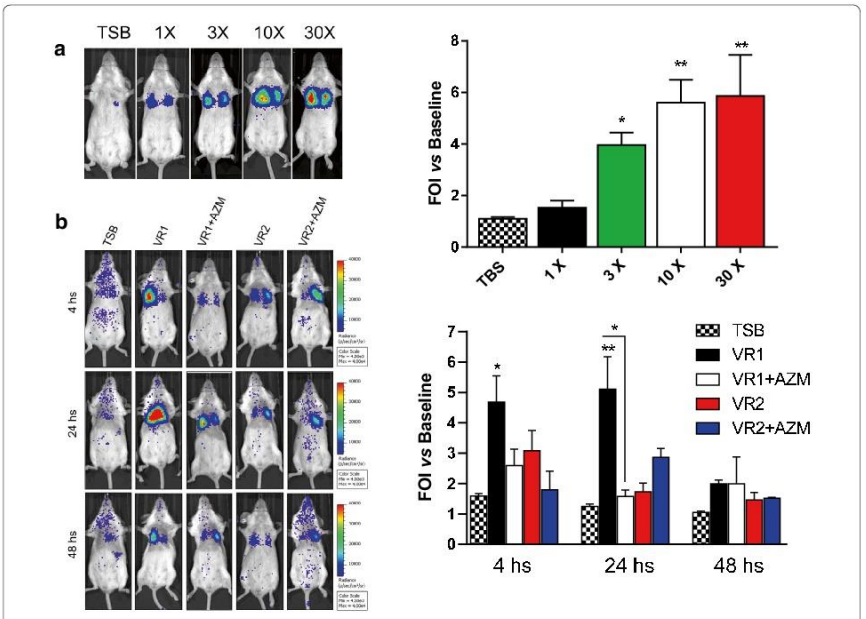

Fig. 4 In vivo imaging of lung inflammation induced by *P. aeruginosa* culture supernatants on IL-8 transiently transgenic mice. **a** Representative images of mice (n = 3 per group) transiently transgenized with bIL-8-Luc and intratracheally instilled with bacterial cell-free 1X, 3X, 10X and 30X supernatants from VR1. The growth medium TSB was used as a control. Mice were monitored at 4, 24 and 48 h post stimulation by BLI drawing a region of interest (ROI) over the chest. **b** Representative images of mice (n = 8 per group) transiently transgenized with bIL-8-Luc and intratracheally instilled with bacterial cell-free, 10X supernatants from VR1 and VR2 strains grown in presence or absence of AZM (VR1 ± AZM and VR2 ± AZM). The growth medium TSB was used as a control. Mice were monitored at 4, 24 and 48 h post stimulation by BLI drawing a region of interest (ROI) over the chest. Data are also presented as light intensity quantification of the ROI using the LivingImage software. The experiment was repeated 3 times and each point represents the mean ± standard error of 8 animals. Data were expressed as FOI over baseline activity of each mice and statistical differences were tested by one way ANOVA followed by Dunnett's post hoc test for group comparisons. Results are reported as mean ± SEM and significance attributed when $P < 0.05$ (*) or $P < 0.01$ (**).

and $4.19 \times 10^3 \pm 0.43$ cells/μL) and the expression of cytokines IL-1β, TNF-α, IL-17, RANTES, KC, IL 12 (p70) and IL 12 (p40) (Figs. 5, 6). Inflammatory cells (WBC $2.39 \pm 0.23 \times 10^3$ and neutrophils recruitment $1.70 \pm 0.0.22 \times 10^3$ cells/μL) and expression of the cited cytokines were lower in SnVR2 with respect to SnVR1. SnVR2 showed a comparable effect on the release of RANTES and IL 12 (p40).

BALF was recovered also from bIL-8 transgenic mice stimulated with SnVR1 + AZM and SnVR2 + AZM in order to evaluate the effect of the antibiotic on the pro-inflammatory activity of both preparations. The challenge with SnVR1 + AZM stimulated at a significant lower level WBC and neutrophils recruitment (respectively $4.07 \pm 0.39 \times 10^3$ and $2.05 \pm 03.4 \times 10^3$ cells/μL) (Fig. 5) and the expression of the cytokines IL-1β, IL-17, RANTES, KC and IL-12 (p70) but not that of TNF-α and IL 12 (p40) in comparison with animals treated with SnVR1 (Fig. 6). A significant difference between the stimulation caused by SnVR2 and SnVR2 + AZM was not observed except for RANTES and IL12-(p40) level (Fig. 6).

Conclusions

The mechanisms and mediators that drive the induction and progression of chronic inflammation and alter lung

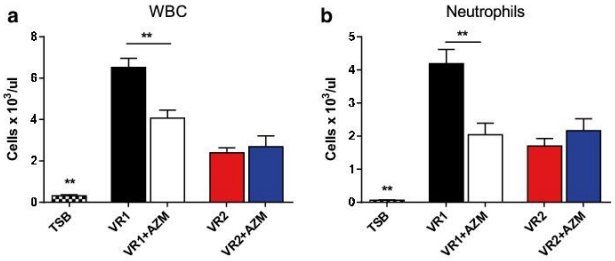

Fig. 5 Immune cell recruitment during lung inflammation caused by *P. aeruginosa* supernatants. Cellular infiltration into the lung of mice intratracheally instilled with bacterial cell-free 10X supernatants from VR1 and VR2 strains grown in presence or absence of AZM (VR1 ± AZM and VR2 ± AZM). TSB is the bacterial growth medium and was used as a control. The amount of white blood cells and neutrophils found in BALF was expressed as number of cells per µl at 24 h post treatment. The experiment was repeated 3 times and each point represents the mean ± standard error of 8 animals. Results are reported as mean ± SEM and significance attributed when $P < 0.05$ (*) or $P < 0.01$ (**).

function in a series of human diseases are not completely understood and this has severely hampered the development of effective treatments [1–3]. Although most of the animal models do not exactly mimic human lung diseases and each model has its own benefits and deficiencies, animal models that accurately reflect human disease pathophysiology continue to be essential for the understanding of pathogenic aspects as well as the development and validation of new therapies. In most mammalian models, TNFα, IL-1β, and IL-8 are central components of a complex cytokine network that initiates, amplifies, and sustains the inflammatory response in tissue [18]. Available evidence also supports the importance of this network in coordinating acute inflammatory responses within the lung. The mouse model used in this study, transiently transgenized with a luciferase reporter gene under the control of the IL-8 bovine promoter, can be easily employed for modeling and monitoring human lung inflammation due to the high similarity existing between respiratory diseases in ruminants and humans without the high costs and demands in terms of maintenance of ruminant models [8].

In the present study, the IL8/luciferase mouse model has been applied to the in vivo monitoring of lung inflammation induced by virulence factors released by *Pseudomonas aeruginosa* and to the evaluation of the anti-inflammatory action of AZM as an inhibitor of the synthesis of bacterial factors involved in pathogenicity. Data here presented show that the *P. aeruginosa* clinical strain VR1, isolated from early lung colonization in a CF patient, synthesizes flagella and biofilm, produces and releases pyocyanin and pyoverdine and proteins with metallo-protease activity. The synthesis and release of these virulence factors significantly decreases when bacteria were grown in the presence of AZM. The pro-inflammatory effect of strain VR1 has been shown in IL-8/luciferase transiently transgenic mice by applying in vivo imaging and further confirmed by the increase in WBC and neutrophils recruitment and cytokine levels in the airways of transgenized mice. On the contrary, the supernatant from bacteria grown in the presence of AZM, a condition associated with a much lower production of virulence factors, stimulated the inflammatory response only at a very reduced level. Similar low levels of IL-8 promoter activation was observed when the supernatant of the *P. aeruginosa* VR2 strain, lacking the specific virulence factors, was instilled in the airways of IL-8/luciferase transgenized mice.

These data support the notion that the clinical benefits associated to AZM treatment in CF patients might be at least in part due to the lowering of the exoproduct synthesis induced by the antibiotic in bacterial cells.

Data obtained in this study demonstrate that the model here described is suitable to non-invasive real time monitoring of lung inflammatory response to bacterial products and to confirm and better understand the mechanism of action of AZM (or any other compound of interest), an antibiotic frequently used in the therapy of CF. The non invasive nature of this mouse model and the possibility for bIL-8-luc transiently transgenized mice to be stimulated with bacterial products for long times [8] enables the monitoring of a biological process longitudinally in the same mouse and represents an obvious advance for functional as well as pharmacological

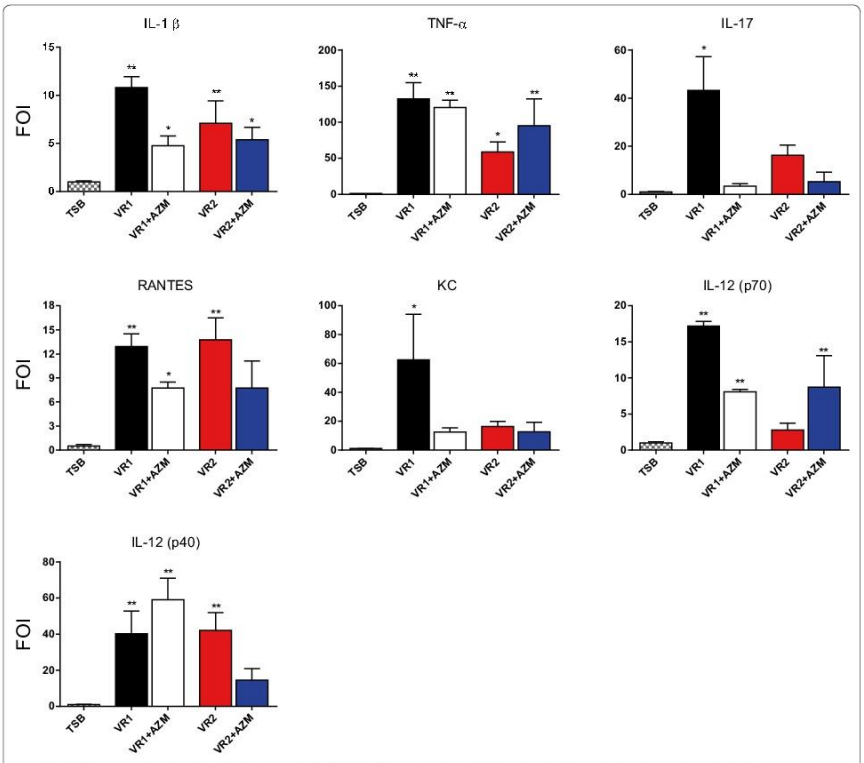

Fig. 6 Cytokines concentration in mice BALF after stimulation with *P. aeruginosa* culture supernatants. Cytokine levels in BALF of bIL-8 transgenized mice 24 h after intratracheally challenge with bacterial cell-free supernatants from VR1 and VR2 strains grown in presence or absence of AZM (VR1 ± AZM and VR2 ± AZM). Data were expressed as FOI over the control (bacterial growth medium TSB) The experiment was repeated 3 times and each point represents the mean ± standard deviation of 8 animals. Results are reported as mean ± SEM and significance attributed when $P < 0.05$ (*) or $P < 0.01$ (**).

studies. The model might be adapted and applied to study the pathogenesis of lung inflammatory diseases such as CF, to identify bacterial/nonbacterial factors with pro-inflammatory activity and to predict the possible therapeutic effect of known and new molecules with a presumptive anti-inflammatory action.

Abbreviations

AZM: azithromycin; NIR: near infrared; BLI: bioluminescence imaging; BALFs: bronchoalveolar lavage fluids.

Authors' contributions

Conception and design, FS, GB, GD, CS, PM, MML. Laboratory testing, FS, FR, GB, AS, PM. Data collection, FS, FR, GB, AS. Data analysis and interpretation: FS, GB, CS, PM, MML, BMA. Drafting of manuscript: FS, GB, GD, GV, CS, PM, MML. All authors read and approved the final manuscript.

Author details

[1] Pharmacology and Toxicology Department Corporate Pre-Clinical R&D, Chiesi Farmaceutici S.p.A. Parma, Largo Belloli, 11/A, 43122 Parma, Italy. [2] Dipartimento di Patologia e Diagnostica, Università di Verona, Verona, Italy. [3] Dipartimento di Scienze Medico Veterinarie, Università di Parma, Parma, Italy. [4] Dipartimento di Scienze Biomediche, Biotecnologiche e Traslazionali, Università di Parma, Parma, Italy. [5] Centro Regionale Fibrosi Cistica, AOUI Verona, Verona, Italy.

Acknowledgements
This work was supported by Fondazione Fibrosi Cistica Project Number 18/2013 and Lega Italiana Fibrosi Cistica (Italian Cystic Fibrosis League) through Veneto Branch—Associazione Veneta Lotta contro la Fibrosi Cistica Onlus.

Compliance with ethical guidelines

Competing interests
FS, GV, are employees of Chiesi Farmaceutici S.p.A., that supported the research work. FR is a consultant of Chiesi Farmaceutici S.p.A.

Received: 15 May 2015 Accepted: 21 July 2015
Published online: 04 August 2015

References

1. Cohen-Cymberknoh M, Kerem E, Ferkol T, Elizur A (2013) Airway inflammation in cystic fibrosis: molecular mechanisms and clinical implications. Thorax 68:1157–1162
2. Dhooghe B, Noël S, Huaux F, Leal T (2014) Lung inflammation in cystic fibrosis: pathogenesis and novel therapies. Clin Biochem 47:539–546
3. Nakou A, Papaparaskevas J, Diamantea F, Skarmoutsou N, Polychronopoulos V, Tsakris A (2014) A prospective study on bacterial and atypical etiology of acute exacerbation in chronic obstructive pulmonary disease. Future Microbiol 9:1251–1260
4. Folkesson A, Jelsbak L, Yang L, Johansen HK, Ciofu O, Høiby N et al (2012) Adaptation of *Pseudomonas aeruginosa* to the cystic fibrosis airway: an evolutionary perspective. Nat Rev Microbiol 10:841–851
5. Sagel SD (2003) Noninvasive biomarkers of airway inflammation in cystic fibrosis. Curr Opin Pulm Med 9:516–521
6. Starkey MR, Jarnicki AG, Essilfie AT, Gellatly SL, Kim RY, Brown AC et al (2013) Murine models of infectious exacerbations of airway inflammation. Curr Opin Pharmacol 13:337–344
7. Vlahos R, Bozinovski S (2014) Recent advances in pre-clinical mouse models of COPD. Clin Sci (Lond) 126:253–265
8. Stellari FF, Franceschi V, Capocefalo A, Ronchei M, Facchinetti F, Villetti G et al (2012) In vivo imaging of transiently transgenized mice with a bovine interleukin 8 (CXCL8) promoter/luciferase reporter construct. PLoS One 7(6):e39716
9. Ansaldi D, Hod EA, Stellari F, Kim JB, Lim E, Roskey M et al (2011) Imaging pulmonary NF-kappaB activation and therapeutic effects of MLN120B and TDZD-8. PLoS One 6:e25093
10. Stellari FF, Lavrentiadou S, Ruscitti F, Jacca S, Franceschi V, Civelli M et al (2014) Enlightened Mannhemia haemolytica lung inflammation in bovinized mice. Vet Res 45:8–13
11. Stellari FF, Sala A, Donofrio G, Ruscitti F, Caruso P, Topini TM et al (2014) Azithromycin inhibits nuclear factor-κB activation during lung inflammation: an in vivo imaging study. Pharmacol Res Perspect 2(5):e00058
12. Bergamini G, Di Silvestre D, Mauri P, Cigana C, Bragonzi A, De Palma A et al (2012) MudPIT analysis of released proteins in *Pseudomonas aeruginosa* laboratory and clinical strains in relation to pro-inflammatory effects. Integr Biol (Camb) C 4:270–279
13. Molinari G, Guzman CA, Pesce A, Schito GC (1993) Inhibition of *Pseudomonas aeruginosa* virulence factors by sub-inhibitory concentrations of azithromycin and other macrolide antibiotics. J Antimicrob Chemother 31:681–688
14. Mizukane R, Hirakata Y, Kaku M, Ishii Y, Furuya N, Ishida K et al (1994) Comparative in vitro exoenzyme-suppressing activities of azithromycin and other macrolide antibiotics against *Pseudomonas aeruginosa*. Antimicrob Agents Chemother 38:528–533
15. Tateda K, Comte R, Pechere JC, Köhler T, Yamaguchi K, Van Delden C (2001) Azithromycin inhibits quorum sensing in *Pseudomonas aeruginosa*. Antimicrob Agents Chemother 45:1930–1933
16. Doring G, Conway SP, Heijerman HG, Hodson ME, Høiby N, Smyth A et al (2000) Antibiotic therapy against *Pseudomonas aeruginosa* in cystic fibrosis: a European consensus. Eur Respir J 16:749–767
17. Institute of Laboratory Animal Resources Commission on Life Sciences, National Research Council (1996) Guide for the care and use of laboratory animals. National Academy Press, Washington, DC
18. Hurley K, Mehta A, Cox S, Ryan D, O'Neill SJ, Reeves EP et al (2013) Airway inflammatory markers in individuals with cystic fibrosis and non-cystic fibrosis bronchiectasis. Inflamm Res 6:1–11

In vivo monitoring of lung inflammation in CFTR-deficient mice

Fabio Stellari*, Gabriella Bergamini*, Francesca Ruscitti, **Angela Sandri**, Francesca Ravanetti, Gaetano Donofrio, Federico Boschi, Gino Villetti, Claudio Sorio, Barouk Maurice Assael, Paola Melotti and Maria del Mar Lleò

Journal of Translational Medicine (2016) 14:226

DOI 10.1186/s12967-016-0976-8

*Equal contribution

Stellari et al. J Transl Med (2016) 14:226
DOI 10.1186/s12967-016-0976-8

Journal of Translational Medicine

RESEARCH Open Access

In vivo monitoring of lung inflammation in CFTR-deficient mice

Fabio Stellari[1*†], Gabriella Bergamini[2†], Francesca Ruscitti[3], Angela Sandri[4], Francesca Ravanetti[5], Gaetano Donofrio[5], Federico Boschi[6], Gino Villetti[1], Claudio Sorio[2], Barouk M. Assael[7], Paola Melotti[7] and Maria M. Lleo[4]

Abstract

Background: Experimentally, lung inflammation in laboratory animals is usually detected by the presence of inflammatory markers, such as immune cells and cytokines, in the bronchoalveolar lavage fluid (BALF) of sacrificed animals. This method, although extensively used, is time, money and animal life consuming, especially when applied to genetically modified animals. Thus a new and more convenient approach, based on in vivo imaging analysis, has been set up to evaluate the inflammatory response in the lung of CFTR-deficient (CF) mice, a murine model of cystic fibrosis.

Methods: Wild type (WT) and CF mice were stimulated with *P. aeruginosa* LPS, TNF-alpha and culture supernatant derived from *P. aeruginosa* (strain VR1). Lung inflammation was detected by measuring bioluminescence in vivo in mice transiently transgenized with a luciferase reporter gene under the control of a bovine IL-8 gene promoter.

Results: Differences in bioluminescence (BLI) signal were revealed by comparing the two types of mice after intratracheal challenge with pro-inflammatory stimuli. BLI increased at 4 h after stimulation with TNF-alpha and at 24 h after administration of LPS and VR1 supernatant in CF mice with respect to untreated animals. The BLI signal was significantly more intense and lasted for longer times in CF animals when compared to WT mice. Analysis of BALF markers: leukocytes, cytokines and histology revealed no significant differences between CF and WT mice.

Conclusions: In vivo gene delivery technology and non-invasive bioluminescent imaging has been successfully adapted to CFTR-deficient mice. Activation of bIL-8 transgene promoter can be monitored by non-invasive BLI imaging in the lung of the same animal and compared longitudinally in both CF or WT mice, after challenge with pro-inflammatory stimuli. The combination of these technologies and the use of CF mice offer the unique opportunity of evaluating the impact of therapies aimed to control inflammation in a CF background.

Keywords: In vivo bioluminescence imaging, Lung inflammation mouse model, Pseudomonas aeruginosa, CFTR-deficient mice

Background

In cystic fibrosis (CF), chronic neutrophilic inflammation with the release of damaging neutrophil products, such as neutrophil elastase, constitutes a key risk factor in early structural lung damage and lung function decline [1]. Bacterial infection stimulates an intense neutrophilic response which fails to eradicate the infection leading to sustained release of pro-inflammatory mediators, continuous influx of inflammatory cells and bacteria persistence [2]. Despite advances in our understanding of the molecular and cellular basis of CF, the paradox of why recruited neutrophils fail to eradicate bacterial infections in the lung remains [2, 3], although recent data from our group indicate a deficit in leukocyte trafficking as a possible mechanism [4]. The progress in understanding the relationship between cystic fibrosis airway inflammation and infection may facilitate the understanding on how to interrupt the self-perpetuating inflammatory response and pursue new directions in treatment.

*Correspondence: fb.stellari@chiesi.com
†Fabio Stellari and Gabriella Bergamini contributed equally to this work
[1] Pharmacology & Toxicology Department Corporate Pre-Clinical R&D, Chiesi Farmaceutici, Largo Belloli, 11/A, 43122 Parma, Italy
Full list of author information is available at the end of the article

Measuring airway inflammation in CF is important for initiating the anti-inflammatory treatment and monitoring its effect. At present, no inflammatory biomarker has been consistently shown to predict clinical efficacy [3]. Frequently, in mouse models, inflammation is induced by instillation of bacterial products with pro-inflammatory activity such as lipopolysaccharide (LPS) and monitored by analyzing the presence of inflammatory markers. Unfortunately, the conventional assessments of inflammation in mice often rely on invasive ex vivo measurements which causes the death of the animal and are consequently particularly onerous when costly transgenic mice are utilized. Moreover, this protocol may not be fully reproducible, probably due to the heterogeneity of airway inflammation in CF. Furthermore, the characterization of pulmonary functions, cellular infiltration and cytokines determination in BALF and the observation of anatomical changes, such as airway remodeling due to inflammation, an approach that, while extensively used and highly validated, precludes the possibility to repeat longitudinally the assessment of test animals [5–7]. However, in vitro and in vivo protocols in animal models have been used to study the mechanism of lung inflammation in chronic diseases and to evaluate the anti-inflammatory role of some candidate molecules [8–10]. Recently emerging non-invasive imaging technologies such as magnetic resonance imaging (MRI), micro-CT and optical imaging have been applied to longitudinal monitoring of airway remodeling and inflammation in murine models [11–14]. The clinical imaging system used in MRI, CT and PET, have been further adapted to murine models of asthma [11, 15–17], to serve as a preclinical and translational step between basic discovery and clinical practice, whereas optical imaging technologies developed in experimental settings may also slow-down their way into the clinical practice, especially in the context of intraoperative activities [18, 19]. Recently a mouse model transiently expressing the luciferase reporter gene under the control of a bovine IL-8 promoter has been generated [20]. Although mice do not express IL-8, the cell signaling and transcriptional apparatus could specifically activate the bovine IL-8 promoter [20]. In the present work, real time monitoring of lung inflammation in CF mice has been successfully applied by taking advantages of the genetic construct carrying the IL-8 promoter/luciferase reporter gene.

Methods

Experimental animals

Gut-corrected CFTR-deficient female C57Bl/6 Cftrtm1-UNCTgN(FABPCFTR)#Jaw and their congenic WT female mice, 6–8 weeks old (Charles River), provided by the (CFaCore facility, Milano, Italy), were used. Prior to use, animals were acclimatized for at least 5 days to the local vivarium conditions (room temperature: 20–24 °C; relative humidity: 40–70 %; 12-h light–dark cycle), having free access to standard rodent chow and softened tap water. All animal experiments described herein were approved by the intramural animal-welfare committee for animal experimentation of Chiesi Farmaceutici and by the Interdeparmental Centre of Experimental Research Service at the University of Verona, and comply with the European Directive 2010/63 UE, Italian D.Lgs 26/2014 and the revised "Guide for the Care and Use of Laboratory Animals".

Collection of bacterial cell-free supernatants

P. aeruginosa strain, VR1 was isolated from a sputum sample of a CF patient followed at the Cystic Fibrosis Center in Verona, Italy. Written informed consent was obtained from the subjects enrolled in the study and approved by the Institutional Review Board of Azienda Ospedaliera Universitaria Integrata (AOUI) Verona as project 1612. The bacterial strain was grown overnight at 37 °C in Bacto™ Tryptic Soy Broth (TSB, Becton, Dickinson and Company) with continuous agitation. The day after, *P. aeruginosa* cells were diluted in TSB to the concentration of 1×10^8 CFU/ml (OD of 0.1 at 600 nm) and grown overnight at 37 °C shaking. The following day, the culture was normalized to an optical density of 0.2 OD at 600 nm. Culture supernatant (VR1Sn) was collected by centrifugation (7000×*g*, 30 min, 4 °C) and filtered through a 0.22 µm Millipore filter to remove any remaining bacteria. VR1Sn was concentrated to 30× using Amicon Ultra-15 30 K (Millipore, Billerica, USA), then centrifuged at 27,000×*g* for 1 h at 4 °C to remove cellular debris and finally sterilized by filtration through a Millipore 0.22 µm filter.

In vivo gene delivery

The bIL-8-Luc plasmid (Dipartimento di Scienze Medico Veterinarie, Università di Parma, Italy) was obtained by sub-cloning the 2030 bp IL8 bovine promoter, amplified by PCR from Madin–Darby bovine kidney (MDBK; ATCC #CCL-22) genomic DNA into the digested pGL-3basic vector (promega) as previously described [20]. We applied in vivo JetPEI (Polyplus Transfection) as a carrier for delivering DNA to lung tissues. The DNA and JetPEI mix was formulated according to the product manual with a final N/P ratio of 7.5. Briefly, 50 µg of bIL-8–Luc and 7.5 µL of JetPEI were both diluted into 200 µL 5 % glucose. The two solutions were then mixed and incubated for 15 min at room temperature. The entire mixture was injected intravenously in mice and the expression of bIL-8–Luc was monitored through imaging with IVIS Spectrum (Perkin Elmer, Massachusetts, USA).

In vivo bioluminescence imaging

Transfection per se causes a mild lung inflammatory response and bIL-8 activation, which is detectable by BLI up to 3–4 days after DNA injection and disappears completely after 1 week [20, 21]. No difference in extension and duration of BLI signal between wild type and CF mice at 3–4 and 7 days of observation after DNA delivery has been observed. (Additional file 1: Figure S1). One week after DNA delivery, before initiating the experiment, all the transient transgenic mice were injected intraperitoneally (i.p.) with luciferin (150 mg/kg) and BLI was recorded in order to check the baseline activation of the IL-8 pathway. Slightly differences in promoter activation detected in the different mice can be normalized by dividing the BLI value obtained from each mouse with the basal photon emission found in the same mouse in order to determine the fold of induction (FOI) as presented in the graphs. This procedure ensures that the data are referred to each individual animal and take in account even slightly different response rates.

Briefly, 10 and 15 min after luciferin injection, mice were lightly anesthetized with isoflurane and images were obtained using the IVIS imaging system: a total of photons emitted from the chest of the mice was quantified using Living Image ® software (Perkin Elmer Inc. Boston, MA, USA).

The following day, mice were intratracheally challenged with *P. aeruginosa* LPS (6.125 µg/mouse), VR1Sn (10×) or human TNF-alpha (1 µg/mouse) using a volume of 50 µl and BLI was recorded at 4, 24, and 48 h. Data were expressed as mean folds of induction (FOI) over the baseline activation of each mouse.

Bronchoalveolar lavage and cytokines

Twenty-four hours after intratracheal challenge, animals were weighted, anaesthetized with isoflurane and sacrificed by bleeding from the abdominal aorta for bronchoalveolar lavage fluid (BALF) collection, performed as previously described [20]. BALF supernatants were frozen at −80 °C for simultaneous quantification of multiple cytokines/chemokines using a Bio-Plex™ Cytokine Assay Kit (Bio-Rad Laboratories, Segrate, Milan, Italy). The cell pellet was resuspended in 0.2 mL of phosphate buffered saline (PBS) and total and differential cell counts were obtained using an automated cell counter (Dasit XT 1800 J, Cornaredo; Milan, Italy).

Histology

Lungs were removed and inflated with a cannula through the trachea by gentle infusion with 0.6 ml of 10 % neutral-buffered formalin. Subsequently, the lungs were placed in 10 % formalin and fixed for at least 24 h. The whole lungs were dehydratated in graded ethanol series, clarified in xylene and paraffin embedded. 5 µm thick sections were cut with a rotary microtome (Reichert–Jung 1150/Autocut) in ventral dorsal plane. For analysis, the sections were stained with hematoxylin-eosin and Giemsa according to standard methods. A previously described lung injury score [22], that included the evaluation of neutrophils in the alveolar and in the interstitial space, the formation of hyaline membranes, the presence of proteinaceus debris and the alveolar septal thickening was applied.

Reagents

In vivo JetPEI DNA transfection reagent (polyplus transfection) was obtained from Euroclone (Milan, Italy), D-luciferin was obtained from Perkin Elmer Inc. (Boston, MA, USA). LPS (from *P. aeruginosa* 0111:B4, product n.L3012) from Sigma (St. Louis, MO) was resuspended in Eagle's minimal essential medium (EMEM).

Data analysis

Experimental values were expressed as the mean and standard error of the mean (SEM). Statistical analysis was performed using one-way analysis of variance followed by Dunnett's t test (*$p < 0.05$, **$p < 0.01$).

Results

The possibility to monitor longitudinally in no-invasive way the activation of IL-8 in the same mice CF compared to WT after intratracheally challenged with inflammatory stimuli such as: human TNF-alpha, LPS P. aeruginosis and with the culture supernatant obtained from the *P. aeruginosa* clinical strain VR1 is step a forward in investigating the molecular mechanism linked to cystic fibrosis and with the advantage of reducing the number of animals required. Starting from the previously acquired assumption that intratracheal instillation of hTNF-alpha 1 week after delivery of the luciferase reporter DNA construct caused activation of bIL-8 in mice that could be easily detected and monitored by IVIS [20]; it was of interest to know if the same system could be applied in CF mice. To this end, CF mice were transiently transgenized with bIL-8-Luc.DNA construct, intratracheally challenged with hTNF-alpha (1 µg/mouse) and compared with WT mice (Fig. 1) Luc expression driven by bIL-8 activation at 4 h after TNF-alpha challenge (Fig. 1e) revealed a significant increase of BLI in CF mice in comparison with WT animals (3.1 and 1.2 FOI, $p < 0.01$) over baseline (untreated mice) (Fig. 1b, d, e). The BLI signal was still detectable without significant differences at 24 h (Fig. 1b, d) in both CF and WT mice (1.5 and 1.2, FOI respectively), while at 48 h the BLI signal was not detectable anymore. CF and WT mice intratracheally treated with saline did not show any BLI signal either

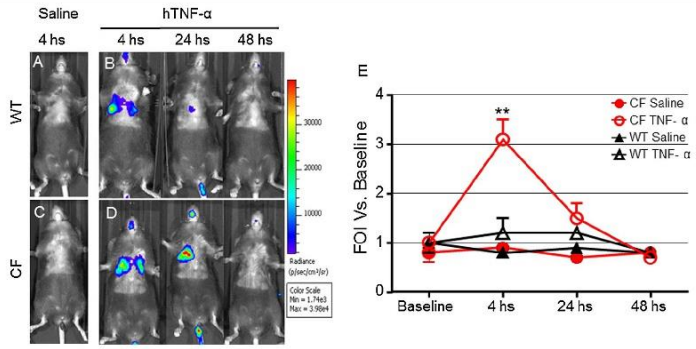

Fig. 1 Representative in vivo images of WT and CF mice transiently transgenized with bIL-8-Luc and intratracheally challenged with hTNF-alpha (1 μg/mouse) and monitoring of bIL-8 activation by BLI. **a, c**: WT and CF mice treated with saline solution (control). **b, d**: WT and CF mice after intratracheal instillation with hTNF-alpha and monitoring of IL-8 activation at 4, 24 and 48 h by BLI. **e**: Time-course of IL-8-Luc activation in WT and CF mice. Results are reported as folds of increase (FOI) over baseline as mean ± SEM, n = 9 each group. Statistical differences were tested by one-way ANOVA followed by Dunnett's t post hoc test for group comparisons. *p < 0.05 and **p < 0.01

at 4 h (Fig. 1a, c) or at later time points of observation. This preliminary set of experiments allowed us to select the optimal transfection conditions and to determine the right time of imaging acquisition. Although the gene delivery technology has been well established [20, 21, 23, 24], every strain of mouse required their own transfection conditions and responded to stimuli in a different manner. C57Bl/6 mice have a black fur that is an obstacle for optical imaging technologies, because black color quenched partially the light even if they were shaved in order to minimize the interference with BLI signal. In the next series of experiments, imaging has been performed only at 4 and 24 h because the BLI signal significantly decreased at 48 h. The same mice challenged with hTNF-alpha, have been reutilized and intratracheally challenged with *P. aeruginosa* LPS (6.25 μg/mouse) after 2 weeks of wash-out. As shown in Fig. 2, both CF and WT mice responded to LPS reaching the maximum BLI signal between 4 and 24 h post-challenge. Interestingly, WT animals challenged with *P. aeruginosa* LPS showed a higher BLI signal compared to CF mice already at 4 h (3.2 and 1.9 FOI respectively) over baseline (Fig. 2b, e, g). However only at 24 h, the BLI signal was significantly higher in CF compared to WT mice (6.7 and 2.1 FOI, $p < 0.05$) (Fig. 2b, e, g). No significant increases in the BLI signal was detected when CF and WT mice were intratracheally treated with the culture medium (EMEM) (Fig. 2a, d). After imaging at 24 h, the same mice were sacrificed for BALFs collection and histological analysis. Right after BALF sampling, lungs were excised and imaging was performed. As clearly shown in ex vivo pictures the BLI signal was well localized in the lung and higher in CF compared to WT mice (Fig. 2c, f), lending support to the positive correlation between in vivo and ex vivo imaging. Formally, information collected by BLI (bioluminescent signal in the lung higher in CF compared to WT mice) and from BALF (WBC and neutrophils counts in BALFs in both mouse strains) cannot directly compared and put "in contrast" to each other. (Fig. 2h). The lungs of CF and WT challenged with either EMEM (Fig. 2i, m) or *P. aeruginosa* LPS (Fig. 2l, n) were fixed in formalin for histological analysis after Giemsa staining. As expected, *P. aeruginosa* LPS-induced lung injury was characterized by neutrophils accumulation, alveolar wall thickening and proteinaceous detritus accumulation in the alveolar space of the lungs of either CF or WT mice when compared to control mice treated with EMEM. Area of emphysema and a slight degree of fibrosis were detected within the lung parenchyma of WT and CF mice without any significant differences as regards the type and degree of histological damage (Fig. 2m, n). Eight in 23 cytokines evaluated in BALFs of WT and CF mice 24 h after stimulation with *P. aeruginosa* LPS, resulted up-regulated when compared to the control animals (Fig. 3). IL-1β, IL-5, KC, IL-6, G-CSF, INFγ, MIP-1α, and TNF-α, are the major pro-inflammatory mediators in acute immune-response and they increased in the same manner in CF and WT LPS challenged mice. Their up-regulation resulted in full agreement between inflammatory cells infiltration and histological analysis (Fig. 2h, m, n).

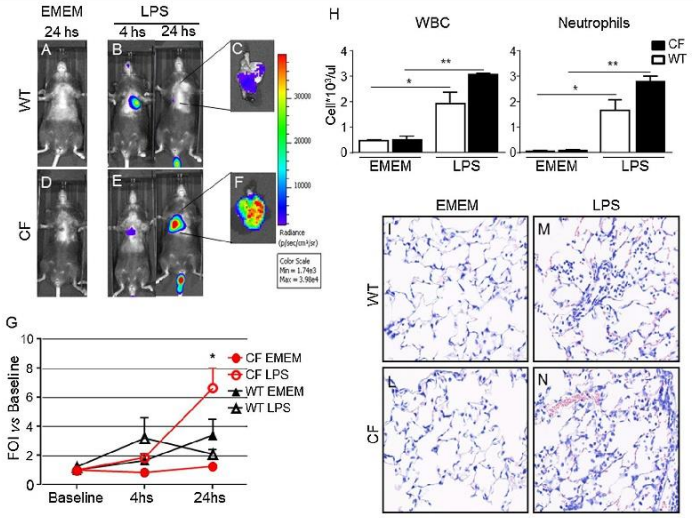

Fig. 2 Representative in vivo images of WT and CF mice transiently transgenized with bIL-8-Luc and intratracheally treated with *Pseudomonas* LPS (6.25 μg/mouse). **a, d**: WT and CF mice treated with EMEM (control). **b, e**: WT and CF mice after intratracheal instillation with LPS and monitored IL-8 activation at 4 and 24 h by BLI. **C, F**: ex vivo images of IL-8 activation in lungs excised from WT and CF mice at 24 hs after LPS challenge. *Panel G*: Time-course of IL-8-luc activation in WT and CF mice. Results are reported as folds of increase (FOI) over baseline as mean ± SEM, n = 6 at each group. **h**: Cellular infiltration into the lung of WT and CF mice after intratracheal instillation with LPS at 24 h. Three mice were used for every time point and the experiment was replicated three times. Values are expressed as mean ± SEM of the three different experiments. Statistical differences were tested by one-way ANOVA followed by Dunnett's t post hoc test for group comparisons. *$p < 0.05$ and **$p < 0.01$ WT and CF TSB vs WT and CF LPS group. (**l**–**n**): Representative photomicrographs of Giemsa stained lung of WT and CF mice after intratracheal instillation with EMEM (l, L) and LPS (M, N) at 24 h. Magnification 40×

In another series of experiments, WT and CF mice were challenged with the supernatant culture (10X) obtained from the *P. aeruginosa* clinical strain VR1 [25]. As recently reported [25], this strain produces and releases in the culture medium a number of virulence factors, such as metalloproteases, pyocianine and pyoverdine, showing pro-inflammatory activity. Intratracheally treatment with VR1Sn was able to activate bIL-8 in transiently transgenic CF and WT mice. (Fig. 4g). WT animals responded with an higher BLI signal at 4 h (1.6 FOI) compared to CF mice, which revealed a very weak signal intensity at the same time point of observation (Fig. 4b, e, g). Nevertheless 24 h after challenge, BLI signal increased significantly in CF compared to WT mice (2.9 and 1.2 FOI, $p < 0.05$) (Fig. 2b, e, g). No significant increases in the BLI signal was detected when CF and WT mice when intratracheally treated with TSB (Fig. 2a, d). Either *P. aeruginosa* LPS or VR1Sn showed a similar behavior on bIL-8 activation. WT animals responded with max BLI signal at 4 h, indicating an early activation of the gene while, on the contrary, CF mice reveled a late response at 24 h. After in vivo imaging at 24 h, mice previously imaged were sacrificed, BALFs collected and lungs removed and subjected to histological analysis and BLI imaging as clearly shown in ex vivo pictures (Fig. 4c, f). The BLI signal was higher in CF confirming the in vivo bioluminescence imaging data. Surprisingly and in contrast with BLI signal, VR1Sn induced an increase in total WBC and neutrophils in BALFs of CF and WT mice, but significant differences were not detectable (Fig. 4h). Lungs coming from TSB or VR1Sn challenged WT and CF mice were fixed in formalin and a Giemsa staining was performed. A widely diffused mononuclear cell infiltrate characterized all the VR1Sn-challenged samples either from CF or WT mice as compared to control mice in which a normal parenchyma was presented (Fig. 4i, l). Histologically, the alveolar space and thicker alveolar septa were filled with acute phase inflammatory cells,

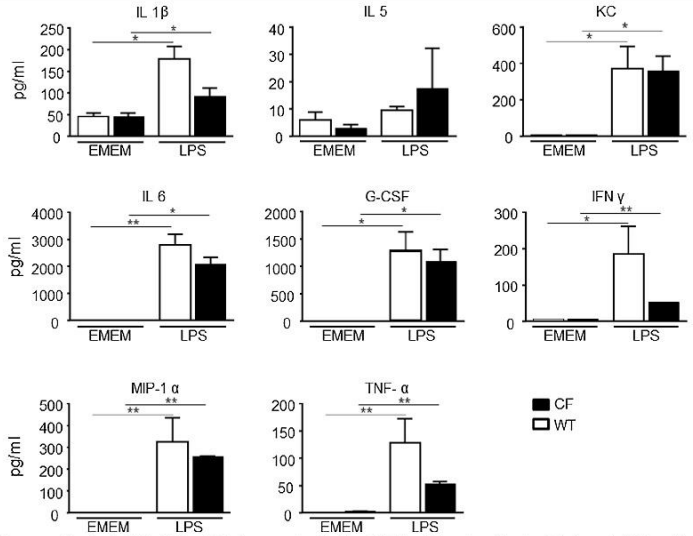

Fig. 3 Cytokines quantification in BALFs. WT and CF mice, treated with either EMEM or LPS and sacrificed at 24 h. A panel of 23 cytokines was analysed using a Bio-Plex™ Cytokine Assay Kit (Bio-Rad Laboratories). Eight resulted up-regulated compared to the control animals: IL-1β, IL-5, KC, IL-6, G-CSF, INFγ, MIP-1α, and TNF-α Three mice were used for every time point and the experiment was replicated three times. Values are expressed as mean ± SEM. Statistical differences were tested by one-way ANOVA followed by Dunnett's t post hoc test for group comparisons. *$p < 0.05$ and **$p < 0.01$

including neutrophils, eosinophils, alveolar macrophages and lymphocytes. Within the alveolar space also proteinaceous detritus were detected. However, the same type and severity of histological damage was observed in WT and CF mice (Fig. 4m, n). Up-regulation of the same set of cytokines after *P. aeruginosa* LPS and VR1 culture supernatant treatment was observed (Fig. 5).

Discussion

The animal model previously developed has been successfully adapted to CFTR-deficient mice. After induction with human TNF-alpha and *P. aeruginosa* LPS, it was possible to detect BLI signal exactly from the thorax areas with higher signals in CF animals with respect to WT mice at 24 h after challenge. Bioluminescent signal was still detectable for as long as 48 h, although at this time point the signal decreased and it became difficult to appreciate the differences between the two types of mice. Further validation by challenging the mice with culture supernatants containing virulence factors released by a clinical strain of *P. aeruginosa* previously characterized [25]. Also in this case, statistically significant differences between WT and CF inflammatory responses were revealed with a stronger response of CF mice as compared to WT animals at 24 h. Lung inflammatory markers, such as immune cells, cytokines and histology, were monitored in BALF after pro-inflammatory stimulation but they did not show significant differences between CF and WT mice. Although surprising at a first glance, we must consider that a differential degree of strain sensitivity to pro-inflammatory stimuli has been reported [26]. Indeed, the same intratracheal challenge consisting in VR1Sn (10X) was used in BALB/C mice and the absolute number of inflammatory cells recruited into the lung 24 h after treatment was much higher than in the C57Bl/6 mouse strain [25], supporting this interpretation. The reporter gene utilized relies on bIL-8 promoter, which responds mainly to NF-κB while additional master genes, like AP-1 (Fos/Jun), NFATs, and STATs, control the expression of several cytokines [27]. Such additional pathways can be activated in different mouse strains that might bypass the need of full NF-κB recruitment. In our

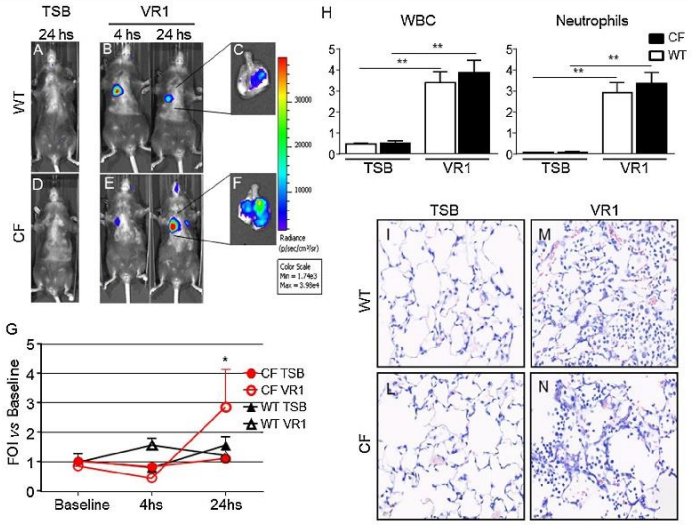

Fig. 4 Representative in vivo images of WT and CF mice transiently transgenized with bIL-8-Luc intratracheally challenged with VR1 culture supernatant (10X/mouse), and monitoring of bIL-8 activation by BLI. **a**, **d**: WT and CF mice after intratracheal instillation with TSB (control). Panel B, E: WT and CF mice after intratracheal instillation with VR1Sn and monitoring of IL-8 activation at 4 and 24 h by BLI. **c**, **f**: ex vivo images of IL-8 activation in lungs excised from WT and CF mice at 24 h. **g**: Time-course of IL-8-luc activation in WT and CF mice after challenge with intratracheal VR1Sn. Results are reported as FOI over baseline as mean ± SEM, n = 6 for each group. *Panel H*: Cellular infiltration into the lung of WT and CF mice after intratracheal instillation with VR1Sn. VR1Sn-induced neutrophils and white blood cells (WBC) recruitment in the airways at 24 h. Three mice were used for every time point and the experiment was replicated three times. Values are expressed as mean ± SEM of the three different experiments. Statistical differences were tested by one-way ANOVA followed by Dunnett's t post hoc test for group comparisons. *p < 0.05 and **p < 0.01 WT and CF TSB vs WT and CF VR1 group. (**i**–**n**) : Representative micro-photographs Giemsa staining of lung of WT and CF mice after intratracheal instillation with TSB(I, L), and VR1Sn (M, N) at 24 h. Magnification 40×

specific case, being the C57Bl/6 mice congenic, the differential response to agonists further highlight the critical role of CF background in controlling inflammatory response.

At the moment we have not an explanation to the fact that we detected a stronger BLI signal in CF mice as compared to WT animals although the immune response, measured with classical BALF markers, was comparable in the two type of mice. However, this undoubtedly might constitute an advantage allowing the detection of CF-specific differences in the inflammatory response also in those cases in which both WT and CF responded equally as regards cell recruitment, cytokines expression and histological changes.

Despite the fact that CFTR-deficient mouse model is considered of limited interest in the field of cystic fibrosis as it does not reproduce and develop the full CF phenotype [28]. Our data support the notion that differential responses in CFTR defective-mice may occur, a fact that is in line with the pro-inflammatory phenotypes recognized in humans.

Conclusions

Non-invasive imaging techniques are increasingly considered in biomedical research and can lead to important insights on disease development on the same mouse model. In this study we combined in vivo gene delivery technology and non-invasive bioluminescence imaging, creating a unique tool to consider CF mice as suitable models in testing anti-inflammatory drugs and in investigating the molecular mechanism linked to cystic fibrosis [4]. Moreover, the possibility to repetitively test a single set of CF animals longitudinally has several advantages as it reduces the number of animals to sacrifice and the costs

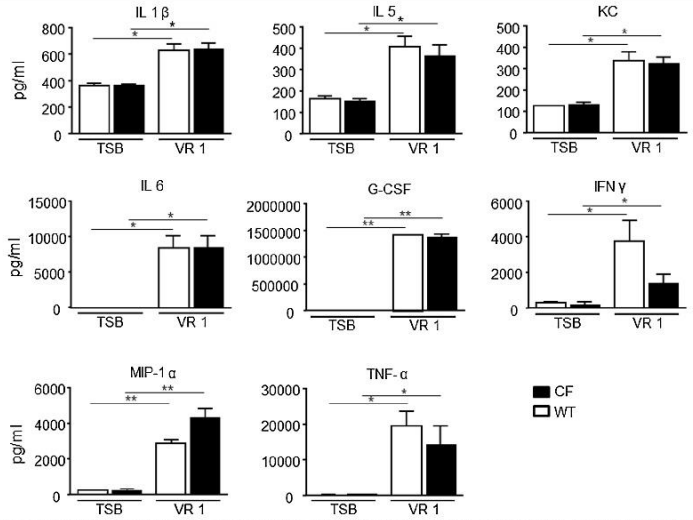

Fig. 5 Cytokines quantification in BALFs. WT and CF mice, treated with either TSB or VR1Sn and sacrificed at 24 h. A panel of 23 cytokines was analysed using a Bio-Plex™ Cytokine Assay Kit (Bio-Rad Laboratories), and eight resulted up-regulated compared to the control animals: IL-1β, IL-5, KC, IL-6, G-CSF, INFγ, MIP-1α, and TNF-α Three mice were used for every time point and the experiment was replicated three times. Values are expressed as mean ± SEM. Statistical differences were tested by one-way ANOVA followed by Dunnett's t post hoc test for group comparisons. *p < 0.05 and **p < 0.01

of housing and increases the data quality by lowering the intra animals variability, since each mouse represent its own control. This principle, applied to a CFTR-deficient murine model, will permit to study the activation of the inflammatory pathways in the CFTR defective lung in response to different agonists and to study/identify bacterial products with pro-inflammatory activity. Furthermore, the model might be used to evaluate, in an in vivo setting, the possible anti-inflammatory effect of drugs and therapeutic treatments in a cystic fibrosis background.

Additional file

Additional file 1: Figure S1. In vivo bioluminescence imaging. Monitoring bIL-8 activation in WT and CF transiently transgenized mice with bIL-8-Luc plasmid at 3, 4 and 7 days after DNA delivery. Results are reported photons/sec/cm2 as mean ± SEM, n = 6 each group. Statistical differences were tested by one-way ANOVA followed by Dunnett's t post hoc test for group comparisons. *p < 0.05 and **p < 0.01.

Abbreviations
BLI: bioluminescent imaging; BALFs: bronchoalveolar lavage fluids; CF: CFTR-deficient mice; WT: wild type mice.

Authors' contributions
Conception and design, FFS, GB, GD, CS, PM, MML. Laboratory testing, FFS, FR, FR, GB, AS, PM. Data collection, FFS, FR, FR, GB, AS, FB. Data analysis and interpretation: FFS, GB, CS, PM, MML, BMA. Drafting of manuscript: FFS, GB, GD, GV, CS, PM, MML. All authors read and approved the final manuscript.

Author details
[1] Pharmacology & Toxicology Department Corporate Pre-Clinical R&D, Chiesi Farmaceutici, Largo Belloli, 11/A, 43122 Parma, Italy. [2] Dipartimento di Medicina, Università di Verona, Verona, Italy. [3] Dipartimento di Scienze Biomediche, Biotecnologiche e Traslazionali, Università di Parma, Parma, Italy. [4] Dipartimento di Diagnostica e Salute Pubblica, Università di Verona, Verona, Italy. [5] Dipartimento di Scienze Medico Veterinarie, Università di Parma, Parma, Italy. [6] Dipartimento di Informatica, Università di Verona, Verona, Italy. [7] Centro Fibrosi Cistica, Azienda Ospedaliera Universitaria Integrata Verona, Verona, Italy.

Acknowledgements
This study has been funded by the FFC #18/2013 from the Italian Cystic Fibrosis Foundation. The authors would like to thank the Cystic Fibrosis animal Core Facility for providing the animals.

Competing interests
FFS and GV are employees of Chiesi Farmaceutici S.p.A., that supported the research work. FR is a consultant of Chiesi Farmaceutici S.p.A.

Received: 1 March 2016 Accepted: 13 July 2016
Published online: 28 July 2016

References

1. Galluzzo M, Ciraolo E, Lucattelli M, Hoxha E, Ulrich M, Campa CC, et al. Genetic deletion and pharmacological inhibition of PI3 K γ reduces neutrophilic airway inflammation and lung damage in mice with cystic fibrosis-like lung disease. Mediators Inflamm. 2015;2015:545417.
2. Cohen-Cymberknoh M, Kerem E, Ferkol T, Elizur A. Airway inflammation in cystic fibrosis: molecular mechanisms and clinical implications. Thorax. 2013;68(12):1157–62.
3. Hauser AR, Jain M, Bar-Meir M, McColley SA. Clinical significance of microbial infection and adaptation in cystic fibrosis. Clin Microbiol Rev. 2011;24(1):29–70.
4. Sorio C, Montresor A, Bolomini-Vittori M, Caldrer S, Rossi B, Dusi S, et al. Mutations of cystic fibrosis transmembrane conductance regulator (CFTR) gene cause a monocyte-selective adhesion deficiency. Am J Respir Crit Care Med. 2015.
5. Belessis Y, Dixon B, Hawkins G, Pereira J, Peat J, MacDonald R, et al. Early cystic fibrosis lung disease detected by bronchoalveolar lavage and lung clearance index. Am J Respir Crit Care Med. 2012;185(8):862–73.
6. Håkansson HF, Smailagic A, Brunmark C, Miller-Larsson A, Lal H. Altered lung function relates to inflammation in an acute LPS mouse model. Pulm Pharmacol Ther. 2012;25(5):399–406.
7. Balloy V, Deveaux A, Lebeaux D, Tabary O, le Rouzic P, Ghigo JM, et al. Azithromycin analogue CSY0073 attenuates lung inflammation induced by LPS challenge. Br J Pharmacol. 2014;171(7):1783–94.
8. Starkey MR, Jarnicki AG, Essilfie AT, Gellatly SL, Kim RY, Brown AC, et al. Murine models of infectious exacerbations of airway inflammation. Curr Opin Pharmacol. 2013;13(3):337–44.
9. Mauffray M, Domingues O, Hentges F, Zimmer J, Hanau D, Michel T. Neurturin influences inflammatory responses and airway remodeling in different mouse asthma models. J Immunol. 2015;194(4):1423–33.
10. Claes AK, Steck N, Schultz D, Zähringer U, Lipinski S, Rosenstiel P, et al. Salmonella enterica serovar Typhimurium ΔmsbB triggers exacerbated inflammation in Nod2 deficient mice. PLoS One. 2014;9(11):e113645.
11. Bianchi A, Ozier A, Ousova O, Raffard G, Crémillieux Y. Ultrashort-TE MRI longitudinal study and characterization of a chronic model of asthma in mice: inflammation and bronchial remodeling assessment. NMR Biomed. 2013;26(11):1451–9.
12. Lederlin M, Ozier A, Dournes G, Ousova O, Girodet PO, Begueret H, et al. In vivo micro-CT assessment of airway remodeling in a flexible OVA-sensitized murine model of asthma. PLoS One. 2012;7(10):e48493.
13. Stellari F, Sala A, Ruscitti F, Carnini C, Mirandola P, Vitale M, et al. Monitoring inflammation and airway remodeling by fluorescence molecular tomography in a chronic asthma model. J Transl Med. 2015;13:336.
14. Ma X, Prakash J, Ruscitti F, Glasl S, Stellari FF, Villetti G, et al. Assessment of asthmatic inflammation using hybrid fluorescence molecular tomography-x-ray computed tomography. J Biomed Opt. 2016;21(1):15009.
15. Blé FX, Cannet C, Zurbruegg S, Karmouty-Quintana H, Bergmann R, Frossard N, et al. Allergen-induced lung inflammation in actively sensitized mice assessed with MR imaging. Radiology. 2008;248(3):834–43.
16. Enright HA, Bratt JM, Bluhm AP, Kenyon NJ, Louie AY. Tracking retention and transport of ultrafine polystyrene in an asthmatic mouse model using positron emission tomography. Exp Lung Res. 2013;39(7):304–13.
17. Thomas AC, Kaushik SS, Nouls J, Potts EN, Slipetz DM, Foster WM, et al. Effects of corticosteroid treatment on airway inflammation, mechanics, and hyperpolarized ^{3}He magnetic resonance imaging in an allergic mouse model. J Appl Physiol (1985). 2012;112(9):1437–44.
18. Crane LM, Themelis G, Arts HJ, Buddingh KT, Brouwers AH, Ntziachristos V, et al. Intraoperative near-infrared fluorescence imaging for sentinel lymph node detection in vulvar cancer: first clinical results. Gynecol Oncol. 2011;120(2):291–5.
19. van Dam GM, Themelis G, Crane LM, Harlaar NJ, Pleijhuis RG, Kelder W, et al. Intraoperative tumor-specific fluorescence imaging in ovarian cancer by folate receptor-α targeting: first in-human results. Nat Med. 2011;17(10):1315–9.
20. Stellari FF, Franceschi V, Capocefalo A, Ronchei M, Facchinetti F, Villetti G, et al. In vivo imaging of transiently transgenized mice with a bovine interleukin 8 (CXCL8) promoter/luciferase reporter construct. PLoS One. 2012;7(6):e39716.
21. Stellari FF, Sala A, Donofrio G, Ruscitti F, Caruso P, Topini TM, et al. Azithromycin inhibits nuclear factor-κB activation during lung inflammation: an in vivo imaging study. Pharmacol Res Perspect. 2014;2(5):e00058.
22. Matute-Bello G, Downey G, Moore BB, Groshong SD, Matthay MA, Slutsky AS, et al. An official American Thoracic Society workshop report: features and measurements of experimental acute lung injury in animals. Am J Respir Cell Mol Biol. 2011;44(5):725–38.
23. Ansaldi D, Hod EA, Stellari F, Kim JB, Lim E, Roskey M, et al. Imaging pulmonary NF-kappaB activation and therapeutic effects of MLN120B and TDZD-8. PLoS One. 2011;6(9):e25093.
24. Stellari FF, Lavrentiadou S, Ruscitti F, Jacca S, Franceschi V, Civelli M, et al. Enlightened Mannhemia haemolytica lung inflammation in bovinized mice. Vet Res. 2014;45:8.
25. Stellari F, Bergamini G, Sandri A, Donofrio G, Sorio C, Ruscitti F, et al. In vivo imaging of the lung inflammatory response to Pseudomonas aeruginosa and its modulation by azithromycin. J Transl Med. 2015;13:251.
26. De Simone M, Spagnuolo L, Lorè NI, Rossi G, Cigana C, De Fino I, et al. Host genetic background influences the response to the opportunistic Pseudomonas aeruginosa infection altering cell-mediated immunity and bacterial replication. PLoS One. 2014;9(9):e106873.
27. Schmeck B, Huber S, Moog K, Zahlten J, Hocke AC, Opitz B, et al. Pneumococci induced TLR- and Rac1-dependent NF-kappaB-recruitment to the IL-8 promoter in lung epithelial cells. Am J Physiol Lung Cell Mol Physiol. 2006;290(4):L730–7.
28. Paroni M, Moalli F, Nebuloni M, Pasqualini F, Bonfield T, Nonis A, et al. Response of CFTR-deficient mice to long-term chronic Pseudomonas aeruginosa infection and PTX3 therapy. J Infect Dis. 2013;208(1):130–8.

An IL-8 Transiently Transgenized Mouse Model for the in Vivo Long-term Monitoring of Inflammatory Responses

Gabriella Bergamini*, Fabio Stellari*, **Angela Sandri***, Maria del Mar Lleò, Gaetano Donofrio, Francesca Ruscitti, Federico Boschi, Andrea Sbarbati, Gino Villetti, Paola Melotti, Claudio Sorio

Journal of Visualized Experiments (2017) e55499

DOI:10.3791/55499

*Equal contribution

Video Article

An IL-8 Transiently Transgenized Mouse Model for the *in Vivo* Long-term Monitoring of Inflammatory Responses

Gabriella Bergamini*[1], Fabio Stellari*[2], Angela Sandri*[3], Maria M. Lleo[3], Gaetano Donofrio[4], Francesca Ruscitti[5,2], Federico Boschi[6], Andrea Sbarbati[7], Gino Villetti[2], Paola Melotti[8], Claudio Sorio[1]

[1]Department of Medicine, General Pathology Division, Cystic Fibrosis Translational Research Laboratory "D. Lissandrini", University of Verona

[2]Corporate Preclinical R&D, Chiesi Farmaceutici S.p.A.

[3]Department of Diagnostic and Public Health, Microbiology Division, University of Verona

[4]Dipartimento di Scienze Medico-Veterinarie, University of Parma

[5]Department of Biomedical Biotechnological and Translational Sciences, University of Parma

[6]Department of Computer Science, University of Verona

[7]Department of Neurological, Biomedical and Movement Sciences, University of Verona

[8]Cystic Fibrosis Regional Center (CFC), AOUI Verona

*These authors contributed equally

Correspondence to: Claudio Sorio at claudio.sorio@univr.it

URL: https://www.jove.com/video/55499
DOI: doi:10.3791/55499

Keywords: Inflammation, gene delivery, *in vivo* monitoring, bioluminescence imaging, interleukin-8, lung

Date Published: 6/13/2017

Citation: Bergamini, G., Stellari, F., Sandri, A., M. Lleo, M., Donofrio, G., Ruscitti, F., Boschi, F., Sbarbati, A., Villetti, G., Melotti, P., Sorio, C. An IL-8 Transiently Transgenized Mouse Model for the *in Vivo* Long-term Monitoring of Inflammatory Responses. *J. Vis. Exp.* (), e55499, doi:10.3791/55499 (2017).

Abstract

Airway inflammation is often associated with bacterial infections and represents a major determinant of lung disease. The *in vivo* determination of the pro-inflammatory capabilities of various factors is challenging and requires terminal procedures, such as bronchoalveolar lavage and the removal of lungs for *in situ* analysis, precluding longitudinal visualization in the same mouse. Here, lung inflammation is induced through the intratracheal instillation of *Pseudomonas aeruginosa* culture supernatant (SN) in transiently transgenized mice expressing the luciferase reporter gene under the control of a heterologous IL-8 bovine promoter. Luciferase expression in the lung is monitored by *in vivo* bioluminescent image (BLI) analysis over a 2.5- to 48-h timeframe following the instillation. The procedure can be repeated multiple times within 2 - 3 months, thus permitting the evaluation of the inflammatory response in the same mice without the need to terminate the animals. This approach permits the monitoring of pro- and anti-inflammatory factors acting in the lung in real time and appears suitable for functional and pharmacological studies.

Video Link

The video component of this article can be found at https://www.jove.com/video/55499/

Introduction

Chronic lung diseases, such as asthma, chronic obstructive pulmonary disease (COPD), cystic fibrosis (CF), and bronchiectasis, are characterized by airway inflammation. Airway inflammation is characterized by edema, cellular infiltration, T lymphocyte and mast cell activation, increased airway secretions, and excessive collagen deposition. CF is a multisystem disorder, and its major cause of mortality and morbidity is lung bacterial infection with increasing pulmonary exacerbation. The decline in lung function predicts a significantly poorer outcome[1,2,3,4].

The inflammation state of the respiratory tract is usually observed through the evaluation of immunological markers recruited during the inflammatory process in material derived from the lower and upper airways, such as sputum, which provides variable results. Bronchoscopies are also performed[5]. Murine models are valuable tools for investigating the pathogenesis and evolution of diseases characterized by airway inflammation and for which effective treatments or cures have not yet been identified. Animal models of lung infection and inflammation have been used to study asthma and host-pathogen interactions, including the role of chemicals that simulate human conditions (*e.g.*, cigarette smoke exposure, LPS, elastase, ovalbumin, poly I:C, *etc.*, as well as combinations of the above)[6]. The measurement of inflammation-related parameters requires the sacrifice of the animals, as invasive approaches are required to measure factors such as bacterial load, cytokines in the lungs, and collected bronchoalveolar lavage (BAL) fluid. Also, histological examinations are often required. The possibility of obtaining information on the inflammatory response kinetics requires the use of numerous mice. Therefore, a technique that would allow for obtaining such information without the need to sacrifice the animals is valuable on technical, ethical, economical, and operational bases.

IL-8 is an essential player in the inflammation process, recruiting leukocytes to the inflamed tissue. It represents a molecular read-out for the study of inflammatory pathway activation. MIP-2 and KC may be functional homologs of human IL-8 in mice. Mice express only one potential IL-8 receptor, a homolog of human CXCR2[7,8], but they are capable of modulating a heterologous IL-8 gene promoter that drives a reporter gene. A

lung inflammation murine model has recently been developed after the observation that a bovine IL-8 promoter/luciferase reporter construct can be transactivated in mice. This feature allows for the utilization of bioluminescence imaging (BLI) to monitor the inflammatory response in living animals[9].

This model has been adapted to study inflammation triggered by bacterial exoproducts (*e.g.*, LPS or products released by bacterial strains) or TNFalpha[10,11]. The drug discovery process is focused on the development and optimization of old and new anti-inflammatory molecules that can treat lung diseases, such as CF, asthma, and COPD. These new chemical entities must be quickly and conveniently tested in animal models that can be linked to specific clinical phenotypes in order to facilitate the design of smart clinical trials.

Protocol

All animal experiments described were approved by the intramural animal-welfare committee for animal experimentation by the Interdepartmental Centre of Experimental Research Service at the University of Verona and comply with the European Directive 2010/63 UE, Italian D.Lgs 26/2014 and the revised "Guide for the Care and Use of Laboratory Animals," Washington, D.C.: National Academy Press, 1996. This protocol and experimentation were approved by the National Institutes of Health (n 273/15). Animals had free access to standard rodent chow and softened tap water and were acclimatized for at least 5 days to the local vivarium conditions (room temperature: 20 - 24 °C; relative humidity: 40 - 70%; light-dark cycle: 12 h) before any treatment.

1. *In Vivo* Gene Delivery

1. Use a laminar flow hood to prepare the *in vivo* delivery reagent/nucleic acid complexes.
2. Define the experimental protocol and parameters following the manufacturer's *in vivo* instructions.
    1. Use a total injection volume of 200 µL of complexes per mouse.
    2. Start with 40 µg of DNA suspended in endotoxin-free water; the optimization range can reach 60 µg.
       NOTE: The final concentration of nucleic acid in the injection volume must not exceed 0.5 µg/µL, according to the manufacturer's instructions.
    3. Use an N/P ratio of 6 - 8 (0.12 - 0.16 µL of delivery reagent per µg of nucleic acid). Calculate the corresponding volume of delivery reagent.
       NOTE: The complexes should be cationic for effective cell entry. The N/P ratio is defined as the number of nitrogen residues (N) on the *in vivo* delivery reagent per nucleic acid phosphate (P) and represents the measure of the ionic balance within the complexes.
3. Dilute the calculated amount (see step 1.2.1) of nucleic acid in 5% glucose (final concentration) using 10% glucose stock solution (provided) and sterile water. Make sure that the dilution volume is half the final injection volume. Vortex gently or mix by pipetting up and down.
4. Dilute the calculated amount (see step 1.2.3) of delivery reagent into half the injection volume of 5% glucose (final concentration) using the 10% glucose stock solution (provided) and sterile water. Vortex gently and spin at 13,000 x g for 15 s.
5. Add the above diluted delivery reagents to the diluted nucleic acid all at once. Mix them by gentle vortexing and spin down at 13,000 x g for 15 s.
6. Incubate the mixture from step 1.5 for 15 min at room temperature.
   NOTE: From this point on, the complexes are stable for 4 h at room temperature and for up to 7 days when stored at 4 °C.
7. Perform tail-vein injections using complexes equilibrated at room temperature. Place the mouse tail into warm water (50 - 53 °C) for 30 s to allow for vein dilation.
    1. Place the mouse inside the restraining device. Insert a 27- to 30-gauge needle in the tail vein at a 20 - 30° angle and slowly inject 200 µL. Upon completion, remove the needle and apply pressure to the injection site.
       NOTE: A slight bulge in the tail during the injection indicates incorrect positioning. If this occurs, remove the needle and repeat the process proximal to the previous site.
8. Visualize gene expression by performing *in vivo* BLI (see step 2) at 24 and 48 h after the intravenous injection.

2. *In Vivo* BLI

NOTE: Beforehand, prepare a fresh stock solution of 15 mg/mL D-luciferin in DPBS, filter-sterilize it using a 0.22-µm filtering unit, and store it at -20 °C.

1. Place the mice into a clear plexiglass anesthesia chamber. Make sure that the isoflurane chamber is full. When ready to anesthetize the animals, ensure that the pump (left) and chamber (right) switches are on. Turn the isoflurane dial to 2.5% for induction and 2% for maintenance. Animals inside the IVIS chamber are kept under 2.5% isofluorane anesthesia during image acquisition.
2. After the mice are fully anesthetized, inject 10 mL/kg bodyweight of the D-luciferin solution by an intraperitoneal route 15 min before imaging.
   NOTE: A kinetic study on D-luciferin should be performed to determine the time of the signal peak after the administration of D-luciferin.
3. Open the *in vivo* imaging system and prepare the imaging chamber by lining it with a piece of black cardstock (discard upon completion). Place the nose cones as needed for correct anesthesia (use one cone per mouse).
   NOTE: The tube that supplies the anesthesia to the instrument is split so that the same concentration of anesthesia is plumbed to the anesthesia manifolds located inside the imaging system.
4. Transfer the mice (up to 5) from the box to the nose cones attached to the manifold in the imaging system and close the door. Image acquisition lasts 5 min.
5. Acquire a BLI using the manufacturer's software, as follows.
    1. Initialize the software. In the *in vivo* imaging system acquisition control panel, put a check mark next to **Luminescent**. Confirm that the Excitation Filter setting is Block and the Emission Filter setting is Open.

2. Click the arrows: for the Luminescent Imaging Mode, select a 5-min exposure time, Binning 8, and F/Stop 1; for the Photograph Imaging Mode, select Binning 4 and F/stop 8.
3. From the Field of View dropdown list, select D, 19 cm, and a Subject Height of 1.5 cm. Click Acquire when ready to acquire the image.

6. When the image acquisition is complete, place the mice back into their cages.
7. Quantify the photons emitted from specific regions using the manufacturer's software.
   1. Click **ROI Tools** in the tool palette. In the **ROI Tools**, select **Measurement ROI** from the Type dropdown list.
   2. Click on the Square icon and draw a squared ROI with the proper dimensions to cover the thorax of one animal. Copy and paste the ROI for each animal to obtain ROIs with the same dimensions. In the ROI Tools panel, click on **Measure ROI** to obtain the measurements of the total intensity in the ROIs.
   3. Observe the ROI Measurements data for all ROIs created in the images or sequences during a session (one ROI per row). Click Export and select the folder where the file will be saved.

3. Mouse Challenge with Pro-Inflammatory Stimuli

NOTE: Prior to the mouse challenge with pro-inflammatory stimuli, check the baseline activation by *in vivo* BLI (see step 2). At least 7 days must pass between *in vivo* gene delivery and mouse challenge to allow the mild and transient inflammation to disappear.

1. Prepare the equipment for intratracheal instillation (refer to **Figure 1** and **Figure 2**).
   1. Connect the 5 ml disposable syringes with the spring (C, E), a 100 µL syringe (B), and a disposable gauge (D) to the 3-way stopcock (A). Place the system on the support (H). Place the system on the support (H).
   2. Connect the PE190 micro medical tubing (F) to the disposable gauge (D) and to the pen century (G).
   3. Fill the 5-mL syringe with 800 µL of air and turn the 3-way stopcock.
      NOTE: Fill the tube with *Pseudomonas aeruginosa* culture supernatant by aspirating 50 µl in the 100 µl syringe.

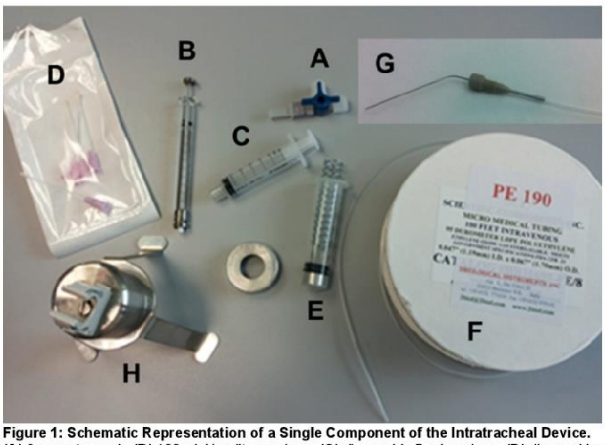

Figure 1: Schematic Representation of a Single Component of the Intratracheal Device.
(A) 3-way stopcock, **(B)** 100-µL Hamilton syringe, **(C)** disposable 5-mL syringe, **(D)** disposable gauge, **(E)** disposable 5-mL syringe with spring, **(F)** PE190 micro medical tubing, **(G)** pen century, and **(H)** support. Please click here to view a larger version of this figure.

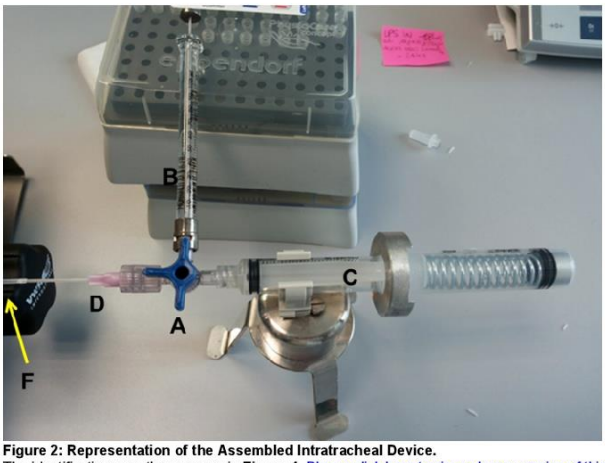

Figure 2: Representation of the Assembled Intratracheal Device.
The identifications are the same as in **Figure 1**. Please click here to view a larger version of this figure.

2. Anesthetize the mice using an isoflurane vaporizer chamber set at 2.5% isoflurane mixed with oxygen.
3. Monitor the animal to evaluate the effects of the anesthetic after 3 - 5 min.
   NOTE: To confirm that the mouse is fully anesthetized, monitor the following signs carefully: slowed breathing rate should slow down, lack of arm stretching when picked up by the neck, and a lack of response when the hind limbs are stimulated. Wait for a few additional minutes and check again before proceeding to the next step if these criteria are not met.
4. Place the anesthetized mouse on the plexiglass intubation platform, hanging it by its incisors, which are placed on the wire.
5. Turn on the laryngoscope with the left hand (for right-handed researchers) and grab a pair of blunt-ended forceps. Use the tip of laryngoscope and the forceps to gently pry open the mouth.
6. Pull the tongue out and hold it to the side using the forceps. Guide the laryngoscope blade towards the back of the mouth. Keep the laryngoscope pressed down very gently at a 90° angle until the opening of the trachea is visible. Hold the laryngoscope in place.
7. Using the other hand, take the delivery tube connected to the end of the PE tubing and insert it into the trachea. Rotate the three-way valve to deliver the inoculum. Pull the tube out of the trachea as soon as possible. Hold the mouse upright for a few seconds to the allow inoculum to be inhaled into the lungs.
   NOTE: Mice will suffocate and die if the trachea is blocked for too long.
8. Remove the mouse from the platform. The recovery time may vary based on strains; monitor the mouse diligently, ensuring that the animal is fully awake within 30 min after the procedure.
9. Intraperitoneally inject 150 mg/kg D-luciferin and image the lungs using an *in vivo* imaging system 4, 24, and 48 h after the intratracheal instillation of the stimuli. Quantify the photons emitted from specific regions using the manufacturer's software.

Representative Results

The bIL-8-Luc transient transgenic mouse model was used for the *in vivo* monitoring of lung inflammation in mice challenged with concentrated bacterial supernatant (30x) containing secreted virulence factors. The induced inflammatory response was detectable by *in vivo* imaging as an increase in the BLI signal. Pro-inflammatory activity was clearly detectable 2.5 h post-instillation, although the BLI signal reached the highest peak between 5 and 24 h and was still detectable at 48 h (**Figure 3**).

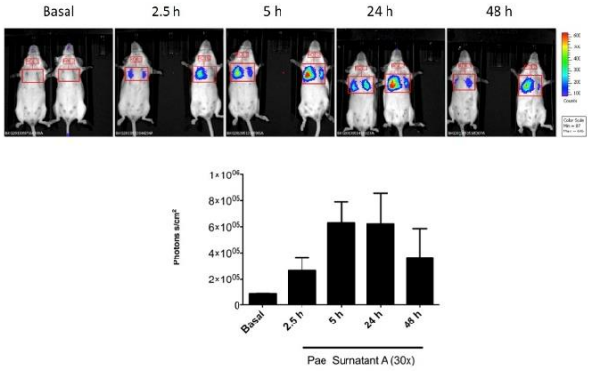

Figure 3: Representative *In Vivo* Imaging of Lung Inflammation Induced by *P. aeruginosa* SN in IL-8 Transiently Transgenic Mice.
Upper panel: Representative images of mice (n= 2 per group) intratracheally instilled with bacterial cell-free 30x SN from a *Pseudomonas aeruginosa* strain (Pae) after transient transgenization with bIL-8-Luc. Mice were monitored by BLI at 2.5, 5, 4, 24 and 48 h post-stimulation, with a region of interest drawn over the chest. Lower panel: Combined data expressed as photons/s/cm^2. Each value represents the mean ± SEM.
Please click here to view a larger version of this figure.

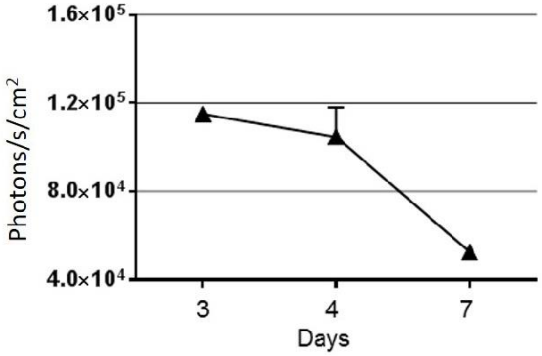

Figure 4: Transient Lung Inflammation Following Transfection.
Decrease of chest BLI from the first assessment (day 3) following the IV inoculation of bIL-8-Luc. Data are expressed as photons/s/cm^2 ± SEM (n= 6).

Discussion

In a previous work[11], a contrast between bIL-8-Luc-dependent BLI and BAL markers was shown. It relied on the differential degree of sensitivity within mouse strains[12]. For this reason, the first application of the bIL-8-Luc model to a different mouse strain requires an initial study of the inflammatory response, both in terms of BLI and more standardized inflammatory markers.

Mice transfection causes mild lung inflammation and the activation of bIL-8-Luc, which is detectable by BLI up to 3 - 4 days after DNA injection (**Figure 4**). It then completely disappears after 1 week[1]. The expression of bIL-8-Luc after gene delivery should always be verified by *in vivo*

BLI, as this is a necessary condition for the success of the following experimental steps. After 7 days and prior to the mouse challenge, baseline activation should be recorded to confirm the disappearance of the transfection-induced inflammation.

This approach has been tested on the acute phase of inflammation, but its application to the chronic phase has not been tested. It is not known how the live microorganism challenge could impact the activity of the promoter used in this setting. An increased understanding of the pathogenesis of acute and chronic inflammation and the consequent alteration of lung function is essential for the development of effective therapies for a number of chronic lung diseases[3,9]. Animal models continue to be necessary for this purpose, although limitations in accurately reflecting human disease pathophysiology are present.

The *in vivo* monitoring of inflammatory parameters in small rodents using luciferase reporter genes derived from other species is of great value. This approach permits the study of the pathophysiology of inflammatory responses, as well as the ability to test interventions aimed at their modulation. This was successfully tested using a previously well-characterized bovine IL-8 promoter/luciferase transiently transgenized (bovinized) mouse model[1]. Moreover, a recent study[10] demonstrated that the model described here is appropriate for monitoring lung inflammatory response induced by bacterial exoproducts and for investigating the mechanism of action of compound(s) of interest. BLI is a non-invasive approach that allows for the longitudinal observation of the lung inflammatory process after intratracheal instillation with relevant stimuli, including *P. aeruginosa* culture supernatant[9,10,11]. This is an obvious advantage of studying acute lung inflammation compared to classical methods, which require the sacrifice of the animals to collect BAL fluid and the lungs. Its value for the study of chronic infection/inflammation has not been addressed.

The present model can be used to deepen the available knowledge on the pathogenesis of lung inflammatory diseases, including the characterization of bacterial/non-bacterial factors with pro-inflammatory activity. Furthermore, it can facilitate the evaluation of the possible therapeutic effects of molecules with known/presumptive anti-inflammatory actions.

Disclosures

The authors have nothing to disclose.

Acknowledgements

This work was supported by the Italian Cystic Fibrosis Foundation Project FFC#18/2013, FFC#29/2015 and by the Italian Cystic Fibrosis League through the Veneto Branch—Associazione Veneta Lotta contro la Fibrosi Cistica Onlus.

References

1. Barnes, P. J. Therapeutic approaches to asthma-chronic obstructive pulmonary disease overlap syndromes. *J Allergy Clin Immunol.* **136**, 531-545 (2015).
2. Cohen-Cymberknoh, M., Kerem, E., Ferkol, T., & Elizur, A. Airway inflammation in cystic fibrosis: molecular mechanisms and clinical implications. *Thorax.* **68**, 1157-1162 (2013).
3. Dhooghe, B., Noel, S., Huaux, F., & Leal, T. Lung inflammation in cystic fibrosis: pathogenesis and novel therapies. *Clin Biochem.* **47**, 539-546 (2014).
4. Durham, A. L., Caramori, G., Chung, K. F., & Adcock, I. M. Targeted anti-inflammatory therapeutics in asthma and chronic obstructive lung disease. *Transl Res.* (2015).
5. Sagel, S. D. Noninvasive biomarkers of airway inflammation in cystic fibrosis. *Curr Opin Pulm Med.* **9**, 516-521 (2003).
6. Starkey, M. R. *et al.* Murine models of infectious exacerbations of airway inflammation. *Curr Opin Pharmacol.* **13**, 337-344 (2013).
7. Cacalano, G. *et al.* Neutrophil and B cell expansion in mice that lack the murine IL-8 receptor homolog. *Science.* **265**, 682-684 (1994).
8. Simonet, W. S. *et al.* Long-term impaired neutrophil migration in mice overexpressing human interleukin-8. *J Clin Invest.* **94**, 1310-1319 (1994).
9. Stellari, F. F. *et al.* In vivo imaging of transiently transgenized mice with a bovine interleukin 8 (CXCL8) promoter/luciferase reporter construct. *PLoS One.* **7**, e39716 (2012).
10. Stellari, F. *et al.* In vivo imaging of the lung inflammatory response to Pseudomonas aeruginosa and its modulation by azithromycin. *J Transl Med.* **13**, 251 (2015).
11. Stellari, F. *et al.* In vivo monitoring of lung inflammation in CFTR-deficient mice. *J Transl Med.* **14**, 226 (2016).
12. De Simone, M. *et al.* Host genetic background influences the response to the opportunistic Pseudomonas aeruginosa infection altering cell-mediated immunity and bacterial replication. *PLoS One.* **9**, e106873 (2014).

